UCRL-ID-124429

EBIT - Electron Beam Ion Trap
N-Division Experimental Physics Annual Report 1995

D. Schneider

October 1996

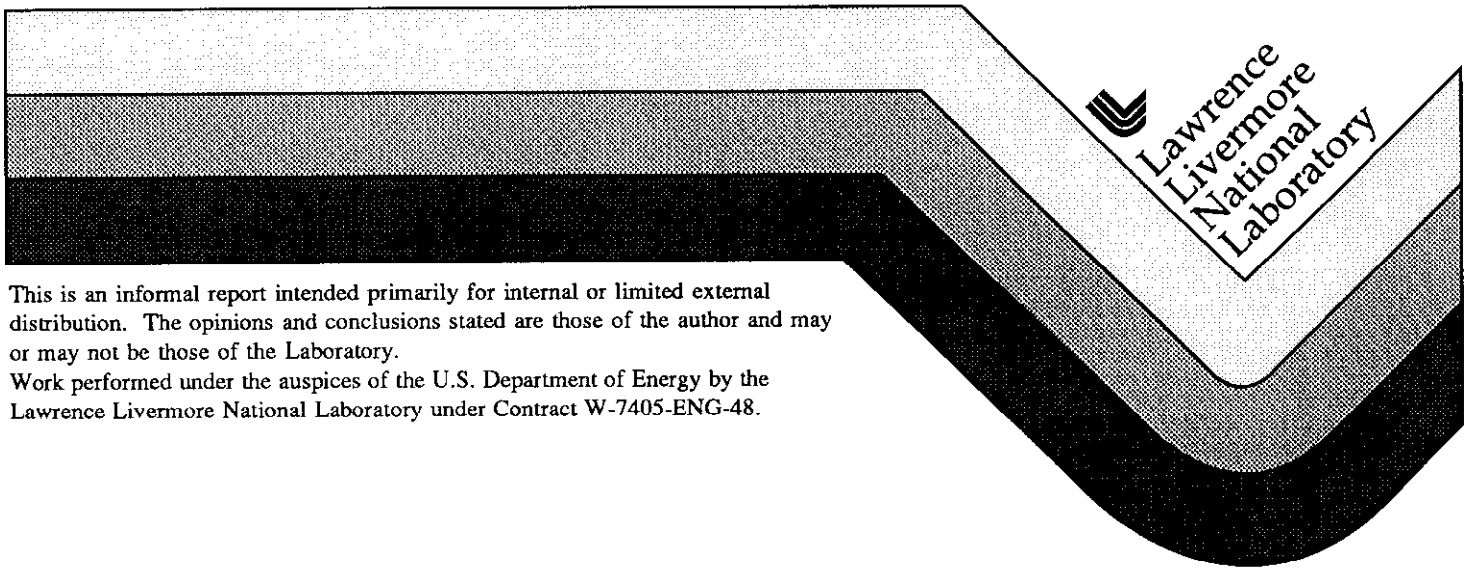

Work performed under the auspices of the U.S. Department of Energy by the Lawrence Livermore National Laboratory under Contract W-7405-ENG-48.

EBIT 95 Annual Report

Table of Contents

EBIT

Electron Beam Ion Trap

N-Division

Experimental Physics

Annual Report
1995

Edited by:
Dieter Schneider

For further information contact:
N Division
Physics & Space Technology Directorate
Lawrence Livermore National
Laboratory
P.O. Box 808, L421
Livermore, CA 94550

Issued October 1996

INTRODUCTION

The multi-faceted research effort of the EBIT (Electron Beam Ion Trap) program in N-Division of the Physics and Space Technology Department at LLNL continues to contribute significant results to the physical sciences from studies with low energy very highly charged heavy ions. The spectroscopy is expanded into the visible regime. The spontaneous emission following the decay of the hyperfine structure level in H-like ^{165}Ho has been observed in an experiment on Super EBIT. The data resulted in a revision of the hitherto accepted nuclear magnetic moment of ^{165}Ho. A microcalorimeter is used to successfully measure x-ray lines from iron that are of astrophysical interest. Radiative lifetime measurements are extended to the millisecond regime, and first high-resolution K x-ray data using a newly implemented transmission spectrometer were measured.

Detailed sputter ion yield measurements using highly charged ion impact on semiconductor surfaces are continued. The energy loss of slow highly charged ions in 100Å thick carbon foils has been studied as a function of ion charges ranging from O^{8+} to Au^{60+}. A significant increase of the energy loss has been found for high charges and defines essential a new regime for energy loss in ion solid interactions. Measurements of secondary electron emission following highly charged ion impact on insulators and metals have been performed and a theoretical effort to model the solid surface response has been started.

Experiments on individually trapped ions are conducted with the EBIT RETRAP system. First charge exchange studies on low energy ions trapped and confined in RETRAP (a cryogenic Penning trap at EBIT) have been completed and a nondestructive method to follow the sequential charge exchange of single ions in RETRAP has been established. A laser laboratory with a laser beam transport system has been installed adjacent to the EBIT facility to allow laser cooling and spectroscopy on highly charged ions in RETRAP and EBIT.

Highly charged ions up to Xe^{54+} and U^{90+} have been extracted from Super EBIT and accelerated to MeV energies by means of high voltage extraction potentials. An Intense EBIT design and construction is well underway and should be completed in 1997.

The EBIT program attracts a number of collaborators from the US and abroad for the different projects. The collaborations are partly carried out through participating graduate students demonstrating the excellent educational capabilities at the LLNL EBIT facilities. Moreover, participants from Historically Black Colleges and Universities are engaged in the EBIT project.

The work was performed under the auspices of the U.S. Department of Energy by the Lawrence Livermore National Laboratory under contract #W-7205-ENG-48. Acknowledgment of funding support from other organizations is noted at individual abstracts of the report.

Dieter H.G. Schneider

I. Atomic Structure Measurements and Radiative Transition Probabilities

Measurements of the Nuclear Charge Radii of Highly Charged Radioactive Isotopes

S. R. Elliott
University of Washington, Seattle, WA 98195
P. Beiersdorfer, and M. H. Chen
Lawrence Livermore National Laboratory, Livermore, CA 94550

The trapping of radioactive nuclides creates new opportunities for novel nuclear physics experiments. Using EBIT, we have performed the first nuclear physics measurements using trapped few-electron, very-high-Z radioactive ions [1]. Employing precision x-ray spectroscopy and exploiting the simplified electronic structure of few-electron ions we isolate the nuclear effects among different isotopes and infer the isotopic variation of the nuclear charge distribution, a fundamental parameter crucial for understanding the collective structure of the nucleus. Its variation, parameterized in terms of the change in mean-square nuclear charge radius ($\delta\langle r^2\rangle$), has been inferred in the high-Z region from muonic-atom x rays [2] and neutral-atom optical isotope shift studies [3]. Our present measurement focuses on the isotopes ^{233}U and ^{238}U for which earlier measurements of $\delta\langle r^2\rangle$ have produced discrepant results, i.e. (-0.520 ± 0.081 fm^2) [4] and (-0.383 ± 0.044 fm^2) [5,6].

Our technique for determining $\delta\langle r^2\rangle$ is based on precise Doppler-shift-free measurements of the n=2 to n=2 x-ray transitions in nearly bare ions of the isotopes in question. Implementation of this technique was previously impossible because of the lack of a facility at which the x-ray transitions from such highly stripped radioactive ions could be generated and measured conveniently and reliably. This situation has changed recently with the successful implementation of a high-energy electron beam ion trap that allows the production of very highly charged ions and of efficient crystal spectrometers that can resolve individual transitions with very high resolution. Moreover, ion traps generally require only minute quantities of material for filling. Thus they are well suited for investigating the properties of isotopes that are rare or radioactive. The transitions studied in the present measurement are the electric dipole, $2s_{1/2}$-$2p_{3/2}$ transitions in the three-electron Li-like ion, the four-electron Be-like ion, the five-electron B-like ion, and the six-electron C-like ion. Because the measurements are for transitions in an inner shell, the electron wavefunction overlap, especially that of the 2s electron, with the nucleus is large. It is thus an excellent probe of the nuclear charge distribution resulting in a relatively large energy shift (ΔE) as different isotopes are measured. Compared to muonic atoms, however, the overlap is modest and large nuclear polarization corrections are avoided. Moreover, the atomic physics of few-electron ions is tractable and deducing $\delta\langle r^2\rangle$ from ΔE is relatively simple. Most importantly, it is not complicated by large specific mass shift corrections necessary in neutral atoms [7]. In other words, in our measurement the coulomb shift (δE_{coul}), which is directly related to $\delta\langle r^2\rangle$, is by far the dominant contribution to ΔE, and other atomic or nuclear contributions are minimal. A further benefit of our technique is that the energy of the $\Delta n=0$ transitions studied falls within a range where high-precision crystal spectroscopy is easily employed.

The ^{233}U ions were introduced into the trap using a novel method [8] relying on a thin wire platinum probe with a plated tip placed near the electron beam. The ions are studied by their characteristic x rays observed through ports in the cryogenic vessels surrounding the trap. The $2s_{1/2}$-$2p_{3/2}$ electric dipole transitions, situated near 4.5 keV, were analyzed in a high-resolution von Hámos-type curved-crystal spectrometer. The x-ray spectrum of ^{233}U was compared with that from ^{238}U. Figure 1 shows the two measured spectra.

We deduced $\delta\langle r^2\rangle^{A,238}$ from δE_{coul} and found $\delta\langle r^2\rangle^{233,238} = -0.457$ fm^2 with a statistical uncertainty of 0.042 fm^2. By deducing $\delta\langle r^2\rangle$ for each charge state separately and then averaging, ensures proper treatment of the electron correlation contribution. The systematic uncertainty in δE_{coul} (8 meV) translates into a systematic uncertainty in $\delta\langle r^2\rangle^{233,238}$ of 0.010 fm^2. Adding the uncertainties in quadrature, the final result is $\delta\langle r^2\rangle^{233,238} = -0.457 \pm 0.043$ fm^2. This result can be compared with that of previous studies; -0.383 ± 0.044 fm^2 [5,6] and -0.520 ± 0.081 fm^2 [4]. The present measurement thus favors neither of the earlier measurements. The weighted mean of all measurements is -0.434 ± 0.028 fm^2. All three experiments are consistent with this mean value to within 1 to 2 standard deviations.

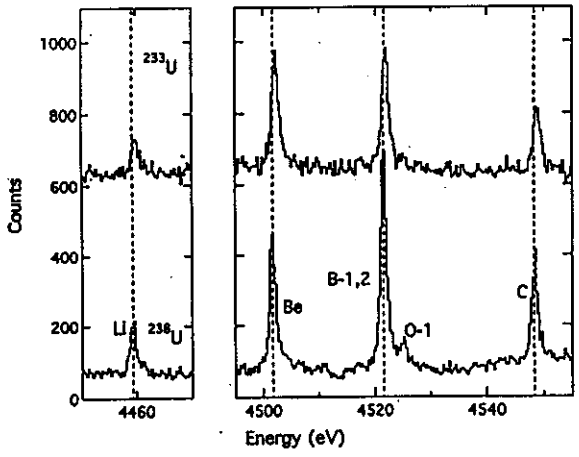

Fig. 1. Crystal spectrometer spectra of the $2s_{1/2}$-$2p_{3/2}$ transitions in U^{86+} through U^{89+} for the two isotopes ^{233}U and ^{238}U. The lines are labeled by the respective charge state of uranium. The ^{233}U is offset by 500 counts/channel. The dashed lines indicate the position of the ^{238}U lines.

References:

[1] S. R. Elliott, P. Beiersdorfer, and M. H. Chen, Phys. Rev. Lett. **76**, 1031 (1996).
[2] R. Engfer *et al.*, At. Data Nucl. Data Tab. **14**, 509 (1974).
[3] P. Aufmuth, K. Heilig, and A. Steudel, At. Data Nucl. Data Tab. **37**, 455 (1987).
[4] J. D. Zumbro *et al.*, Phys. Rev. Lett. **53**, 1888 (1984).
[5] A. Anastassov *et al.*, Hyper. Inter. **74**, 31 (1992).
[6] R. T. Brockmeier, F. Boehm, and E. N. Hatch, Phys. Rev. Lett. **15**, 132 (1965).
[7] W. H. King, Isotope Shifts in Atomic Spectra (Plenum Press, New York, 1984).
[8] S. R. Elliott, and R. E. Marrs, Nucl. Instr. and Meth. **B100**, 529 (1995).

Direct Observation of the Spontaneous Emission of the Hyperfine Transition F=4 to F=3 in Ground State Hydrogen-like $^{165}Ho^{66+}$ in an Electron Beam Ion Trap

José R. Crespo López-Urrutia, Peter Beiersdorfer, Daniel Savin, and Klaus Widmann
Lawrence Livermore National Laboratory, Livermore, CA 94550, USA

Measurements of the hyperfine splitting (HFS) of the ground state of hydrogen-like ions provide a very sensitive tool to explore QED and nuclear contributions to the electron energy. Only the spontaneous 1s hyperfine transitions in H, D and He^{+} have been observed experimentally; recently the fluorescence of laser pumped H-like Bi^{82+} was detected in a heavy-ion storage ring [1] resulting in the first measurement of the HFS in a multiply charged ion.

We have measured the F=4 to F=3 hyperfine transition of the 1s level of H-like $^{165}Ho^{66+}$ using passive emission spectroscopy [2]. The ions were produced and stored in a high energy electron beam ion trap (SuperEBIT). Holmium was injected into the trap using a metal vapor vacuum arc (MEVVA) source. A prism spectrograph and a cryogenically cooled CCD camera detector are used for detection. With the holmium MEVVA on, at a beam energy of 132 keV and 285 mA beam current, the trap contained 0.5% Ho^{67+}, 6 % Ho^{66+}, 40 % Ho^{65+}, 25% Ho^{64+} and also some lower charge states .Without holmium injection, the trap was filled by slow accumulation of heavy elements emanating mainly from the heated cathode. The thermal background radiation and the atomic line emission from the gas injector were eliminated by subtracting from every spectrum taken with holmium in the trap another one taken without holmium under otherwise identical conditions. During the long integration times (1 h) used for the individual exposures, cosmic rays were also detected by the CCD on individual pixels. Their contribution was largely reduced by a computer program discarding all pixels showing anomalous deviations. The remaining baseline fluctuation was mainly due to the statistical variation of the thermal radiation background in the trap. To obtain spectra from the two-dimensional images, the pixel counts on the CCD detector were integrated along one dimension. The result of the addition of 18 background corrected spectra (36 hours of data) is displayed in Fig 2. A single feature at (5726.4 ± 1.5) Å with a peak height 10 times larger than the standard deviation of the background and a FWHM of 15 Å appeared with a total number of around 4000 counts above the background. This feature was attributed to the hyperfine transition in Ho^{66+}. To exclude the possibility that the line was emitted by a lower charge state, the beam energy was then lowered to make sure that no H-like Ho^{66+} could be produced, while keeping the lower charge states in the trap more or less unchanged. No lines were observed under such conditions.

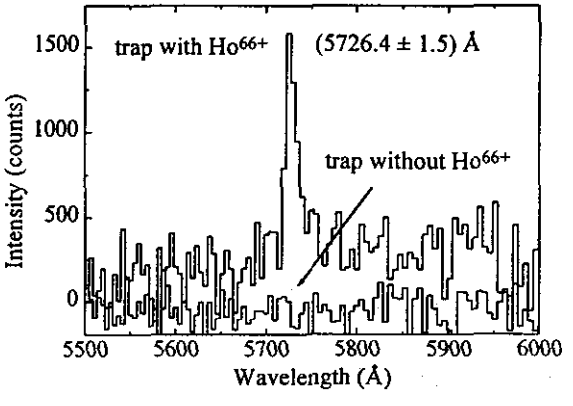

Figure 1. The F=4 to F=3 hyperfine transition in hydrogen-like Ho^{66+} and its baseline.

The main process populating the upper F level of the H-like ion is collisional ionization of He-like ions, were one of the two 1s electrons is removed leaving an H-like ion behind with similar probability for population in either the F=4 or F=3

state. The large population of He-like ions in the trap is thus simultaneously ionized to H-like state and excited to the F=4 level.

We used neutral atoms from the gas injector excited by the electron beam at low energies to generate a large number of calibration lines. Possible instrument and beam shifts were continuously monitored by observing the position of the NeI line at 5852.48 Å. Our experimental result of (5726.4 ± 1.5) Å (air) corresponds to a (5727.9 ± 1.5) Å vacuum wavelength and an energy difference between the F=4 and F=3 levels of (2.1645 ± 0.0006) eV.

The energy difference between the two levels in a H-like ion is given by Shabaev [3] as

$$\frac{\alpha^4 Z^3}{n^3}\cdot\frac{\mu_I}{I}\cdot\frac{m_e}{m_p}\frac{(I+j)\cdot m_e c^2}{j\cdot(j+1)\cdot(2l+1)}\left[A\cdot(1-\delta)\cdot(1-\varepsilon)+\kappa_{rad}\right] \qquad (1)$$

with following terms: α, fine-structure constant; Z, nuclear charge; n, j, l: principal, total moment and orbital moment electron quantum numbers; μ_I, nuclear magnetic moment; m_e, m_p: electron, proton mass; I, nuclear spin; A, relativistic factor; δ, nuclear charge distribution correction; ε, nuclear magnetization distribution (Bohr-Weisskopft) correction; κ_{rad}, QED radiative correction. Using this formula and μ_I = 4.173(27) n.m. as tabulated by Lederer and Shirley in [4], Shabaev [3] predicts a vacuum wavelength of 5639 Å. This value differs from our measured value by 89 Å. We use instead μ_I = 4.132(5) n.m., from a newer measurement of μ_I (Nachtsheim [5]) with five times smaller uncertainty, in Equ. (1) and add the QED contributions calculated by Persson et al. [6] and Schneider et al. [7], to obtain a transition energy of 2.1675 eV, and a vacuum wavelength of 5720.15 Å. This differs from our measured vacuum wavelength (5727.9 ± 1.5) Å by only 0.14 %. We emphasize that this good agreement was only reached after using the updated value for the nuclear magnetic moment and the QED corrections.

Our method can be readily applied to other H-like ions with HFS in the visible or UV range; an extension to the IR seems also feasible. Future possibilities include the use of laser spectroscopy for lifetime determination, since the count rate at the present is too low to allow a measurement with meaningful accuracy.

References

[1] I. Klaft et al. Phys. Rev. Lett. 73, N18, 2425 (1994)
[2] José R. Crespo López-Urrutia, Peter Beiersdorfer, D.Savin, and Klaus Widmann, PRL 76, N5, 826 (1996)
[3] V M Shabaev, J. Phys. B: At. Mol. Opt. Phys. 27, 5825 (1994)
[4] E. Browne et al. in *Table of Isotopes*, ed. C. M. Lederer and V. S. Shirley (7th ed.; New York: Wiley)(1978)
[5] G. Nachtsheim, *Präzisionsmessung der Hyperfeinstruktur-Wechselwirkung von ^{165}Ho im Grundzustand*" Ph.D. Thesis, Bonn 1980 (unpublished)
[6] H. Persson et al., PRL 76, No 9, p. 1433 (1996).
[7] S. M. Schneider, W. Greiner, and G. Soff, Phys. Rev. A50, 118 (1994)

This work was in part supported by the Office of Basic Energy Sciences and was performed under the auspices of the U.S.D.o.E. by Lawrence Livermore National Laboratory under contract # W-7405-ENG-48.

Search for $^3S_1$-$^3P_2$ Decay in U^{90+}

P. Beiersdorfer, S. R. Elliott, A. L. Osterheld, K. Widmann
Lawrence Livermore National Laboratory, Livermore, CA 94551
Th. Stöhlker
Gesellschaft für Schwerionenforschung, D-64220 Darmstadt, Germany

Heliumlike ions represent the simplest atomic system for developing and testing theoretical approaches for calculating the atomic structure of multi-electron ions. In this case the nonrelativistic Schrödinger equation can be solved with high accuracy so that many-body relativistic and QED effects can be isolated and compared with measurements. These effects are largest for the energy of the $1s^2$ ground state. In heliumlike U^{90+} QED effects represent 262.8 eV of the 132,902-eV ground state energy. QED effects are considerably smaller for the energy of a 2s electron (about 49 eV for U^{90+}). However, because QED effects are yet smaller for 2p electrons (8–9 eV for U^{90+}) the size of the QED effects can be maximized relative to the transition energy by studying 2s–2p transitions. Measurements of 2s–2p transitions thus provide important tests of structure calculations complementary to measurements involving transitions to the ground state.

Two 2s–2p transitions are possible in heliumlike ions: 1s2s $^3S_1$ – 1s2p $^3P_0$ and 1s2s $^3S_1$ – 1s2p $^3P_2$. A measurement of the former transition in heliumlike U^{90+} was made by Munger and Gould [1]. By contrast, the latter transition has been observed only for elements as heavy as krypton [2]. In low-Z ions the 1s2p $^3P_2$ level decays exclusively to the 1s2s $^3S_1$ level. However, in higher-Z ions the levels decays increasingly via a magnetic quadrupole transition to the $1s^2$ ground state, as illustrated in Fig. 1. This trend reverses in very high-Z ions, where relativistic effects enhance the probability for dipole-allowed decay to the 1s2s $^3S_1$ level. Detection of this transition in high-Z ions is thus not precluded by an overwhelmingly large radiative branch to the $1s^2$ ground state.

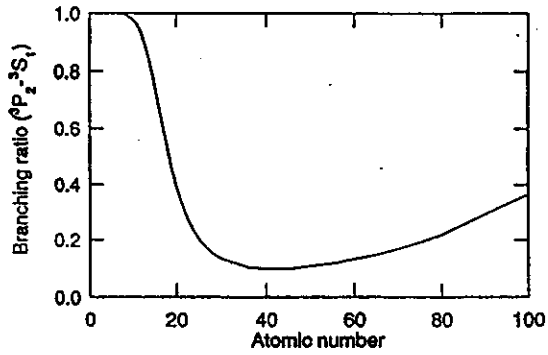

Fig. 1. Probability for dipole-allowed radiative decay of the 1s2p $^3P_2$ level to the 1s2s $^3S_1$ level. The transition competes with magnetic quadrupole decay to the $1s^2$ ground state.

The predicted energy of the 1s2s $^3S_1$ – 1s2p $^3P_2$ transition in heliumlike U^{90+} is 4510.012 eV [3]. The transition is, thus, expected to fall inbetween the 2s–2p transitions in berylliumlike U^{88+} and boronlike U^{87+} situated at 4501.72 and 4521.39 eV, as measured earlier by us at the Livermore high-energy EBIT facility [4]. A major difficulty in identifying the 1s2s $^3S_1$ – 1s2p $^3P_2$ transition is given by the small size of the excitation rates of the 1s2p $^3P_2$ level from the ground state, which

is only a few percent of the excitation rates of the 2s–2p transitions in berylliumlike and boronlike uranium.

Using the EBIT facility, we performed extensive surveys of the relevant spectral region [5]. A weak feature with intensity just above the level of background fluctuations was observed at the predicted location of the $1s2s\ ^3S_1 - 1s2p\ ^3P_2$ transition, as illustrated in Fig. 2. The feature was observed in spectra where the intensity of the $2s_{1/2}$–$2p_{3/2}$ transition in lithiumlike uranium, and thus the ionization balance, was optimized; it appeared absent in spectra where the average ionization balance was lower. The measured energy of the feature is 4510.05±0.24 eV, which agrees closely with the values predicted for the $1s2s\ ^3S_1 - 1s2p\ ^3P_2$. Detailed spectral modeling calculations, however, indicate the possibility that a weak transition in berylliumlike U^{88+} is situated within 4 eV of the location of the heliumlike $^3S_1 - ^3P_2$ transition. This transition connects the level $1s^22p_{1/2}2p_{3/2}\ ^3P_1$ with the $1s^22s_{1/2}2p_{1/2}\ ^3P_0$ metastable ground level in berylliumlike uranium. The accuracy with which the energy of the berylliumlike transition can be predicted is insufficient to rule out a blend with the heliumlike $^3S_1 - ^3P_2$ transition. Better theoretical calculations and additional measurements will be required to firmly identify the $^3S_1 - ^3P_2$ transition and ascertain its QED component.

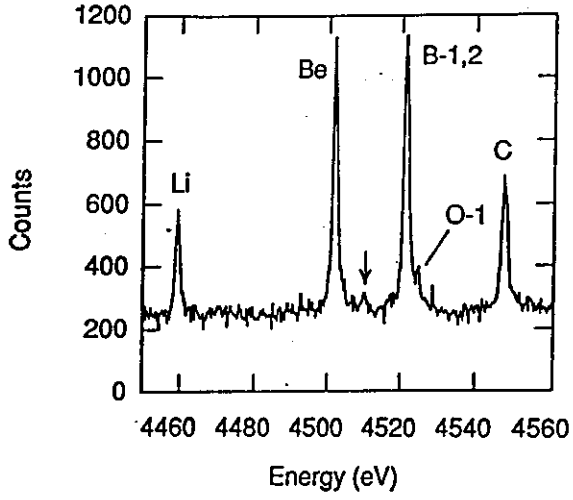

Fig. 2. Crystal-spectrometer spectra of the $2s_{1/2}$–$2p_{3/2}$ transitions in the energy region 4450 to 4560 eV. Transitions in lithiumlike, berylliumlike, boronlike, carbonlike, and oxygenlike uranium are labeled by Li, Be, B, C, and O, respectively. The predicted location of the $^3S_1 - ^3P_2$ transition in U^{90+} is 4510.012 eV and is indicated by an arrow.

References:

[1] C. T. Munger and H. Gould, Phys. Rev. Lett. **57**, 2927 (1986).

[2] S. Martin et al., Europhys. Lett. **10**, 645 (1989).

[3] G. W. F. Drake, Can. J. Phys. **66**, 586 (1988).

[4] P. Beiersdorfer, D. Knapp, R. Marrs, S. Elliott, M.Chen, Phys. Rev. Lett. **71**, 3939 (1993).

[5] P. Beiersdorfer, S. R. Elliott, A. L. Osterheld, Th. Stöhlker, J. Autrey, G. V. Brown, A. J. Smith, and K. Widmann, Phys. Rev. A **53**, 4000 (1996).

This work was supported by the LLNL Research Collaborations Program for Historically Black Colleges and Universities and the DOE Office of Basic Energy Sciences, Division of Chemical Sciences.

X-ray Spectroscopy of Highly Charged Californium Ions

P. Beiersdorfer,[a] J. R. Crespo López-Urrutia,[a] S. R. Elliott,[b] and K. Widmann[a]
[a]*Lawrence Livermore National Laboratory, Livermore, CA 94551*
[b]*Department of Physics, University of Washington, Seattle, WA 98195*

The ions studied with EBIT in one form or another have included virtually all elements from hydrogen up to uranium. A variety of fundamental physics issues call for studying elements with the highest atomic number Z possible. These include, for example, studies of quantum electrodynamics (QED), or, more generally, studies of the Lamb shift, which is comprised of energy shifts due to electron self energy, the finite nuclear mass, and the vacuum polarization. The Lamb shift increases as Z^4 and thus becomes a major energy term in ions with the highest nuclear charge. If any new physics is to be discovered that is not included in the Lamb shift, it is expected to be in the highest-Z elements.

While all transuranic elements are unstable, there are eight transuranic elements with lifetimes of several hundred days or longer. These elements, covering atomic numbers 93 through 100, are typically highly radioactive and are poisonous even in microscopic quantities. EBIT, however, uses only about 10^6 ions to fill its trap. This is such a small quantity that even transuranic elements could, in principle, be injected into EBIT.

Recently, a technique was developed to fill the EBIT trap which requires only small quantities of material. This technique employs a thin wire coated with the material of interest that is brought near the electron beam where ion sputtering slowly transfers the material to the trap [1]. This method has first been demonstrated on gold; later it was used to introduce ^{233}U into the trap [2].

We have employed the coated-wire technique to introduce ^{249}Cf into EBIT. Californium (Z=98) is the highest-Z element with a lifetime of years or more. A platinum wire was electrolytically coated with 5 nanograms or 20 nCi of ^{249}Cf, which was inserted into the EBIT trap. The trap was operated with a continuous 95-mA electron beam at 145 keV. The x-ray emission was monitored with a 6-cm diameter, 3-cm deep Ge detector that viewed the EBIT trap through one of its radial ports. Several minutes were required before any radiation from Cf was noticeable in the x-ray spectrum. A spectrum collected for a total of 120 minutes is shown in Fig. 1. The spectrum shows two features that are attributed to the n=2 to n=1 transitions in highly charged Cf at approximately 111.5 and 117.5 keV. The lower-energy feature corresponds to transitions of an electron in the $2s_{1/2}$ and $2p_{1/2}$ subshells to the $1s_{1/2}$ K-shell vacancy; the higher-energy feature corresponds to transitions of an electron in the $2p_{3/2}$ subshell. The intensity of the lower-energy feature is clearly higher than that of the higher-energy feature. The dominance of the lower-energy feature is a diagnostic signature of the fact that the x-ray emission comes from very high charge states, in particular, from Cf ions with a (nearly) vacant L-shell [3]. The ratio contrast markedly from the ratio that would be observed from low-charge state ions or neutrals, where the higher-energy feature, or so-called $K\alpha_1$ line, is about twice the size as the lower-energy feature, or so-called $K\alpha_2$ line.

For comparison, we also show in Fig. 1 a spectrum of uranium. It was collected over a similar time span as the californium. Similar ratios of the j=1/2 and j=3/2 features are observed. Unlike californium, uranium was not introduced via the wire probe. Instead it accumulated in the trap under some operating conditions without external introduction. Its presence in the trap is attributed to uranium deposited on the drift tubes and electrodes in prior experiments. The uranium signal is about the same size as the californium signal. Moreover, signals from lower-Z elements, such as barium or osmium, were observed in our spectra that also competed in intensity with that observed from californium. Our experiment, thus, indicates that it will be necessary to increase the amount of Cf plated on the wire in order to increase the Cf signal over that from elements entering the trap via other channels. This is easily possible, as the amount of Cf coated on the wire is still much smaller than radiologically or toxicologically possible.

The present experiment with ^{249}Cf can be considered a successful first step that demonstrates the possibility of introducing transuranic elements into the trap for further study. The use of transuranic elements on EBIT will increase in the future, and spectroscopic measurements will undoubtedly become a standard technique for these highest-Z elements.

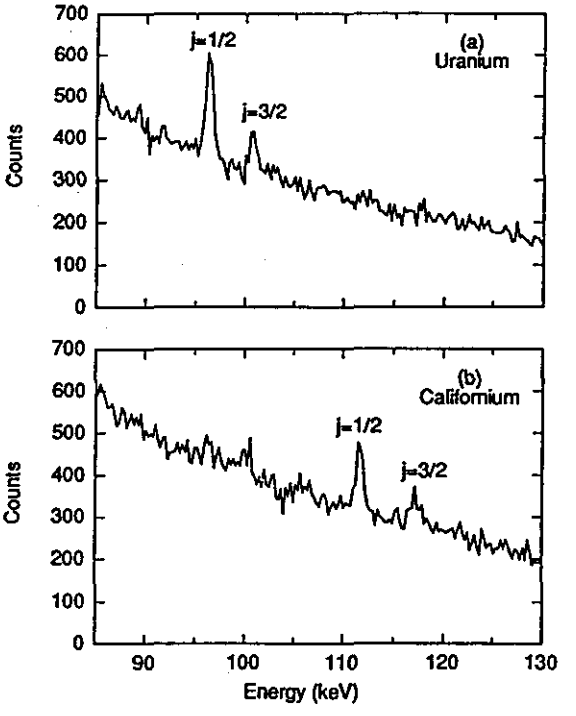

Fig. 1. X-ray spectra of (a) highly charged ^{238}U and (b) highly charged ^{249}Cf recorded with a Ge detector on SuperEBIT. The low-energy and high-energy features correspond to transitions from electrons with angular momenta j=1/2 and j=3/2, respectively. The background is caused by bremsstrahlung from the 145-keV electron beam used to produced and excite the highly charged ions.

References:

[1] S. R. Elliott, and R. E. Marrs, Nucl. Instrum. Meth. **B100**, 529 (1995).

[2] S. R. Elliott, P. Beiersdorfer, and M. H. Chen, Phys. Rev. Lett. **76**, 1031 (1996).

[3] P. Beiersdorfer, A. Osterheld, S. R. Elliott, M. H. Chen, D. Knapp, K. Reed, Phys. Rev. A **52**, 2693(1995).

This work was supported by the DOE Office of Basic Energy Sciences, Division of Chemical Sciences.

Measurements of Line Overlap for Resonant Spoiling of X-ray Lasing Transitions in Nickellike Tungsten

S. R. Elliott*, P. Beiersdorfer, B. J. MacGowan, and J. Nilsen
Lawrence Livermore National Laboratory, Livermore, CA 94551

Modification of the x-ray laser kinetics by resonant photo-pumping is of practical and scientific interest. For example, resonant photo-pumping has been proposed as an efficient way to achieve lasing. Conversely, resonant photo-pumping may be used to spoil lasing. This allows tailoring of the laser to yield monochromatic output that suits available x-ray optics. It also enables one to probe the laser kinetics and to obtain a better understanding of the underlying principles of x-ray lasing. The success of photo-pumping hinges on sufficient overlap of the emission and absorption lines as the difference of the energies of the two lines must be within the line widths determined by the plasma dynamics, such as Doppler and opacity broadening. Typically, an overlap of a few parts in 10^4 is required. Due to correlation effects, high-n levels of multi-electron ions are difficult to calculate and are reliable to roughly a part in 10^3. These differences are large enough to preclude accurate predictions of successful overlaps. As a result, precise measurements of the overlaps are needed. We have made measurements [1] of candidate resonances for spoiling of x-ray laser transitions in the nickel-like tungsten W^{46+} laser shown to lase at 43.18 Å. This lasing wavelength is within the "water window" between the carbon and oxygen K edges. As such it may be well suited for applications such as short-pulsed x-ray microscopy.

The 43-Å lasing transition proceeds from level $(3d_{3/2}^9 4d_{3/2})_{J=0}$ to level $(3d_{3/2}^9 4p_{1/2})_{J=1}$. Raising the population of the lower level will diminish or destroy the population inversion necessary for lasing and thus will spoil the 43-Å laser. This is accomplished by pumping with an appropriate pump line whose wavelength is nearly coincident with that of the dump transition from level $(3d_{3/2}^9 4p_{1/2})_{J=1}$ to the $^1S_0$ ground level. The energy of the $4p_{1/2}\rightarrow 3d_{3/2}$ dump transition was predicted by Maxon et al. to be 1728 eV, or 7.175 Å [2] and 1726 eV or 7.181 Å by Quinet and Biemont [3]. A candidate pump line is provided by the $2p_{3/2}\rightarrow 1s_{1/2}$ Ly-α_1 line in hydrogenic Al^{12+} at 7.1709 Å [4]. Other candidate pump lines are the $2p_{1/2}\rightarrow 1s_{1/2}$ Ly-α_2 line in hydrogenic Al^{12+} (predicted at 7.1763 Å [5]), the transition from $(2p_{1/2}^5 3d_{3/2})_{J=1}$ to the $^1S_0$ ground level in neonlike bromine Br^{25+} (predicted at 7.1700 Å [5]), and the transition from $(3d_{3/2}^9 4f_{5/2})_{J=1}$ to the $^1S_0$ ground level in nickellike erbium Er^{40+} (predicted at 7.1760 Å [3,6]).

The data were measured on the Lawrence Livermore National Laboratory electron beam ion trap (EBIT). Spectra are recorded with an evacuated flat-crystal spectrometer. The Lyman lines provide excellent reference lines relative to which the $4p_{1/2}\rightarrow 3d_{3/2}$ tungsten line can be measured. Setting the values of the Ly-α_1 and Ly-α_2 lines to 7.17091 and 7.17632 Å [4], respectively, we find 7.1733±0.0003 Å for the tungsten line. Similarly, we measured the wavelength of the $4f_{5/2}\rightarrow 3d_{3/2}$ transition in nickellike erbium Er^{40+} and that of the $3d_{3/2}\rightarrow 2p_{1/2}$ transition in neonlike bromine Br^{25+}. We find 7.1837±0.0013 and 7.1685±0.0002 Å, respectively.

The measured location of the candidate pump lines relative to the measured position of the $4p_{1/2}\rightarrow 3d_{3/2}$ dump transition in tungsten is shown schematically in Fig. 1b. The best resonance is found with the $2p_{3/2}\rightarrow 1s_{1/2}$ Ly-α_1 line in hydrogenic Al^{12+}. The two lines differ by 2.4±0.3 mÅ or 335 ppm. Figure 1a also gives a schematic overview of the predicted locations of the various

lines. A comparison of the predicted and measured locations illustrates the unequivocal need for precise measurements of candidate resonances.

Figure 1c shows the measured position of the lines represented by Gaussians of width similar to that expected in a 500-eV plasma. It is clear from this figure that the overlap is marginal. However this poor overlap may be improved by relative motion of the W and Al ions. Since the W line lies nearly equidistant between the Al Ly-α lines, any such motion would improve the overlap.

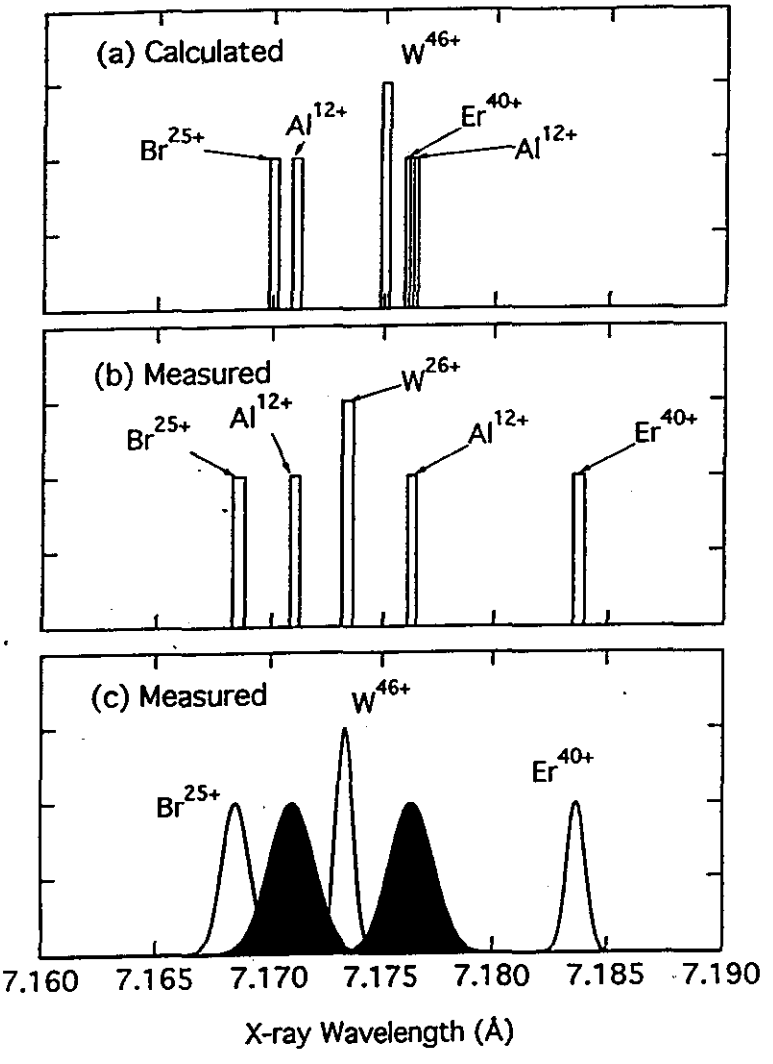

Fig. 1. Comparison of predicted (a) and measured (b) location of the 3d-4p transition in nickel-like W^{46+} anf of various candidate resonant photopumping transitions. The bars are labeled by the ion in consideration. In (c) all lines are indicated at their measured locations by Gaussians with widths equal to that expected for a 500-eV plasma.

Previous measurements implied possibly good overlap between the W line measured at 7.170(5) Å [7] and the Br line measured at 7.173(2) Å [8], and between the W line and Ly-α_1 calculated to be at 7.171 Å [4]. The present experiment improves the precision of the measured lines by more than an order of magnitude and shows that no overlap exists between the W and Br lines. In fact, among the candidate resonances investigated only two are found that are possibly sufficient to allow photo-pumping. The first is the resonance between the $2p_{3/2} \rightarrow 1s_{1/2}$ Ly-α_1 line in hydrogenic Al^{12+} and the $4p_{1/2} \rightarrow 3d_{3/2}$ transition in nickel-like tungsten W^{46+}. The two lines differ by 335 ppm, which approximately equals the Doppler broadening of the aluminum line in a 500-eV plasma. Moreover, the tungsten line differs only 420 ppm from the $2p_{1/2} \rightarrow 1s_{1/2}$ Ly-α_2 line in hydrogenic Al^{12+}, and the Ly-α_2 line may also contribute to pumping the nickel-like transition. The fact that the tungsten line lies in-between the Ly-α lines is especially important in cases where plasma motion shifts the wavelength of the tungsten line (or that of the aluminum lines). Such a shift would improve the resonance.

* Present address: Nuclear Physics Laboratory, GL-10, University of Washington, Seattle, WA 98195

References:

[1] S. R. Elliott, P. Beiersdorfer, B. J. MacGowan, and J. Nilsen, Phys. Rev. **A52**, 2689 (1995).

[2] S. Maxon, S. Dalhed, P. L. Hagelstein, R. A. London, B. J. MacGowan, M. D. Rosen, G. Charatis, G. Busch, Phys. Rev. Lett. **63**, 236 (1989).

[3] P. Quinet and E. Biemont, Physica Scripta **43**, 150 (1991).

[4] W. R. Johnson and G. Soff, At. Data Nucl. Data Tables **33**, 405 (1985).

[5] J. A. Cordogan and S. Lunell, Phys. Scr. **33** 406 (1986).

[6] J. Nilsen, Phys. Rev. A **40**, 5440 (1989).

[7] P. Mandelbaum, M. Klapisch, A. Bar-Shalom, J. L. Schwob, and A. Zigler, Physica scripta 27, 39 (1983); and A. Zigler, H. Zmora, N. Spector, M. Klapisch, J. L. Schwob, and A. Bar-Shalom, J. Opt. Soc. Am. **70**, No. 1, 129 (1980).

[8] J. F. Seely, T. W. Phillips, R. S. Walling, J. Bailey, R. E. Stewart, and J. H. Scofield, Phys. Rev. A **34**, 2942 (1986).

Measurements of the Neonlike 4d → 2p Resonance Line

Joseph Nilsen, Peter Beiersdorfer, Klaus Widmann, Vincent Decaux, and Steven R. Elliott*
Lawrence Livermore National Laboratory, Livermore, CA 94550

Neonlike ions are of considerable interest in the study of highly ionized plasmas because the closed-shell structure of their ground state makes them abundant over a wide range of densities and temperatures. They have been used for diagnostic purposes and many X-ray lasers are based on the collisional excitation of these ions. The strong nuclear field of these highly charged ions provide a perfect testbed for studying the nonperturbative aspects of relativistic and quantum electrodynamic(QED) theory, especially issues such as the correlation corrections and the electron self energy. Over the last several years many authors have studied the n = 3 excited states of high-Z Ne-like ions but only a few calculations and no high resolution measurements have been made for the n = 4 excited states. To provide an experimental benchmark for the theoretical predictions, we use EBIT to measure the n = 4 resonance lines of selected high Z ions.

Looking at the oscillator strengths of the seven n = 4 → n = 2 Ne-like lines we choose to study the strongest line, which is the $2p_{3/2}\ 4d_{5/2}$ (J = 1) → ground state transition, commonly referred to as 4D. This line has a typical oscillator strength of 0.5. Above Z = 40, there are no level crossings to perturb the systematics of calculating the energy levels.

We studied four different materials, Ba, Pr, Ir, and Pt, the first two in EBIT and the rest in Super-EBIT. The wavelengths of the Ne-like lines are determined relative to the wavelengths of Ly-α and He-α lines of the appropriate elements. A typical set of spectra showing the 4D line in Ne-like Ir and the He-α lines in krypton is shown in Fig. 1. To record the data the von Hamos spectrometer uses a LiF(200) crystal(2d=4.027 Å) bent to a radius of curvature of 30 cm and a position-sensitive proportional counter. To determine the wavelength of the 4D line in Ne-like Ir, we set the wavelength of the He-α krypton line, labeled w, to 0.945410 Å, and use the 1.705 mÅ separation between lines w and z, to establish the dispersion. Line z is the $1s2s\ ^3S_1 \rightarrow 1s\ ^1S_0$ forbidden line. We find 0.949875 Å ± 0.024 mÅ for the wavelength of the Ne-like Ir line. In a similar fashion, Table I presents the measured wavelengths and energies for line 4D for all four materials. Shown in parenthesis are the uncertainties in the last digit. Table I also presents the energy differences between theory and experiment calculated with the multi-configuration Dirac-Fock(MCDF) atomic physics code of Grant and coworkers in the extended average level(EAL) mode, using the Z-expansion(MZ) method, and using the model potential(RPTMP) method. All three methods agree well at lower Z but diverge significantly at higher Z. The experimental data shows the best agreement with our MCDF results. Given the strong Z dependence of the QED terms as compared with the rather constant difference between the MCDF calculation and the experiments, the likely difference lies with the residual electron correlation energy. A more complete description of the calculations and experiments can be found in our recent paper.[1]

---

*Present address:*Department of Physics, University of Washington, Seattle, WA 98195*

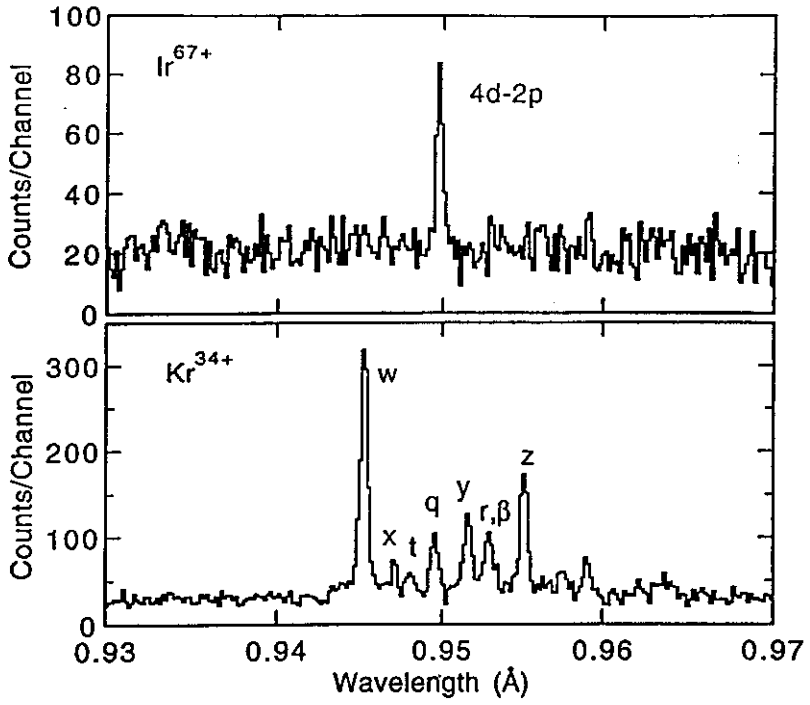

Fig. 1. Top: spectrum of neonlike iridium showing the 4D line. Bottom: spectrum of heliumlike krypton. The heliumlike lines are denoted w, x, y, and z and are used as reference lines. Transitions in lithiumlike krypton (t, q, r), berylliumlike krypton (β), and boronlike krypton (unlabeled) are also seen.

Table I. Measured wavelengths and energies (in units of 10^4 cm^{-1}) of the Ne-like $2p_{3/2}$ $4d_{5/2}$ ($J = 1$) → ground state transition, referred to as 4D. The uncertainties in the last digit are given in parenthesis. Also given are the energy difference ΔE (in units of 10^4 cm^{-1}) between the MCDF, RPTMP, and MZ codes and the measured energy.

Z	Wavelength (Å)	E_{expt}	ΔE_{MCDF}	ΔE_{RPTMP}	$\Delta E_{MZ\_}$
56 (Ba)	1.93028(10)	5180.60(27)	-0.82	0.91	0.08
59 (Pr)	1.71634(3)	5826.35(10)	-0.68	0.99	0.55
77 (Ir)	0.949875(24)	10527.70(27)	-0.85		6.0
78 (Pt)	0.923286(36)	10830.88(42)	-0.58		6.9

References

1. J. Nilsen, P. Beiersdorfer, K. Widmann, V. Decaux, and S. R. Elliott, "*Energies of neonlike n = 4 to n = 2 resonance lines,*" Physica Scripta **54**, 183-187 (1996).

Measurement of the 3.92-ms Radiative Lifetime of the 1s2s $^3S_1$ Level in Heliumlike N^{5+} in the Magnetic Trapping Mode

J. Crespo López-Urrutia, P. Beiersdorfer, K. Widmann
Lawrence Livermore National Laboratory, Livermore, CA 94550

Measurements of the radiative lifetimes of long-lived excited levels in multiply charged ions are of fundamental atomic physics interest, as they provide empirical input to complex structure calculations. They are also of great interest to plasma diagnostics, especially in astrophysics, where transitions from long-lived metastable levels are used to provide electron density information. Measurements have been performed with a variety of different trapping methods. These include the use of Penning, Paul, or Kingdon traps, where multiply charged ions are captured after being produced in electron cyclotron or electron beam ion sources [1] and the use of ion storage rings [2].

The utility of EBIT for measuring radiative lifetimes has been demonstrated in measurements of the 91.5-μs lifetime of the $^3S_1$ level in heliumlike neon [3] and the 13.6-μs lifetime of the $^3S_1$ level in heliumlike magnesium [4]. The technique we employed in these measurements relied on modulating the energy of the electron beam, above and below the excitation threshold of the $^3S_1$ level, and determining the lifetime of the metastable $^3S_1$ level from its fluorescent decay while the beam energy was below threshold. For measuring the lifetime of the $^3S_1$ level in heliumlike nitrogen we developed and successfully demonstrated a new technique for measuring lifetimes of metastable levels [5]. While the earlier method relied on modulating the electron beam energy, the method employed in measuring nitrogen relied on modulating the electron beam current, i.e., by switching between the electron trapping mode, where the electron beam is on, and the magnetic trapping mode, where the electron beam is off.

Our measurement was performed by producing N^{5+} in the electron trapping mode at a beam energy of 700 eV. This energy is well above the threshold for exciting the heliumlike $n=2 \rightarrow n=1$ transitions, including excitation of the $^3S_1$ level. The production of these K-shell x-rays, which have energies near 460 eV, was recorded with a windowless SiLi detector, as shown in Fig. 1. We then switched to the magnetic trapping mode. The K-shell x-ray intensity dropped precipitously, as collisional excitation ceased . The signal intensity then drops exponentially, as is evident in Fig. 1. The exponential decay takes place with a decay time of 3.92±0.13 ms and equals the radiative decay of the $^3S_1$ level.

The radiative lifetime of N^{5+} measured is over forty times longer than the longest radiative lifetime measured on EBIT before employing the electron trapping mode. It thus demonstrates the utility of the magnetic trapping mode, first discovered and analyzed in Fourier-transform ion cyclotron resonance measurements on EBIT [6]. Since ions in this mode remain trapped for seconds [5], measurements of yet much longer radiative lifetimes appear possible.

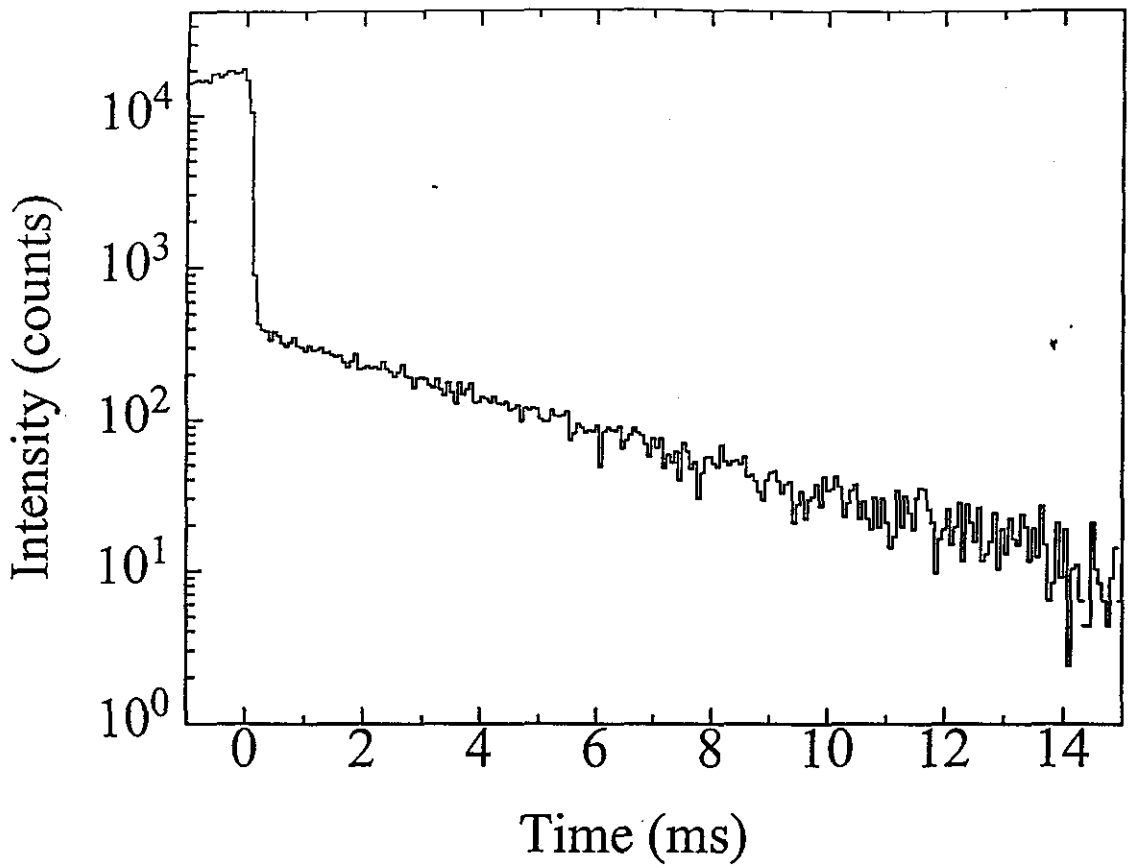

FIG. 1. Evolution of the n=2 → n=1 x-ray emission from N^{5+} as the mode of operation of EBIT is switched from the electron trapping mode to the magnetic trapping mode at t = 0 ms. The exponential decay of the x-ray signal is caused by the radiative decay of the metastable $1s2s\ ^3S_1$ level in heliumlike nitrogen.

References:

[1] L. Yang and D. A. Church, Phys. Rev. Lett. **70**, 3860 (1993).

[2] H. T. Schmidt, P. Forck, M. Grieser, D. Habs, J. Kenntner, G. Miersch, R. Repnow, U. Schramm, T. Schüssler, D. Schwalm, and A. Wolf, Phys. Rev. Lett. **72**, 1616 (1994).

[3] B.J. Wargelin, P. Beiersdorfer, and S.M. Kahn, Phys. Rev. Lett. **71**, 2196 (1993).

[4] G. S. Stefanelli, P. Beiersdorfer, V. Decaux, K. Widmann, Phys. Rev. A **52**, 3651 (1995).

[5] P. Beiersdorfer, L. Schweikhard, J. Crespo López-Urrutia, and K. Widmann, Rev. Sci. Instrum. (in press).

[6] P. Beiersdorfer, B. Beck, R. E. Marrs, S. R. Elliott, and L. Schweikhard, Rapid commun. Mass Spectrom. **8**, 141 (1994).

This work was supported by the NASA X-Ray Astronomy Research and Analysis Program under grant NAGW-4185.

II. Spectral Diagnostics for High Temperature Laboratory and Astrophysical Plasmas

Iron K-shell emission from ionizing plasmas

V. Decaux, P. Beiersdorfer
Lawrence Livermore National Laboratory, Livermore, CA 94551
S. M. Kahn
Columbia University, New York, NY 10027
V. L. Jacobs
Naval Research Laboratory, Washington, D. C. 20375

Transient ionization conditions play an important role in astrophysical plasmas, as in the shock-front-heated regions of young supernova remnants or impulsively heated gas in solar flares. For these cases, as pointed out by Mewe and Schrijver [1], the establishment of ionization balance lags behind the sudden increases in electron temperature, which dramatically affects the emitted X-ray spectra. Integrating over time, Kα emission from all existing charge states of iron (Fe I - Fe XXVI) can be observed. This is in sharp contrast to the more traditional situation found in plasmas for which collisional ionization equilibrium has been established, where the Kα spectrum is known to be dominated by the emission from Fe XXV and Fe XXVI, since K-shell transitions cannot be excited at the lower electron temperatures where the less ionized species are prevalent. Also, while dielectronic recombination (DR) is usually the dominant line formation process in equilibrium plasmas with a Maxwellian electron distribution, this process plays only an insignificant role in ionizing plasmas.

During the past few years, we have performed a laboratory simulation of X-ray line formation under transient ionization conditions, using the Livermore Electron Beam Ion Trap (EBIT). Our early efforts focused on the lowest ionization stages Fe X - Fe XVII [2]. During the past year, we focused on the intermediate charge states Fe XVII - Fe XXV [3]. Since our spectral resolution ($\lambda/\Delta\lambda \geq 2000$) exceeds that of present and near-future satellite measurements (the resolution of EBIT is about three times better than that of ASTRO-E), our measurements are well suited to serve as benchmarks for detailed models of transient ionization in astrophysical plasmas, which have not previously been tested to this level of accuracy. The electron density in EBIT is similar to the electron density of solar flares, which is on the order of 10^{11} - 10^{12} cm^{-3}. We measured in our experiment the transient spectral structure as a function of time, at a beam energy of 12 keV and in the wavelength range from 1.84 - 1.94 Å, in which the Kα emission features of the charge states Fe XVIII - Fe XXV are prominent. The first three spectra, recorded in the intervals 0-20 ms, 20-40 ms, and 40-60 ms after injection of iron into EBIT, are shown in Fig. 1. These measurements provide the first experimental validation of the theoretical predictions of Mewe and Schrijver [1], with which good overall agreement is found.

Focusing on the charge states Fe XVII - Fe XXI, we compared the experimental data with a complete theoretical model including all relevant excitation mechanisms; we were able to deduce from our spectroscopic data the ionization time $\eta = N_e t$, where N_e is the electron density and t is the time measured from the beginning of the ionization process [3]. This quantity is of fundamental importance and is the principal parameter used to characterize ionizing plasmas. In the case of supernova remnants, where the time since the explosion is known, the value of the density N_e can be inferred, if the parameter η is determined spectroscopically. As a result of the good agreement between the experimental and theoretical results for spectral line ratios within each charge state, we were able to reproduce accurately the experimental data by adjusting only the charge-state population fractions. For the case of the charge states Fe XVII - Fe XXI, the result of this fit to the experimental data was compared to the result of a theoretical

time-dependent charge-state balance model. This is shown in Fig. 2, where the results of this comparison (evaluated as the sum of the squared differences between the calculated and measured charge-state population fractions) is plotted against values of the assumed electron density in the range from $1 - 3 \times 10^{12}\text{cm}^{-3}$ (or, equivalently, η because t is known in our measurements). We were then able to determine the value of N_e for which the model result is in best agreement with the experimentally-determined charge-state population fractions. Figure 2 shows that the best agreement is found for $N_e = 1.7 \pm 0.3 \times 10^{12}\text{cm}^{-3}$, in excellent accord with the empirical estimate of $1.5 \times 10^{12}\text{cm}^{-3}$ obtained from the known beam current density (5300 A cm^{-2}) and beam energy (12 keV) in our experiment on EBIT. Our 20% accuracy in the spectroscopic determination of N_e (or η) implies that the ionization timescale and thus the age of a given supernova remnant can be inferred from spectral observations with similar accuracy, provided that the same level of statistics and spectral resolution can be achieved in such measurements.

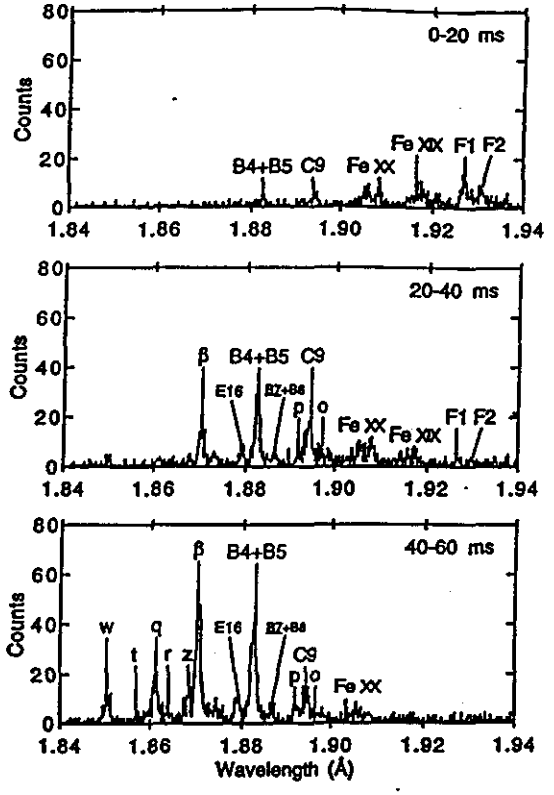

Figure 1: K-shell spectra of iron in the region 1.84-1.94 Å recorded at a beam energy of 12 keV in the intervals 0-20 ms, 20-40 ms, and 40-60 ms after injection of iron into EBIT.

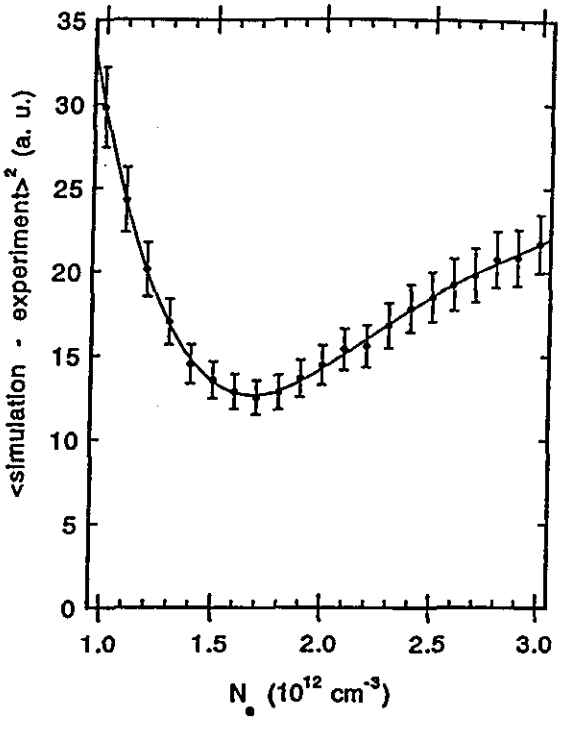

Figure 2: Sum of the squared differences between the calculated and measured charge-state population fractions as a function of the assumed electron density.

References:

[1] R. Mewe and J. Schrijver, A & A 87, 261 (1980).

[2] V. Decaux, P. Beiersdorfer, A. Osterheld, M. Chen, and S. M. Kahn, ApJ 443, 464 (1995).

[3] V. Decaux, P. Beiersdorfer, S. M. Kahn, and V. L. Jacobs, ApJ (to be published).

This work was supported by NASA's X-Ray Astronomy Research and Analysis Program under grant NAGW-4185.

The First on–line EBIT Plasma Measurement with a Microcalorimeter

M. Le Gros, E. Silver
Smithsonian Astrophysical Observatory, Boston, MA 02138

P. Beiersdorfer, J. Crespo López–Urrutia, K. Widmann
Lawrence Livermore National Laboratory, Livermore, CA 94550

S. Kahn
Columbia University, NY 10027

To make the greatest use of the improved spectroscopic capabilities of the AXAF, ASTRO-E, XMM, and other future x–ray astronomy missions, better knowledge of fundamental atomic properties are needed. The spectra that have been obtained from such missions as ASCA and DXS have revealed deficiencies in the current plasma codes. The dependence of key diagnostic x–ray lines on density, temperature, and excitation conditions that exist in astrophysical sources is important input to improving the plasma codes. The EBIT provides a unique capability for measuring atomic structure and cross sections in the isolated–ion limit, and for efficiently expanding the experimental data base of atomic energy levels, oscillator strengths and transition cross–sections.

The microcalorimeter is the ideal spectrometer for the EBIT–type plasma. Briefly, the efficiency of the microcalorimeter will greatly shorten the measurement time by several orders of magnitude compared to the integration time required by crystal spectrometers whose efficiencies are about 0.1%. The microcalorimeter will simultaneously obtain the required spectra for all of the relevant spectral components identified above. An important feature of the microcalorimeter is that it is insensitive to the polarization of the x–ray emission.

In our recent verification experiment, we produced both He–like and Ne–like Fe plasmas. For normalization purposes, the EBIT incorporates a 200 mm^2 germanium detector placed 20 cm from the plasma as a monitor. The count rate of 2×10^3 Hz measured by this detector indicated that the x–ray emission of the EBIT was about 5×10^6 Hz into 4π. Given the geometrical constraints of the EBIT environment at the time of this experiment, we were only able to field a single pixel detector with an area of 0.25 mm^2, 1.5 m from the EBIT plasma. Consequently, the microcalorimeter count rate was only about 50 counts per hour. Even at this low rate, we have successfully obtained the first microcalorimeter spectrum of He–like iron (Fe XXV); the instrument has almost zero background. This is shown in Figure 1. To produce these x–rays, the electron excitation energy was 9 keV. Changing the plasma conditions and reducing the excitation energy to 2 keV permitted us to measure the Ne–like L x–rays, also shown in Figure 1.

These experiments demonstrate the great utility of our microcalorimeter as a high-resolution spectrometer on EBIT, initiating a new era in high-resolution laboratory spectroscopy for astrophysics. We are developing a dedicated multi–channel instrument to perform extensive follow–on experiments. This new instrument will have sub-10eV energy resolution and a total detector area of 2 mm^2.

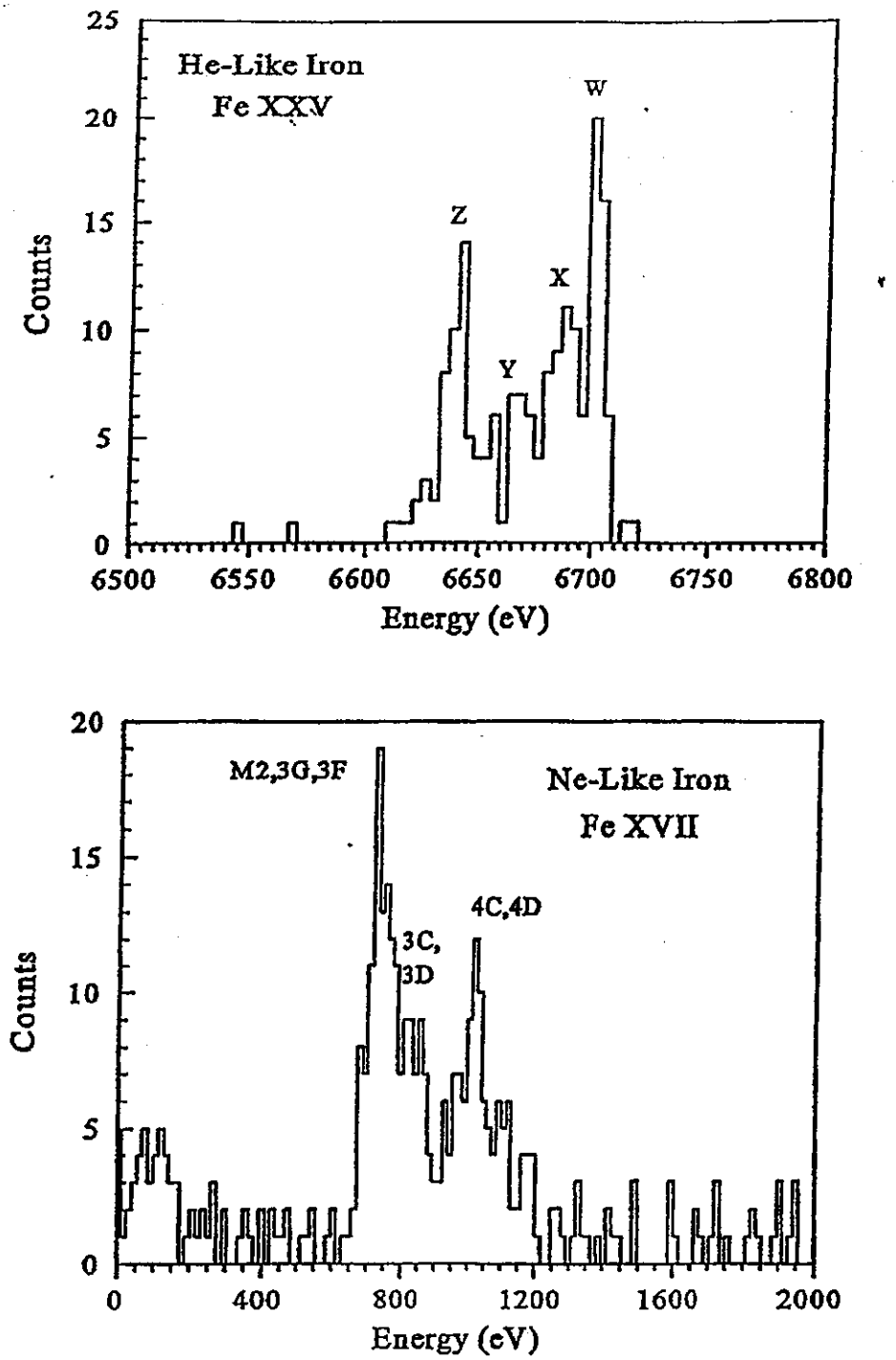

Fig. 1. The first laboratory spectrum of heliumlike Fe XXV and Fe XVII made with a microcalorimeter.

The EBIT-related portion of this work was supported by the NASA X-Ray Astronomy Research and Analysis Program under grant NAGW-4185.

Fe XXIV Line Emission Produced by Electron Impact Excitation

D. W. Savin
Space Sciences Laboratory, University of California, Berkeley, CA 94720
P. Beiersdorfer, J. Crespo López-Urrutia, V. Decaux, D. A. Liedahl, K. J. Reed, K. Widmann
Livermore National Laboratory, Livermore, CA 94550
S. M. Kahn
Department of Physics, Columbia University, New York, NY 10027.

Recent Advanced Satellite for Cosmology and Astrophysics (ASCA) observations in the 0.7-2.0 keV spectral band have revealed major discrepancies between spectroscopic data from cosmic X-ray sources and model predictions using standard plasma emission codes [1-3]. These discrepancies appear to indicate the existence of errors in the atomic data used in the plasma emission codes. This is most clearly demonstrated in the observation by Fabian et al.[1] of the cooling flow in the Centaurus cluster of galaxies. Cooling flows are optically thin, quasi-static plasmas, with no significant radiative transfer or transient effects, and are believed to be the simplest class of cosmic X-ray sources. Thus, the discrepancies reported by Fabian et al. indicate errors in the atomic data, and for their observations have been attributed to errors in the Fe XXIII and XXIV electron impact excitation (EIE) rate coefficients [4].

To address this issue we have carried out a series of broadband, high resolution measurements of Fe XXIV n=n' → n=2 line emission (hereafter, n' → 2). Using EBIT, we have measured EIE generated 3 → 2 and 4 → 2 line emission from Fe XXIV initially in the ground level. In specific, we have carried out line ratio measurements for the 3p $^2P_{3/2}$ → 2s $^2S_{1/2}$, 3d $^2D_{5/2}$ → 2p $^2P_{3/2}$,and the 4p $^2P_{3/2,1/2}$ → 2s $^2S_{1/2}$ transitions all relative to the 3p $^2P_{1/2}$ → 2s $^2S_{1/2}$ transition (hereafter, 3 $^2P_{3/2}$ - 2 $^2S_{1/2}$, 3 $^2D_{5/2}$ - 2 $^2P_{3/2}$, 4 $^2P_{3/2,1/2}$ - 2 $^2S_{1/2}$, and 3 $^2P_{1/2}$ - 2 $^2S_{1/2}$, respectively).

Two flat crystal spectrometers (FCSs) have been used to detect X rays from EBIT[5]. Representative iron 3 → 2 and 4 → 2 spectra collected for the present results are shown in Figs. 1a and 1b. The spectra were collected using a thallium hydrogen phthalate crystal in first order. The spectra consist entirely of lines of Fe XXII, XXIII, and XXIV[6,7].

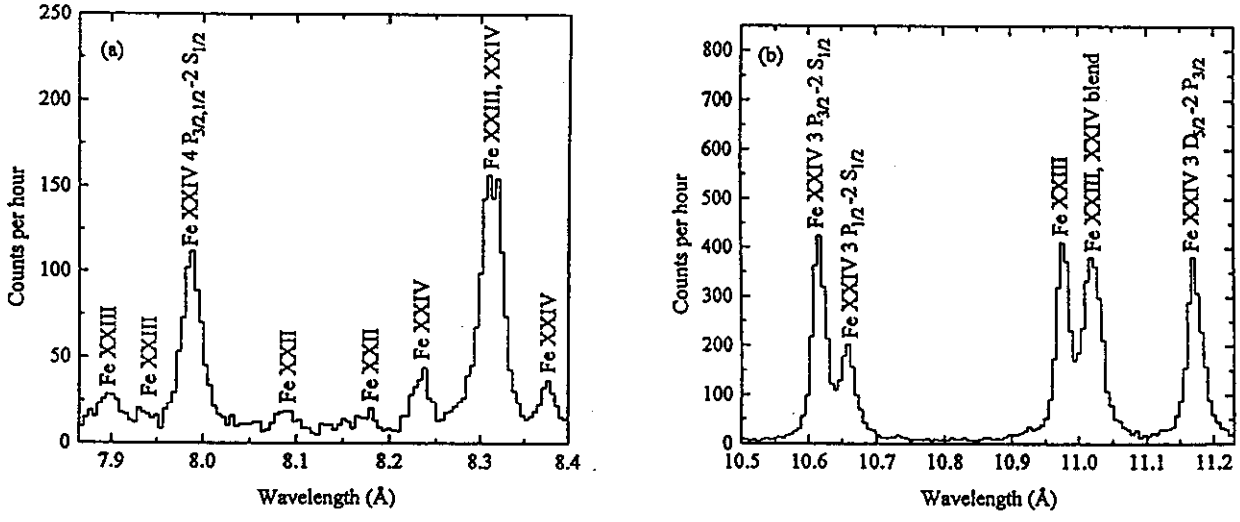

Figure 1: (a) Fe XXIV 4 → 2 spectrum at an electron beam energy of 4500 eV recorded for 155 min; (b) Fe XXIV 3 → 2 spectrum at an electron beam energy of 4500 eV recorded for 155 min.

FCSs are inherently narrowband devices. The Fe XXIV $3\ ^2P_{3/2} - 2\ ^2S_{1/2}$, $3\ ^2P_{1/2} - 2\ ^2S_{1/2}$, and $3\ ^2D_{5/2} - 2\ ^2P_{3/2}$ all lie close together in wavelength and may be simultaneously observed using a single FCS. The Fe XXIV $4\ ^2P_{3/2,1/2} - 2\ ^2S_{1/2}$ and $3\ ^2P_{1/2} - 2\ ^2S_{1/2}$ lines lie far apart in wavelength. Broadband measurements are carried out using 2 FCSs to observe simultaneously different narrowband regions (each containing lines of interest). The broadband X-ray detection efficiency for one of the FCSs was measured absolutely. The second FCS was then cross-calibrated to the first FCS for detection of the $3\ ^2P_{1/2} - 2\ ^2S_{1/2}$ reference line. The dominant uncertainty in all line ratio measurements is attributed to a combination of counting statistics, background level determination, line blending, and line shape determination.

Predicted line ratios have been calculated using the fully relativistic distorted wave (RDW) code of Zhang, Sampson & Clark[8] and the quasi-relativistic distorted wave Hebrew University-Lawrence Livermore Atomic Code (HULLAC)[9,10]. The $(3\ ^2P_{3/2} - 2\ ^2S_{1/2})/(3\ ^2P_{1/2} - 2\ ^2S_{1/2})$ and $3\ ^2D_{5/2} - 2\ ^2P_{32})/(3\ ^2P_{1/2} - 2\ ^2S_{1/2})$ line ratios predicted by RDW and by HULLAC all lie within 1σ of the measured values. The measured $4\ ^2P_{3/2,1/2} - 2\ ^2S_{1/2})/(3\ ^2P_{1/2} - 2\ ^2S_{1/2})$ line ratio at 4.5 keV was 0.492 ± 0.074. The quoted uncertainty represents the total experimental uncertainty at a confidence level believed to be equivalent to a 1σ statistical confidence level. The line ratios predicted by RDW and by HULLAC are 0.409 and 0.386, respectively, and lie within 1.1σ and 1.4σ of the measured value, respectively. This is within the 90% confidence limits (1.65σ) of the measurement. Overall, we find good agreement between our measurements and the RDW and HULLAC calculations[11].

The importance and need of accurate atomic data for modeling cosmic X-ray sources has now been demonstrated observationally[1-3], theoretically[4], and experimentally[11]. The importance and need will become even more apparent after the planned launches of the Advanced X-ray Astrophysics Facility, the X-ray Multimirror Mission, and ASTRO-E. Fe XXIV is a relatively easy system for theoretical calculations. Other Fe L-shell ions possess two or more electrons in their L-shell and line emission from these ions is expected to be more challenging to calculate accurately. EBIT experiments can provide benchmark measurements for these more challenging calculations. With EBIT we plan to carry out further broad-band, high resolution measurements of Fe L-shell line emission.

References:

[1] A. C. Fabian et al., Astrophys. J. **436**, L63 (1994).
[2] S. A. Drake et al., Astrophys. J. **436**, L87 (1994).
[3] N. E. White et al., Pub. Astron. Soc. Japan **46**, L97 (1994).
[4] D. A. Liedahl, A. L. Osterheld, & W. H. Goldstein, Astrophys. J. **438**, L115 (1995).
[5] P. Beiersdorfer and B. J. Wargelin, Rev. Sci. Instrum. **65**, 13 (1994).
[6] R. L. Kelly, J. Phys. Chem. Ref. Data, **16**, Suppl. 1 (1987).
[7] B. J. Wargelin et al. (in preparation).
[8] H. L. Zhang, D. H. Sampson, and R. E. H. Clark, Phys. Rev. A **41**, 198 (1990).
[9] M. Klapisch et al., J. Opt. Soc. Am. **67**, 148 (1977).
[10] A. Bar-Shalom, M. Klapisch, and J. Oreg, Phys. Rev. A **38**, 1773 (1988).
[11] D. W. Savin, P. Beiersdorfer, J. Crespo López-Urrutia, V. Decaux, E. M. Gullikson, S. M. Kahn, D. A. Liedahl, K. J. Reed, and K. Widmann, Astrophys. J. (in press).

This work was supported by the NASA High Energy Astrophysics X-Ray Astronomy Research and Analysis grant NAGW-4185.

Forbidden optical lines in highly charged ions

José R. Crespo López-Urrutia, P. Beiersdorfer, K. Widmann, and V. Decaux
Lawrence Livermore National Laboratory, University of California,
P.O. Box 808, Livermore, CA 94551

Many forbidden transitions in highly charged ions produced in an electron beam ion trap (EBIT) have wavelengths in the visible range. They can be used as diagnostic tools in high temperature plasmas, allowing for the identification of ionic species and their densities and temperatures. Advantages compared to x-ray diagnostics include large collection efficiencies, good spectral resolution, possible implementation of laser fluorescence methods and the use of optical fibers for remote, gamma radiation insensitive control of plasma devices. Previous work in tokamaks and other plasma sources was limited to ions comparatively low charge states, and the data analysis was often hindered by the difficult identification of the radiating species in the plasma. Collisional quenching and Stark broadening also limit the observability of lines in the visible range in those plasmas. In contrast, lines with transition rates on the order of ms up to fractions of a second are not collisionally depopulated in EBIT, because of the low collision frequency within the trap. With its well-defined ion charge balance and selectivity and the capability of exciting the ions with monoenergetic electrons, EBIT offers a superior tool for studies in the visible range. We have set up an apparatus for spatially resolved visible spectroscopy of the trap region in Super-EBIT (Fig. 1). A cryogenically cooled CCD with an appropriate imaging objective was used. It allows simultaneous measurement of the whole visible spectrum or part of it (see Fig. 2 for an example). As a first application, we have studied the trap geometry, the cooling gas injection mechanism and the spatial distribution of charged states within the trap [1]. As seen in Fig. 3, two regions appear clearly distinguishable: (a) the trap between the upper and lower drift tubes, where the highly charged ions are stored, and (b) the crossing of the electron beam with the ballistic atomic beam of the cooling gas injector, comprising the central portion of the trap. The central region of the trap (3 mm) displayed atomic lines from the cooling gas with narrow spatial profile. The trapped ions are stored in a longer (20 mm) and wider cylinder (≈ 300 μm diameter). The lines that appear in this region are

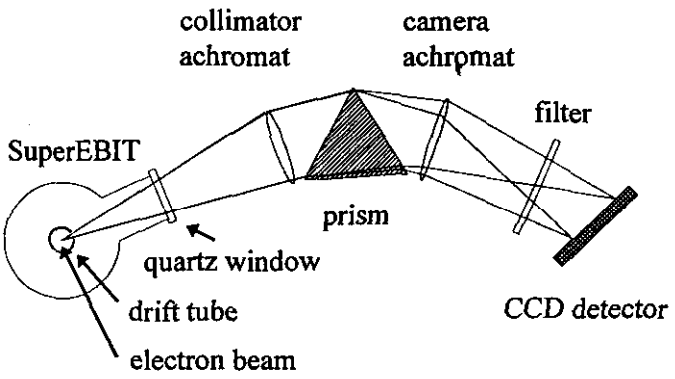

Figure 1. Stigmatic spectrograph arrangement.

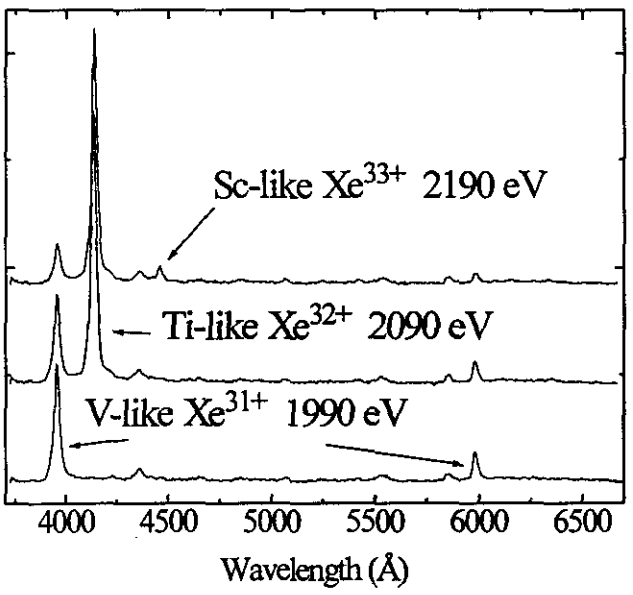

Figure 2. Spectra of Xe at different electron beam energies.

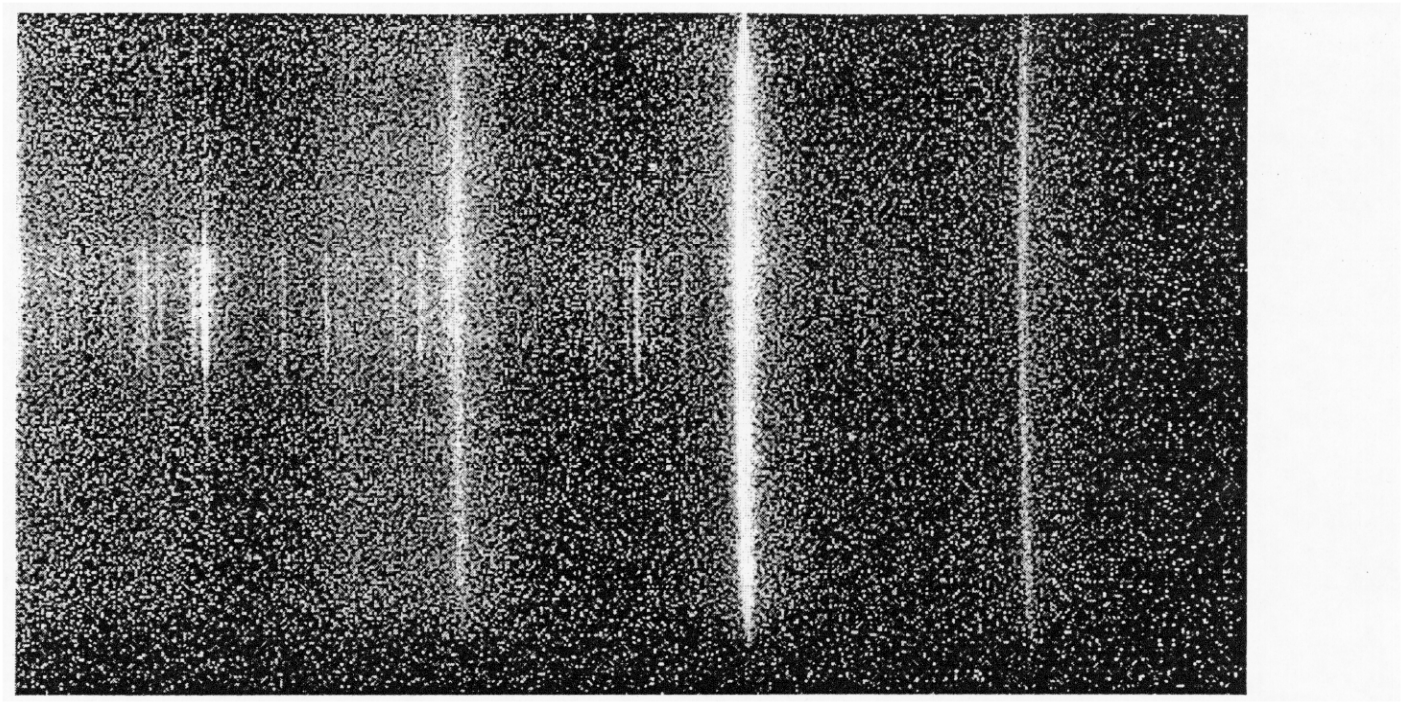

Figure 3. Spatially resolved spectrum of the trap. Neutral Xe atoms from the gas injector cross the narrow electron beam (70 μm) at the center region (5 mm), are excited and decay by fast optical transitions (t ≈ ns) immediately. Some of them are ionized and remain tied in the potential well of the electron beam, filling the whole trap length (20 mm). Their metastable levels decay slowly (t ≈ ms); the forbidden lines display source broadening corresponding to the high ion temperature and spatial radial spread.

mostly M1 transitions of high-Z ions with $3d^n$ configurations and mid-Z ions with $2p^m$ configurations (Fig. 2).

We have observed, among other, the forbidden lines in the visible spectrum of highly charged Fe, Ar, Cl, Mg, and lines from Ne, O, N, C ions excited with electrons in the energy range 150 eV-150 keV. We reproduced the experiments performed at the NIST EBIT [2] with Xe and Ba, extending the spectral coverage, the resolution and the observed charge states. The analysis and interpretation of the data are in progress. Possible applications include diagnostics of magnetic plasma devices and interpretation of astrophysical data.

References

[1] "Optical Diagnostics of highly charged ions in Super-EBIT", ICPEAC 1995, Whistler, BC, Canada
[2] C. A. Morgan et al., Phys. Rev. Lett. 74, N10, 1716 (1995)

High-Resolution Measurement, Line Identification, and Spectral Modeling of the Kβ Spectrum of Heliumlike Ar^{16+}

P. Beiersdorfer, A. Osterheld, T.W. Phillips
Lawrence Livermore National Laboratory, Livermore, CA 94551
M. Bitter, K.W. Hill, S. von Goeler
Princeton Plasma Physics Laboratory, Princeton, NJ 08543

K-shell x-ray spectra involving transitions from levels with principal quantum number n=3 to levels with n=1, so-called Kβ spectra, are important spectral diagnostics of laser-produced plasmas [1,2]. The spectra are used for inferring the electron density and temperature of high-density plasmas generated in the core of imploding target capsules employed in inertial confinement fusion (ICF) research, as well as for determining the mixing of pusher and fuel materials. For measurements of the fuel density and temperature, argon has been the element of choice because it is readily incorporated as a dopant (≤ 0.2%) in the deuterium fuel and because heliumlike Ar^{16+} is copiously produced in plasmas generated at present-generation ICF facilities such as the NOVA laser facility [2]. The electron density of the fuel is inferred from the stark-broadened profile of the Kβ emission of heliumlike Ar^{16+}, which in contrast to the Kα or Ly-α emission from heliumlike Ar^{16+} or hydrogenlike Ar^{17+}, respectively, is optically thin [1,2]. The fuel temperature is determined from the ratio of the Kβ and Ly-β emission from Ar^{16+} and Ar^{17+}, respectively [2], or from the line shape of the Ar^{16+} Kβ emission including neighboring dielectronic satellites from Ar^{15+} [3]. The diagnostic use of Kβ spectra for such high-density plasma sources requires reliance on theoretical atomic physics parameters such as line positions, dielectronic resonance strengths, electron-impact excitation and radiative rates. In order to infer the electron density from Kβ emission of heliumlike Ar^{16+} it is necessary, for example, to account for overlap with the emission from lithiumlike Ar^{15+} [3,4]. In particular, lithiumlike satellite transitions of the type $1s2\ell3\ell' \rightarrow 1s^2 2\ell$ and $1s3\ell3\ell' \rightarrow 1s^2 3\ell$ need to be taken into account. These satellite transitions broaden the heliumlike Kβ emission feature and would result in an overestimate of the density if ignored in modeling calculations [2-4]. A test of the atomic data is desirable to ascertain the reliability of the modeling calculations. Such a test can be accomplished by measuring spectra from plasmas with well-defined temperature and density, especially if non-spectroscopic methods are used to determine temperature and density.

We have performed a detailed analysis of the Kβ spectrum of heliumlike Ar^{16+} recorded with a high-resolution crystal spectrometer on the Princeton Large Torus (PLT) tokamak [5]. PLT plasmas are well diagnosed by non-spectroscopic techniques. The peak electron temperature is about 2.3 keV; the peak electron density does not exceed 2×10^{13} cm^{-3}. The spectral measurements thus tested atomic theory in the low-density, so-called collisionless, limit. While a large numbers of tokamak measurements of the n=2 to n=1 K-shell transitions have been reported, this is only the second such measurement for the n=3 to n=1 K-shell transitions, following our earlier paper on the the Kβ spectrum of Fe^{24+} recorded on the TFTR tokamak [6].

Our measurements included the positions and strengths of the $1s2\ell3\ell' \rightarrow 1s^2 2\ell$ and $1s3\ell3\ell' \rightarrow 1s^2 3\ell$ lithiumlike satellite lines populated by dielectronic recombination as well as transitions of the type $1s2\ell3\ell' \rightarrow 1s^2 2\ell$ excited by electron collisions. They also include satellite lines in

berylliumlike Ar^{14+} of the type $1s2\ell2\ell'3\ell'' \rightarrow 1s^22\ell2\ell'$, as illustrated in the spectrum in Fig. 1. Calculated and measured line positions are generally in good agreement differing no more than ± 2 mÅ.

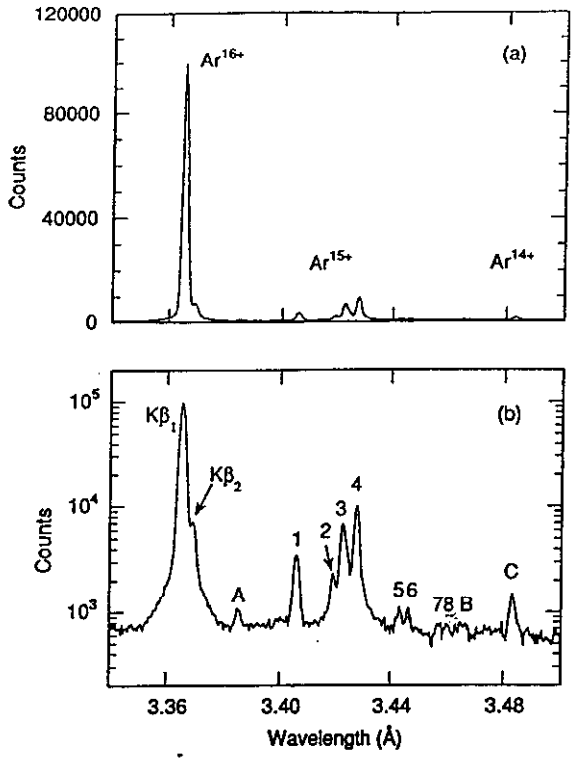

Fig. 1. Kß spectrum of argon: (a) linear, (b) logarithmic scale. The positions of features from heliumlike Ar^{16+}, lithiumlike Ar^{15+}, and berylliumlike Ar^{14+} are marked in (a). Individual features are labeled in (b) according to the notation used in Ref. [5]. The data were accumulated from 23 discharges.

A detailed comparison of the measured argon spectrum with theoretical data was made and good agreement is obtained for the intensity of most dielectronic satellite transitions. The intensity of the dielectronic satellite lines relative to lines excited by electron impact is sensitive to the electron temperature. The temperature inferred from most ratios, involving either lithiumlike or berylliumlike dielectronic satellite lines, agreed within experimental uncertainties with the electron temperature determined by non-spectroscopic means. The good agreement demonstrates that the Kβ emission from heliumlike ions can be used as a reliable electron temperature diagnostic for low-density plasmas, including to those of solar flares and the solar corona.

An exception to the good agreement was given by the $1s3\ell3\ell'$ lithiumlike satellites. These were found to be 50% stronger than predicted. Moreover, we found that intensity estimates based solely on the electron-impact excitation of the heliumlike 1s3p levels underestimate the $K\beta_2$: $K\beta_1$ line ratio by nearly a factor of two relative to the measured value, as illustrated in Fig. 2. Follow-up measurements to address these issues that are especially important in the analysis of high-density plasmas are in progress on EBIT.

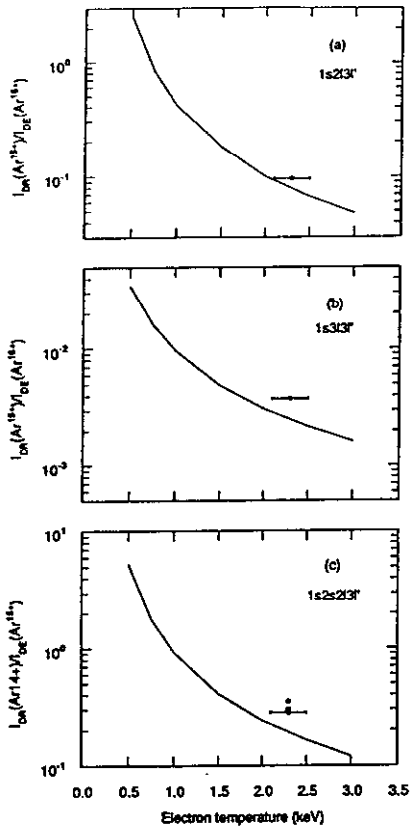

Fig. 2. Predicted temperature dependence of the relative intensities of the heliumlike Kß lines and comparison with the measured value. The predicted intensites are based on the relative collisional excitation rates only and do not include cascade contributions or blends with high-n satellites.

References:

[1] A. Hauer, K. B. Mitchell, D. B. van Hulsteyn, T. H. Tan, E. J. Linnebur, M. Mueller, P. C. Kepple, and H. R. Griem, Phys. Rev. Lett. **45**, 1495 (1980); B. Yaakobi, S. Skupsky, R. L. McCrory, C. F. Hooper, H. Deckman, P. Bourke, and J. M. Soures, Phys. Rev. Lett. **44**, 1072 (1980); J. D. Kilkenny, Y. Lee, M. H. Key, and L. G. Lunney, Phys. Rev. A **22**, 2746 (1980).

[2] B. A. Hammel, C. J. Keane, D. R. Kania, J. D. Kilkenny, R. W. Lee, R. Pasha, R. E. Turner, and N. D. Delameter, Rev. Sci. Instrum. B, 5017 (1992); B. A. Hammel, C. J. Keane, M. D. Cable, D. R. Kania, J. D. Kilkenny, R. W. Lee, and R. Pasha, Phys. Rev. Lett. **70**, 1263 (1993); B. A. Hammel, C. J. Keane, T. R. Dittrich, D. R. Kania, J. D. Kilkenny, R. W. Lee, and W. K. Levedahl, **51**, 113 (1994).

[3] C. J. Keane, B. A. Hammel, D. R. Kania, J. D. Kilkenny, R. W. Lee, A. L. Osterheld, L. J. Suter, R. C. Mancini, C. F. Hooper, Jr., and N. D. Delameter, Phys. Fluids B **5**, 3328 (1993).

[4] R. C. Mancini, C. F. Hooper, N. D. Delameter, A. Hauer, C. J. Keane, B. A. Hammel, and J. K. Nash, Rev. Sci. Instrum. **63**, 5119 (1992).

[5] P. Beiersdorfer, A. L. Osterheld, T. W. Phillips, M. Bitter, K. W. Hill, and S. von Goeler, Phys. Rev. E **52**, 1980 (1995).

[6] A. J. Smith, M. Bitter, H. Hsuan, K. W. Hill, S. von Goeler, J. Timberlake, P. Beiersdorfer, and A. Osterheld, Phys. Rev. A **47**, 3073 (1993).

III. Ion/Surface Interaction Studies

Neutralization of Slow Highly Charged Ions in Thin Carbon Foils

T. Schenkel[1,2], M. A. Briere[3], D. H. Schneider[1]

[1] Lawrence Livermore National Laboratory

[2] J. W. Goethe University Frankfurt, Germany

[3] presently at: Physics Dept., Univ. of Rhode Island, S. Kingston, RI

One of the key question in highly charged ion (HCI) solid interaction studies is that of the time scale for neutralization and de-excitation of HCI in solids. An understanding of how long it takes to dissipate tens to hundreds of keV of neutralization energy is crucial in the development of HCI based materials analysis and modifications techniques, since it is this neutralization time that defines the available energy density in any given HCI - solid interaction system.

We have analyzed the charge states of O^{7+}, Ar^{16+}, Ar^{18+}, Kr^{33+}, and Th^{65+} ions (kinetic energy: 7.5 keV * q) after transmission through 10 nm thick carbon foils using an experimental setup as shown in Fig. 1. HCI where extracted from EBIT II with an extraction potential of 7 kV. After m/q analysis the HCI impinged on a carbon foil target under normal incidence. The target bias was - 500 V. Secondary electrons, emitted during HCI impact on the foil where used as start signals in a time of flight (TOF) coincidence. The mass to charge ratio of transmitted ions was analyzed electrostatically in the electrical field between two parallel plates, and detected by a position sensitive micro channelplate (PS-MCP) detector. The PS-MCP rear plate signal was used to stop the TOF coincidence, which was implemented as a means to reduce the signal background. Studies on the energy loss of HCI in thin films using this technique will be described in an upcoming report. The targets consisted of one or two carbon foils with a nominal thickness of 10 nm, mounted on a copper mesh (ACF-Metals, Tucson, AZ). Background gas-pressures were kept at $2*10^{-10}$ torr in the scattering chamber and at $3*10^{-9}$ torr in the beam line.

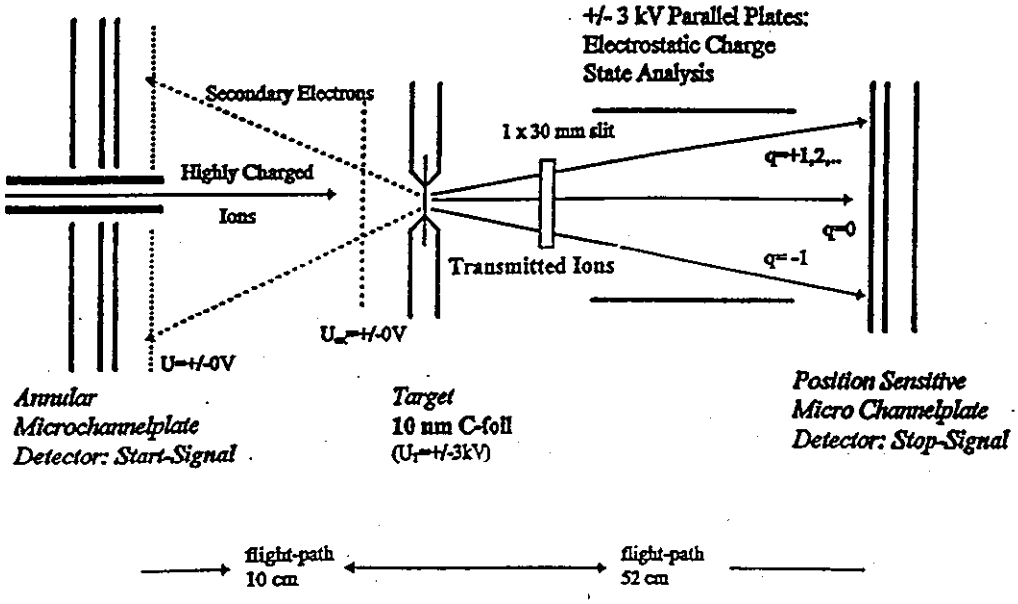

Fig. 1: Experimental setup for charge state analysis of HCI transmitted through thin carbon films.

Fig. 2 shows examples of charge state distributions of HCI after transmission through one and two carbon foils. Data represent projections of a two dimensional position distribution on the axis perpendicular to the direction of electrostatic charge state separation.

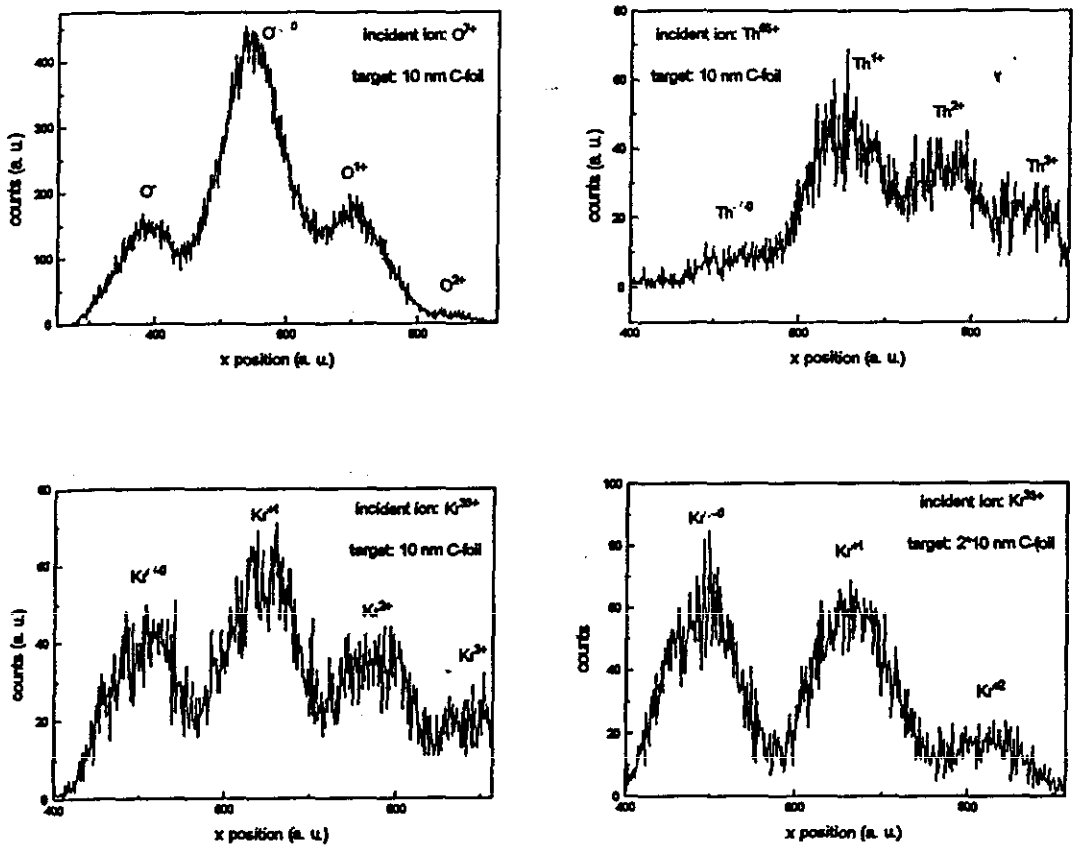

Fig. 2: Charge state distributions of HCI after transmission through one or two 10 nm thick carbon foils.

All highly charged ions up to Th^{65+} neutralize very efficiently and reach average charge states of neutral and one plus in the 10 nm thick carbon foil. The total time for de-excitation can be calculated from the initial velocity, target thickness, and the critical distance for first capture of electrons from the target conduction band. The later has been derived in the context of the "Classical Over the Barrier Model" [1] as (in atomic units):

$$R_c = 1/2 * W_\phi \sqrt{8 * q + 2}$$

The available neutralization time is then given by $dt_{neutr} = (R_c + \Delta x)/v$.

(Initial velocity corrections due to image charge interaction of incoming HCI with the target [2] are neglected as small contributions in the velocity regime used in this study).

Describing the available time for neutralization this way assumes that ions leave the thin film in a largely de-excited state. While little is known about the excitation states of slow, very highly charged ions after transmission of thin films, the following arguments can be

made in support of the assumption that the degree of excitation of transmitted ions is small. Flight times of transmitted ions from the foil to the detector were typically ~ 700 ns. Populations of excited states would be expected to result in de-excitation along the flight path to the detector, accompanied by autoionizing transitions, which would then increase the resulting final charge states. The observed low average charge states of ~ 1+, thus set an upper limit to the post scattering contributions to the observed final charge state.

As shown in Fig. 2 for Kr^{33+}, the average final charge states after passage of two, stacked, 10 nm thick carbon foils is lower then the corresponding value after one foil. This result reflects further relaxation of any excited states that were present after passing the first foil, and evolution of the ion charge state to an (dynamical) equilibrium value at a given velocity during the slow down process in the target material [see also Ref. 3, and references therein]. The results of this study are summarized in Tab. 1.

incident ion species	q_{ave} (10 nm C-foil)	q_{ave} (2 * 10 nm C-foil)	v_{in} (10^5 m/s)	dt_{neutr} (fs)	E_{pot} (keV)
O 7+	+/- 0	-	7.96	14	1.17
Ar 16+	0.8 +	0.6 +	7.61	15	5.8
Ar 18+	1+	-	8.07	14.5	14.4
Kr 33+	1.1 +	0.7 +	7.45	16.5	36.5
Th 65+	1.6 +	1.1 +	6.37	21	113

Tab. 1: Average charge states of ions after transmission through one and two 10 nm thin carbon foils. Relative errors in the average charge states are +/- 5%. Ions start out with incident velocities v and potential energies corresponding to their initial charge states. Given neutralization times apply for transmission through one 10 nm thick foil only.

Up to the highest charge states of 65+ for thorium ions, the neutralization process is essentially completed after passage of 10 nm of material, and within 20 fs. In that time 113 keV of neutralization energy have been dissipated in the target through emission of secondary particles and excitation of target atoms. Due to the short neutralization time and assuming an HCI solid interaction area with a 1 nm radius, the corresponding power density reads impressive, as $3 * 10^{19}$ W/cm^3 or 600 kJ/cm^3 are dissipated, nominally enough to doubly charge every carbon atom along a 10 nm column. Reports on studies of the response of solids to this extreme disruption of their local charge equilibrium are included in this volume.

References:

[1] J. Burgdörfer, et al., Phys. Rev. A 44, (1991), 5674
[2] F. Aumayr, et al., PRL 71, (1993), 1943
[3] R. Herrmann, et al., Phys. Rev. A 50, (1994). 1435

techniques, investigating whether single HCI can locally induce the phase transition from an amorphous, magneto optical inactive phase, to a polycrystalline, magneto optical active phase.

References: [1] T. Kessler. et al., Nucl. Instr. and Meth. B 89 (1994) 140; and T. Kessler, C. Maurer, T. Schenkel, et al., to be published
[2] P. Hansen, et al., Philips Technical Review, V41 (1983/84)'33
[3] D. B. Poker, et al (eds.), "Ion-Solid Interactions for Materials Modification and Processing", MRS Proceedings, V396, Pitsburg,1996

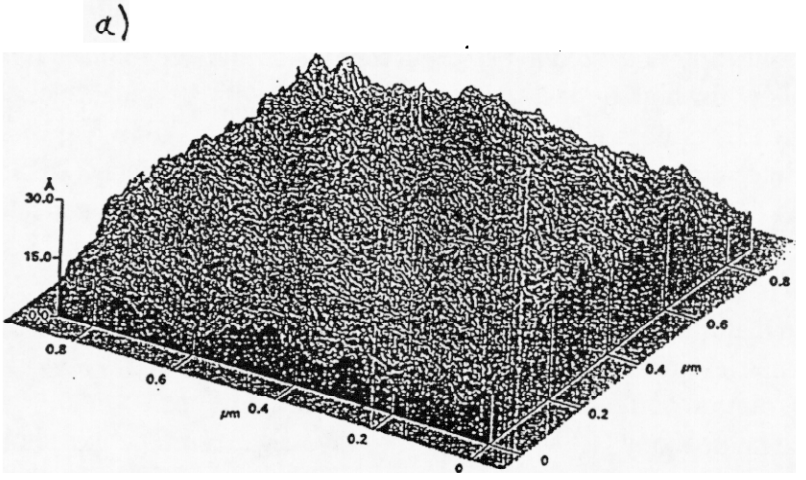

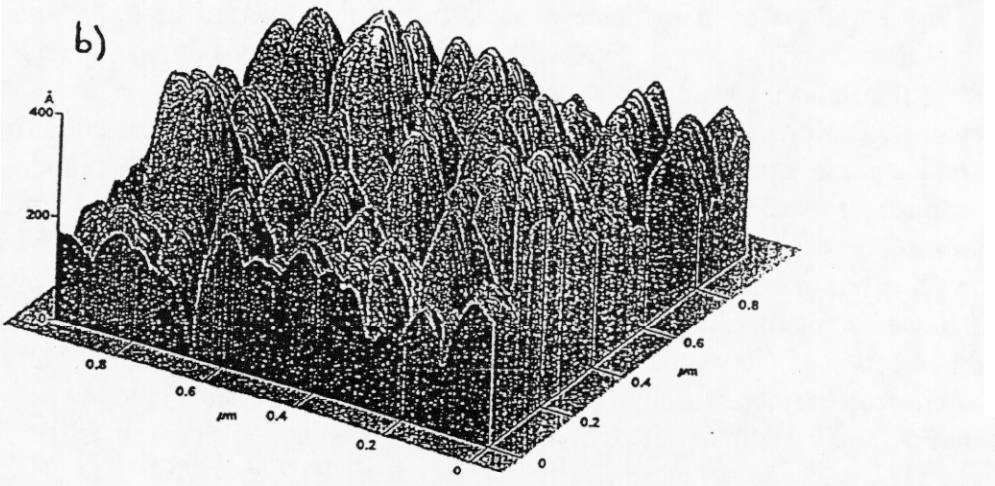

Fig. 1: AFM surface morphology measurements of a) as deposited, amorphous, and b) electron beam annealed, polycrystalline garnet films. Only the annealed, polycrystalline films are magneto optically active, and exhibit the Faraday effect.

Atomic Force Microscopy Studies of Phase Transitions in Magneto-Optical Garnet Films

T. Schenkel[1,2], T. Kessler[2], K. Bethge[2], D. H. Schneider[1]

[1] Lawrence Livermore National Laboratory, Physics & Space Technology Directorate

[2] Institute of Nuclear Physics, J. W. Goethe University Frankfurt, Germany

Magneto-optic garnets are of great technological interest because of their utilization in memory- and opto-electronical devices, and as display materials [1]. Garnet films for use as display materials have been developed by Kessler et al. [1]. A crucial factor in this development was the optimization of Faraday-Rotation (rotation of the polarization plane of linearly polarized light) [2] in the film, while keeping the film thickness small to allow for high optical transmission. Films with a typical thickness of 1 - 2 μm were deposited by radiofrequency magnetron sputtering on AF45 glass. Film stoichiometry was determined by Rutherford Backscattering Spectrometry (RBS) at the Frankfurt 7 MV Van de Graaff accelerator before and after the films were annealed in an oven (several minutes at 700°C), or with an electron beam (electron energy: 15 keV, current density: 370 $\mu A/cm^2$). It was found that excess amounts of oxygen and bismuth are driven out of the material in the course of the annealing process. Examples of typical garnet film stoichiometries are $GdBi_2Fe_5Ga_{1.5}O_{17}$ before and $Gd_2BiFe_5Ga_{1.5}O_{12}$ after annealing. Faraday rotation could only be observed in annealed films.

Atomic force microscopy (AFM) was used to investigate surface morphology changes due to the annealing process. AFM measurements were performed using a Park Scientific Autoprobe LS in contact mode at constant force. The nominal rigidity of standard Si_3N_4 tips was 0.3 N/m, tip radii were nominal 40 nm. A typical example of AFM surface morphology measurements on as-deposited and as-annealed garnet films is shown in Fig. 1. The as-deposited films show a surface roughness of several nanometers. On the annealed films, micro crystallites with heights of several tens of nanometers indicate that the annealing process results in a phase transition of the garnet material from an amorphous (as deposited) to a polycrystalline phase. It is this phase transition to a polycrystalline phase, accompanied by stoichiometry changes in the film, that modify the magneto optical properties of the material such that it now exhibits the Faraday effect.

Phase-Transitions of materials induced by heating, electron beams or ion beams [e. g. 3], as well as non-thermal chemical reactions induced by the tunneling current from a scanning tunneling microscope, have been investigated for many years. In the context of ion solid interaction studies with slow, highly charged ions (HCI) at the LLNL EBIT, the finding of electron beam induced phase transitions in magneto optical garnets is of significance in the development of highly charged ion based materials modification techniques. The basic idea of these efforts is to use single HCI, e. g. Au^{69+}, as a very efficient tool to introduce several hundreds of keV of electronic excitation energy into a nanometer size volume of material, thus inducing phase transitions and non-thermal chemical reactions on a nanometer scale. We are currently using magneto-optical garnet films as a test material in the development of HCI based nano-engineering techniques, investigating whether single HCI can locally induce the phase transition from an

Cluster Ion Emission in the Interaction of Slow Highly Charged Ions with Surfaces

T. Schenkel[1,2], D. H. Schneider[2]

[1]Physics & Space Technology Directorate, Lawrence Livermore National Laboratory

[2]Institute for Nuclear Physics, J. W. Goethe University, Frankfurt, Germany

Production of high yields of secondary cluster ions is one of the characteristic features of highly charged ion (HCI) induced sputtering of materials [1-3]. The change in cluster intensities as a function of cluster size in sputtering of different materials has been used as a signature for the presence of distinct cluster production and sputtering mechanisms. One basic question is whether clusters are emitted from a surface as an intact entity, or rather form at the surface from independently excited atoms.

The collision cascade model has been very successful in the description of secondary particle emission in the interaction of keV, singly charged ions with surfaces [4]. Independent atom-atom collisions along a collision cascade result in the ejection of surface and near surface atoms. Secondary particle yields increase proportional to the nuclear stopping power of incident ions at a given velocity, in a given material. In experimental studies, most of the secondary particles are found to be neutral, and significant contributions from molecular secondary particles (both charged and neutral) are observed. In the "statistical molecule emission" picture [5] it is assumed that clusters form at a surface after the constituting atoms have received kinetic energy in independent, random collisions from the same collision cascade. Clusters can form if the center of mass energy of contributing atoms and molecules is smaller than the dissociation energy of the cluster. This combinatorial model predicts an exponential decay of secondary cluster yields with increasing cluster size [6]. Complementary, an emission-as-entity model predicts a power law dependency of the yields of emitted clusters with increasing cluster size. The assumption is now that momentum is transferred to surface near target molecules due to the propagation of a pressure pulse or a shock wave [7,8], resulting in the emission of large clusters. The predicted exponent for the power law is ~ 2 [6,8].

Using Th^{70+} ions (E_{kin} = 3 keV / amu) from EBIT as a primary beam in a Time-of-Flight Secondary Ion Mass Spectrometry experiment [2], we have investigated negative secondary clusters ion production from thin SiO_2 films (150 nm thermal oxide on silicon substrate) and from highly oriented pyrolytic graphite (HOPG) samples (Fig. 1). Corresponding cluster yield vs size dependencies are shown in Fig. 2. In the case of $(SiO_2)_nO^-$ clusters, a fit to an exponential decay function (~ exp(-b*n) results in a too rapid decrease of the heavy cluster yields. A power law fit (~ n^a) describes the yield decrease vs size well in the cluster size range from n=3 to ~ n=20. A least square fit yields a power law exponent of a=-2.5, much larger than the exponents of a $\in$ [-5.5, -9], which were found in singly charged ion induced cluster emission studies [6], and very close to predictions of the shock wave model. The generation of a shock wave in solids at highly charged ion impact is consistent with the "Coulomb explosion" model, which has been

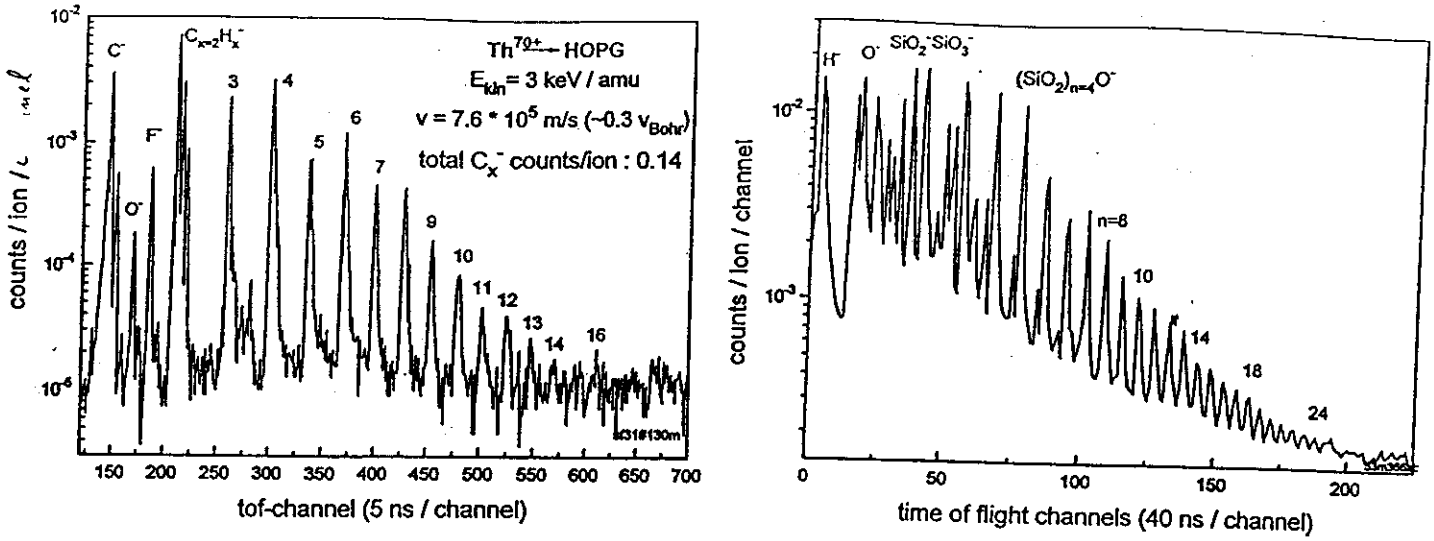

Fig. 1: Negative secondary ion production from HOPG and SiO_2 (150 nm thermal oxide on silicion) at Th70+ impact.

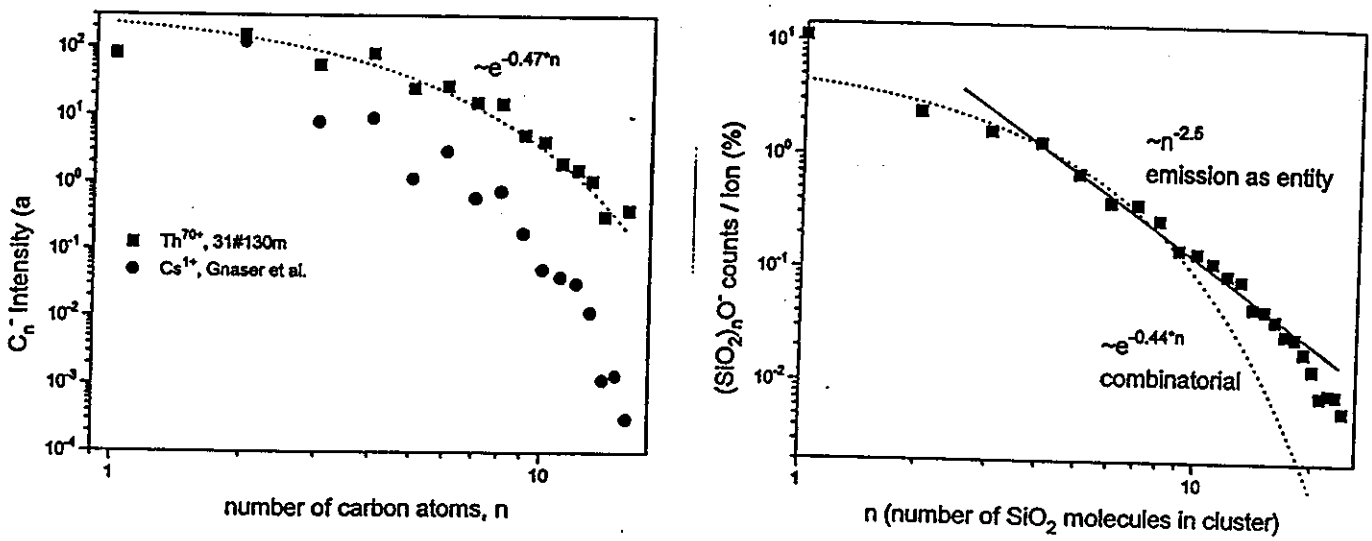

Fig.2.: Negative cluster intensities vs cluster size n, for sputtering of HOPG and thin SiO_2 films by Th^{70+} (10 keV / amu). Cs^{1+} (14.5 keV) sputtering of HOPG from Ref. 9.

suggested to describe strongly increased secondary ion yields, and defect production in the interaction of highly charged ions with surfaces [1,2].

In the case of HOPG, the yield vs size dependency exhibits an odd-even oscillation, well known from singly charged ion induced sputtering [9]. The same change in periodicity around n=10 was observed for HCI induced cluster production. It has been found in UV photoelectron spectroscopy [9] studies that carbon clusters with n<10 have linear chain like structures, while larger ones form monocyclic rings. Favoring of odd or even numbered carbon clusters reflects changes in cluster electron affinities which are in turn sensitive to these different cluster geometries. The striking difference between HCI and singly charged ion induced cluster sputtering is the rate of intensity change with increasing cluster size. In the HCI case the intensity vs size dependency can be described with an exponential decay function, indicating the applicability of a combinatorial cluster formation model [3]. The reproduction of odd-even oscillations also suggest that the basic cluster formation process is similar for both cases. The reason for the much slower decrease of cluster intensity with cluster size in HCI induced sputtering of HOPG is presently not well understood. The question of the presence of a Coulomb explosion like relaxation of HOPG surfaces at HCI impact and the generation of corresponding shock waves can not be resolved here and will be addressed in an upcoming report.

Investigations of secondary cluster ion production as a function of incident ion charge states (and HCI potential energies, respectively), and as a function of incident ion velocity will be used to further differentiate contributions from different cluster production mechanisms. Improving the mass resolution of our TOF-SIMS spectrometer will allow us to study the production of doubly charged negative carbon cluster ions [10]. Using laser post-ionization, we will extent our investigations to secondary neutral cluster production in highly charged ion solid interactions.

References:

[1] D. Schneider, M.A. Briere, Physica Scripta, V 35 (1996) 228
[2] M. A. Briere, T. Schenkel, D. Schneider, Proceedings of SIMS X, Münster, 10/95
[3] G. Schiwietz, et al., Nucl. Instr. and Meth. B 100 (1995) 47
[4] P. Sigmund in R. Behrisch (ed.), Sputtering by Particle Bombardment (Springer, Berlin. Heidelberg, New York, 1982)
[5] W. Gerhard, Z. Physik B22, 31 (1975)
[6] S. R. Coon, et al., Surface Science 298 (1993) 161
[7] R. E. Johnson, et al., Phys. Rev. B, V40 (1989) 49
[8] I. S. Bitensky, E. S. Parilis, Nucl. Instr. and Meth. B 21 (1987) 26
[9] H. Gnaser, H. Oechsner, Nucl. Instr. and Meth. B 82 (1993) 518
[10] S. N. Schauer, P. Williams, R. N. Compton, Phys. Rev. Lett. 65 (1990) 625

Direct Comparison of Collisional and Electronic Contributions to Secondary Ion Yields Using a Highly Charged Ion Neutralizer

T. Schenkel[1,2], M. A. Briere[3], K. Visbeck[1], A. E. Schach von Wittenau[1],

K. Bethge[2], H. Schmidt-Böcking[2], and D. H. Schneider[1]

[1] Physics & Space Technology Directorate, Lawrence Livermore National Laboratory

[2] Institute for Nuclear Physics, J. W. Goethe University Frankfurt, Germany

[3] presently at: Dept. of Physics, University of Rhode Island, S. Kingston, RI

In order to be able to directly compare the contributions to secondary ion yields from collisional and electronic, i. e. charge state dependent, processes, a highly charged ion "neutralizer" was built. Fig. 1 shows a schematic of the experimental setup. Highly charged ions (HCI) are extracted from EBIT and transmitted through a ~10 nm thick carbon foil, mounted on a high transmission grid. Measurements of transmitted ion charge state distributions show (see elsewhere in this report) that HCI reach charge state equilibrium inside the foil, while the total energy loss in the foil amounts to ~ 40 keV, or ~ 13 % of an initial kinetic energy of 308 keV. Equilibrium charge states of Xe^{44+} ions at ~ 300 keV ($v = 6.5 * 10^5$ m/s $= 0.3\ v_{Bohr}$) were found to be ~ 1.5 + (see [1] for comparison with high energy equilibrium charge states), and this "inverse stripping device" makes use of the fact that EBIT HCI are very slow on an atomic velocity scale. Given straightforward incident energy adjustment by tuning of the foil bias, transmitted ions in charge state equilibrium can be used as an important reference beam. Sputtering and secondary ion production has been studied extensively with beams of singly charged ions. Sputtering occurs as a consequence of collisional momentum transfer and yields are known to scale linearly with the nuclear stopping power [2, 3]. Fig. 2 and 3 show examples of negative secondary ion spectra, as measured by time-of-flight secondary ion mass spectrometry. Spectra are normalized to the number of incident ions. When using HCI, data were recorded over several minutes, with a typical incident ion flux of ~ 500 HCI / s. The secondary ion detection efficiency of ~ 10% is not included. Flight time start signals are provided by secondary electrons, emitted at HCI impact. When the neutralizer foil was used, start signals could be taken from secondary electrons emitted from the carbon foil at HCI impact, or alternatively, secondary electrons from kinetic emission processes at impact of xenon ions in charge state equilibrium could be used. Secondary ion production efficiencies increase by two orders of magnitude when highly charged ions are used as compared to ions in charge state equilibrium. Fig. 4 shows this increase over the whole range of currently available ion charge, from low charge state Xe ions, up to Th^{70+} for a) Si^+ and b) Si^- secondary ions sputtered from a float zone silicon target. The native oxide had been removed using a standard wet etching procedure. Si^+-yields increase by a factor of 330 when Th^{70+} is used instead of low charge state Xe ions. Positive secondary ion yield vs charge data show a stronger augmentation in ion production for incident ion charge states in excess of 52+ for gold ions, indicating the

presence of a threshold charge for the onset of "Coulomb explosion" sputtering [4-6]. In comparison, earlier reported positive secondary ion yield increases with ion charge from thin silicon dioxide films on silicon [4], showed a strong increase for charges q>25 for Xe ions. The higher charge (and HCI potential energy, respectively) required for the onset of strong electronic sputtering is in agreement with predictions of Coulomb explosion models [4-6]. Model predictions are currently being tested in experimental studies of total ablation rates in HCI solid interactions.

Secondary ion production with singly charged ions is routinely used for highly sensitive surface analysis (SIMS-Secondary Ion Mass Spectrometry, e. g. [7]). A useful yield increase in access of two orders of magnitude could mark a significant competitive advantage of slow, highly charged ions over conventional singly charged ions.

References:

[1] K. Shima, T. Mikumo and H. Tawara, At. Data Nucl. Data Tables **34**, 357 (1986)
[2] J. P. Biersack, Nucl. Instr. and Meth. **B 27** (1987) 21
[3] H. Jacobsson and G. Holmen, Nucl. Instr. and Meth. **B 82** (1993) 291
[4] E. S. Parilis, et al., Atomic Collisions on Surfaces, (Elsevier, North Holland, 1993)
[5] D. H. Schneider, M. A. Briere, Physica Scripta **53**, 228, (1996)
[6] R. L. Fleischer, P. B. Price and R. M. Walker, Nuclear Tracks in Solids, (University of California Press, Berkeley, 1975)
[7] A. Benninghoven, Surface Science **299/300** (1994) 246

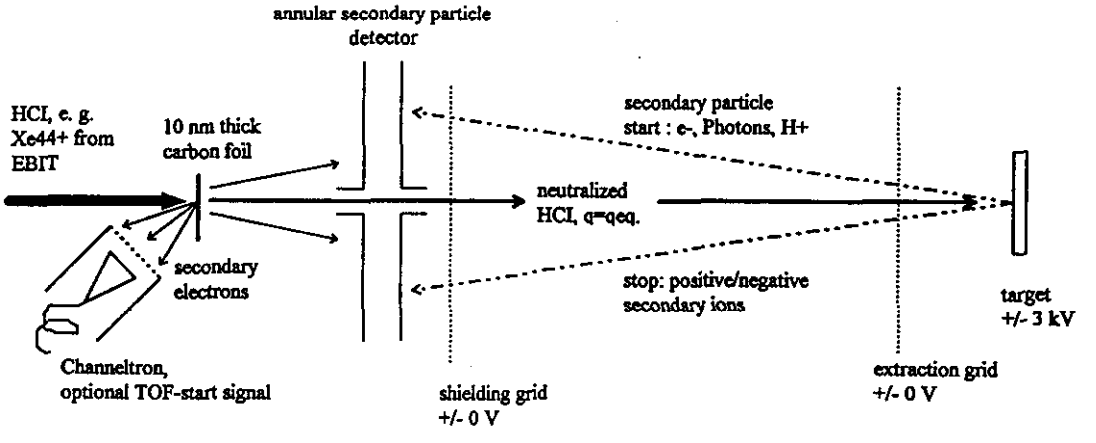

Fig. 1: Schematic of the time-of-flight secondary ion mass spectrometry setup with HCI neutralizer.

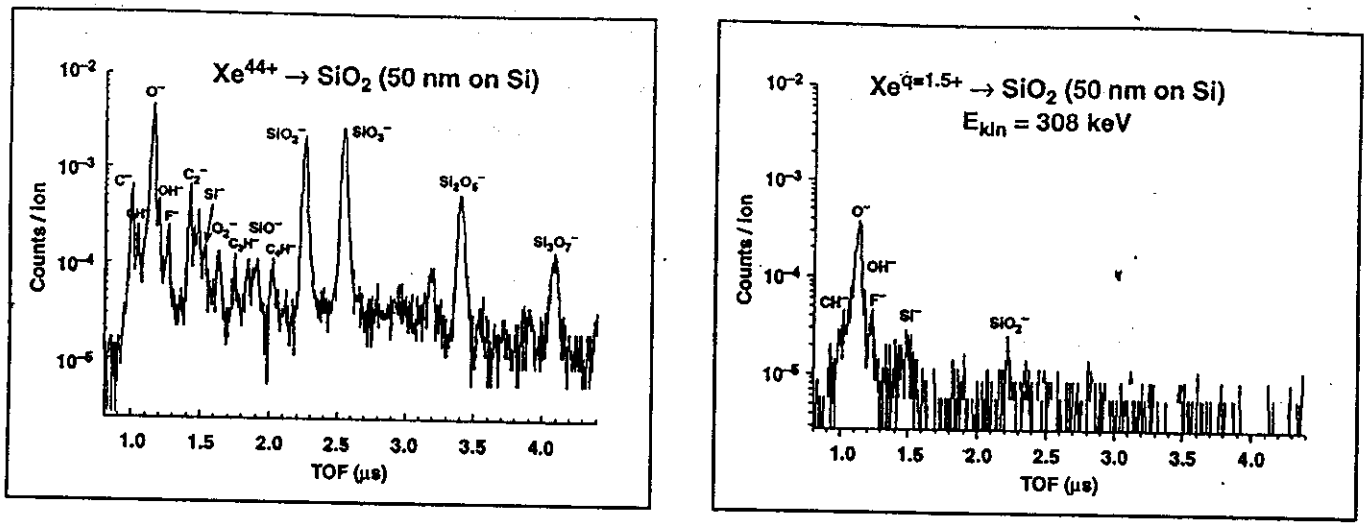

Fig. 2: Direct comparison of negative secondary ion production from SiO_2 (50 nm on Si), Xe^{44+} and $Xe^{1.5+}$ at a constant kinetic energy of 2.27 keV / amu.

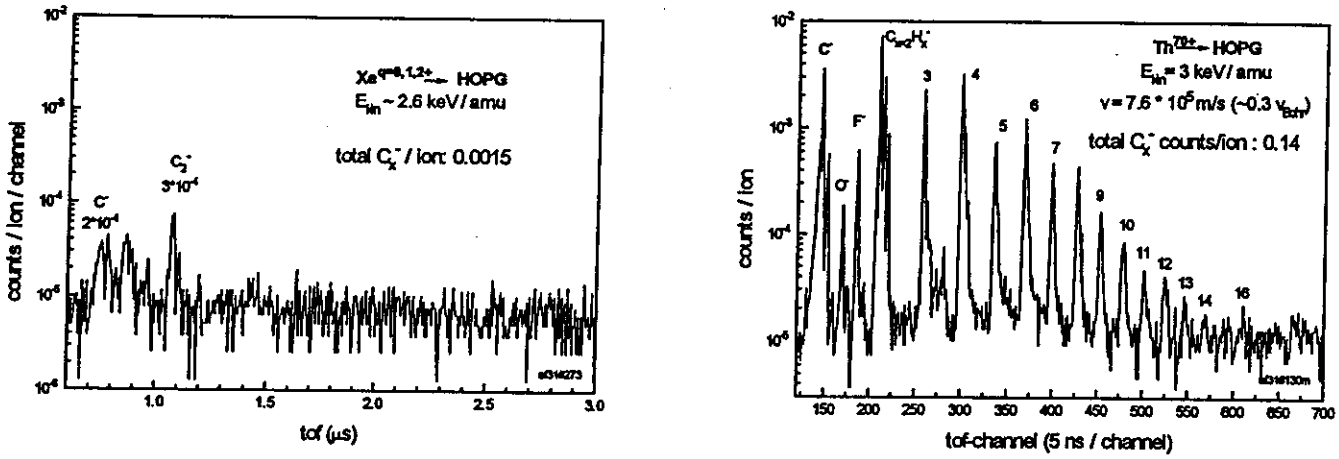

Fig. 3: Comparison of negative secondary ion production from a highly oriented pyrolytic graphite sample at impact of Th^{70+} and $Xe^{1.5+}$ at energies of 3 and 2.27 keV / amu.

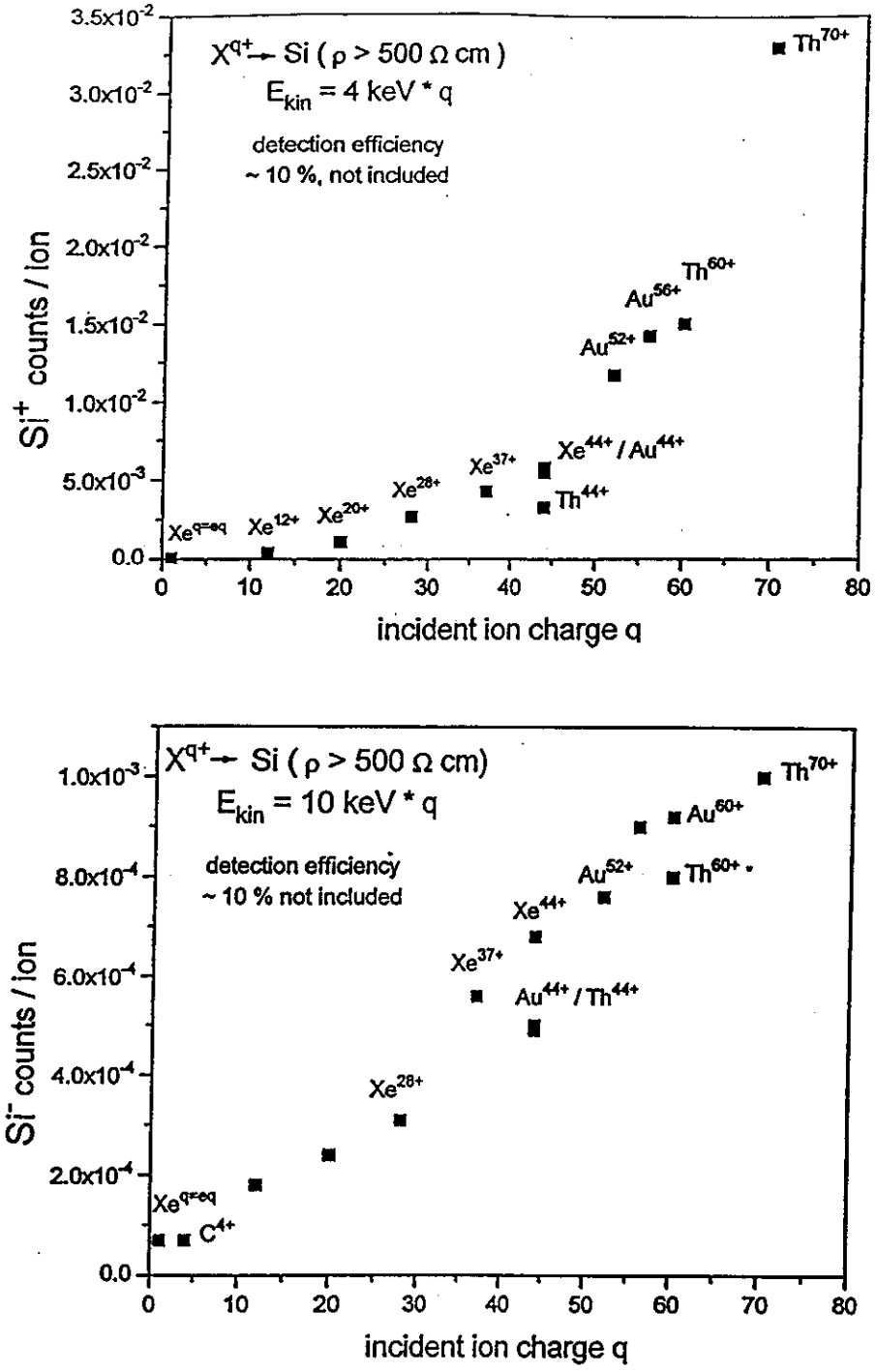

Fig. 4: a) Positive and b) negative secondary ion production from a cleaned, float zone silicon target as a function of incident ion charge q.

Electron Emission in the Interaction of Slow Highly Charged Ions with Thin Insulators and Metal Surfaces

T. Schenkel[1,2], A. V. Barnes[3], K. Bethge[2], H. Schmidt-Böcking[2] and D. H. Schneider[1]

[1] Physics & Space Technology Directorate, Lawrence Livermore National Laboratory

[2] Institute for Nuclear Physics, J. W. Goethe University Frankfurt, Germany

[3] Dept. of Physics and Astronomy and Center for Molecular and Atomic Studies at Surfaces, Vanderbilt University, Nashville, TN

Electron yields have been determined for the interaction of highly charged ions (O^{q+}, $3 \le q \le 7$; Xe^{q+}, $16 \le q \le 52$; Au^{q+}, $44 \le q \le 69$; Th^{q+}, $44 \le q \le 75$; corresponding potential energies 0.1 keV$< E_{pot} <$ 198 keV), with thin SiO_2 films (150 nm thick thermal oxide films on silicon substrates), and Au surfaces, at normal incidence and impact energies of $E_{kin} = 9$ keV * q. Analysis of measured electron emission statistics was used to determine integrated electron emission yields (Fig. 1). Total electron yield values from HCI impact on Au surfaces were utilized for calibration [1,2]. It was found that the number of electrons emitted per incident highly charged ion from SiO_2 films increases proportionally to the incident ion charge up to the highest charge states (Fig. 2), following previously determined general trends in electron emission from metal surfaces [1,2]. Electron yields changed by less than 15% when the incident velocity of Xe^{44+} ions was varied between $4.5*10^5$ m/s and $9.8 * 10^5$ m/s. In a regime dominated by collisional electron emission (incident H^+ and O^{3+} ions), the electron yields are slightly higher for insulators [3], whereas for incident ion charge states $q>3$, more electrons are emitted from metal than from insulator surfaces. This result is in agreement with theoretical predictions of shorter above surface neutralization / deexitation times in HCI insulator interactions [4]. As an HCI approaches a surface, neutralization begins when it reaches a critical distance for capture of target electrons into highly excited Rydberg states. This distance [5] is expected to be larger for materials with high workfunctions and for wide band gap materials, like SiO_2. For metals, most secondary electrons are emitted in above surface autoionization processes in the course of hollow atom de-excitation. A shorter distance of first electron capture leads to a shorter above surface neutralization time, resulting in lower above surface secondary electron emission yields from insulators than from metals at HCI impact. In this picture the excitation state of an HCI impinging on an insulator surface will be higher than for impact on a metal surface. The dynamics of below surface de-excitation of hollow atoms, sub-surface electron emission, and the question of target lattice response mechanisms in insulators, poor conductors and metals are currently being addressed in systematic studies.

References:

[1] J. McDonald, et al., PRL 68 (1992), 2297

[2] F. Aumayr, et al., PRL 71 (1993), 1943

[3] R. A. Baragiola, in "Low Energy Ion-Surface Interactions", J. W. Rabalais (ed.), John Wiley & Sons, New York, 1994, P. 243

[4] J. Burgdörfer, et al., Aust. J. Phys., 1996, 49, 527

[5] J. Burgdörfer, et al., Phys. Rev. A 44 (1991) 5674

Fig. 2 shows examples of charge state distributions of HCI after transmission through one and two carbon foils. Data represent projections of a two dimensional position distribution on the axis perpendicular to the direction of electrostatic charge state separation.

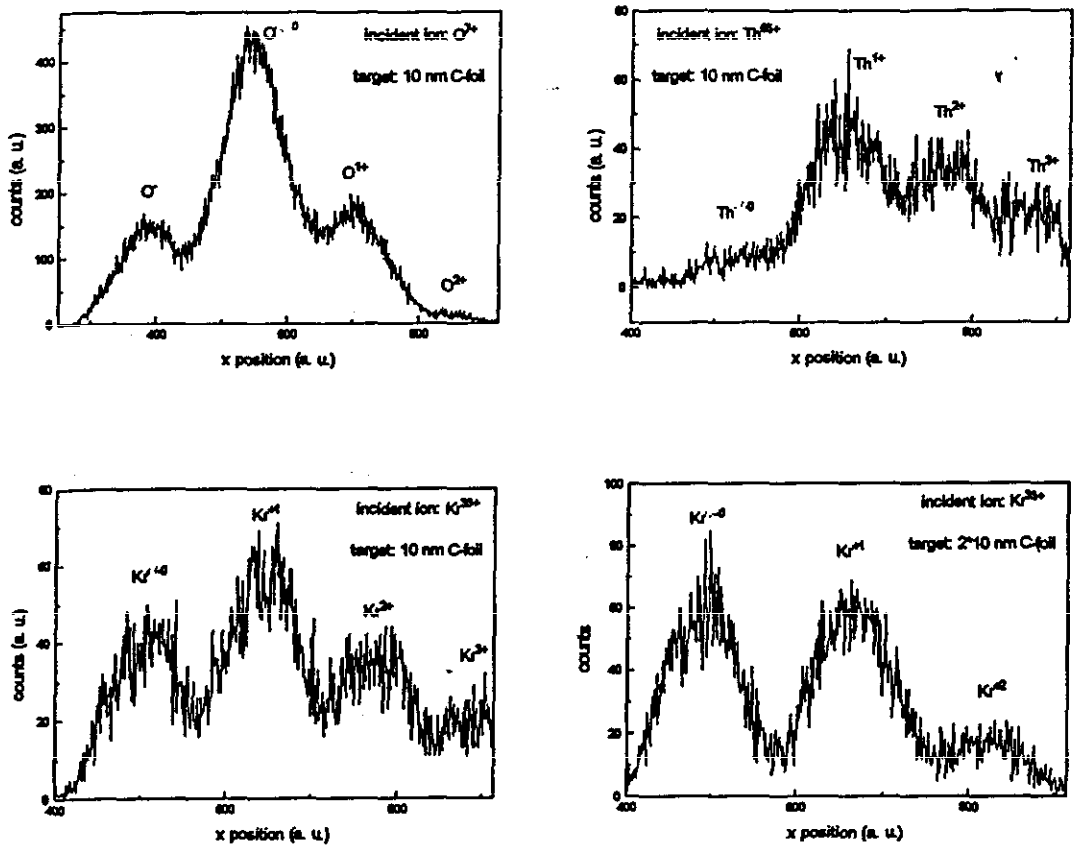

Fig. 2: Charge state distributions of HCI after transmission through one or two 10 nm thick carbon foils.

All highly charged ions up to Th^{65+} neutralize very efficiently and reach average charge states of neutral and one plus in the 10 nm thick carbon foil. The total time for de-excitation can be calculated from the initial velocity, target thickness, and the critical distance for first capture of electrons from the target conduction band. The later has been derived in the context of the "Classical Over the Barrier Model" [1] as (in atomic units):

$$R_c = \tfrac{1}{2} * W_\phi \sqrt{8 * q + 2}$$

The available neutralization time is then given by $dt_{neutr} = R_c + \Delta x / v$.

(Initial velocity corrections due to image charge interaction of incoming HCI with the target [2] are neglected as small contributions in the velocity regime used in this study).

Describing the available time for neutralization this way assumes that ions leave the thin film in a largely de-excited state. While little is known about the excitation states of slow, very highly charged ions after transmission of thin films, the following arguments can be

Simulation of the Electron Emission from Insulators Induced by Highly Charged Ions

Oleg Pankratov, Tsukiyo Tanaka and Dieter Schneider

Lawrence Livermore National Laboratory
Livermore, CA 94550

It is very well known that the exposure of any solid surface to slow highly charged ions (HCI) leads to electron emission. Remarkably, the number of emitted electrons exceeds by far the charge of the ion. This is particularly well pronounced for sufficiently high ionic charges. For example, the impact of Th^{80+} with the gold surface produces more than 250 electrons [1]. Theoretical analysis of Bardsley and Penetrante [2] shows that the electrons are emitted by means of a field emission mostly before the ion strikes the surface. Due to the enormous electric field of the ion the electron emission is similar for metals and insulators. However, the consequences are very different. In case of a metallic substrate the local charge neutrality of the solid is maintained due to the electron supply from the bulk. For insulators or poor conductors the electron emission from the spot below the incoming ion leads to formation of a localized depletion region. Due to a very high ionization of this region the ions of a solid experience a strong Coulomb repulsion which may cause a so called "Coulomb explosion" [3-4] and creates a crater on the surface. A peculiar feature of this mechanism is that the surface damage is not related to a direct impact of the HCI and may actually occur before the ion strikes the surface. The idea of a "Coulomb explosion" was quite extensively discussed in the past [3-6], but has never been subjected to a quantitative theoretical analysis. To evaluate the importance of this mechanism of a surface damage through HCI , one needs to calculate the shape of a depletion region and a degree of ionization.

As a first step in this direction we performed a calculation of electron emission from insulators. Following Bardsley and Penetrante, we consider electron emission using a Nordheim-Fowler formula for the field emission. In contrast to the case of a metallic substrate one has to consider the positive charge of holes which are left in a solid. Also an additional charge of electrons which return from vacuum to the substrate must be taken into account. We investigate the most simple model of an insulator completely neglecting the conductivity in the bulk and at the surface. In such a model each emission event creates an immobile positive hole in a surface region. The electrons which return to the substrate and "stick" to the surface are assumed to be immobile. The electric charge of the holes and these "surface electrons" must be taken into account in a calculation of the electric field distribution and the total force which determines the motion of the HCI. The figure below shows the numbers of holes, "surface electrons" and free electrons in a vacuum above the surface as a function of the distance between the ion and the surface. It

is interesting to note the qualitatively different motions of different HCIs. Ar^{10+} hits the surface whereas Xe^{44+} and U^{90+} are repelled by the positive charge of the depletion region. That is why the ion-surface separation which has been initially decreasing, starts increasing. This effect apparently cannot occur for metallic substrates where the ion motion is dominated by the attractive image force.

References:

[1] D. Schneider and M. Briere, Phys. Scripta, 53, 228 (1996).
[2] J.N.Bardsley and B.M.Penetrante, Com. At. Mol. Phys. 27, 43 (1991).
[3] R.L.Fleischer, P.B. Price, and R. M. Walker, Journ. Appl. Phys. 36, 3645 (1965).
[4] E.S. Parilis. Proc. Int. Conf. on Atomic Collision Phenomena in solids, Amsterdam, p. 324 (1970).
[5] I.S. Bitensky and E.S. Parilis, Journ. de Physique, C2-227 (1989).
[6] Y. Yamamura, S.T. Nakagawa, H. Tawara, Nucl. Ins. Meth. B98, 400 (1995).

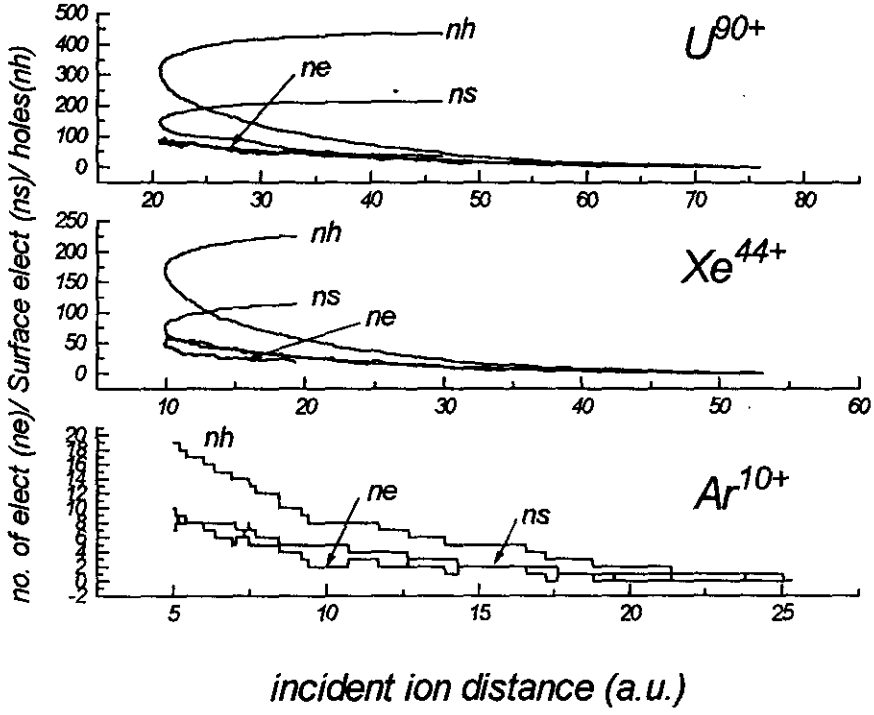

Time for the Empty L Shell of a Hollow Atom to be Filled

J.P. Briand and B. d'Etat-Ban
Universite Pierre et Marie Curie, Paris, France
D. Schneider, M.A. Briere, V. Decaux, J.W. McDonald, and S. Bardin
Lawrence Livermore National Laboratory, Livermore, CA

The dynamics of the first capture and decay processes occurring during the interaction of slow highly charged ions below a surface has been studied in looking at the x rays emitted directly, or in coincidence, by impinging bare or hydrogenlike ions of various atomic numbers on solid targets. Results on the decay processes of these hollow atoms, mainly formed below the surface, for argon, iron, and krypton ions are presented. By measuring the changes of the numbers of electrons in the L and M shells of the ions, compared to the lifetime of the K shell, it has been possible to evaluate the mean time for the filling of the L and M shells. These measurements are compared with a model of interaction of the ions with the surface(1).

Beams of Fe^{25+}, Fe^{26+}, Kr^{35+}, and Kr^{36+} ions at 7 kV/q kinetic energy were prepared at the Lawrence Livermore National Laboratory (EBIT) source and sent onto metallic targets. The x rays emitted in flight by these ions were observed with intrinsic germanium detectors of 200 mm^2 area and 180 eV resolution at 6 keV. The spectra have been presented in Ref. 1 and the 1994 EBIT Annual Report. The Kα lines observed are made of a complex array of KL^2 satellite lines corresponding to the transitions of L electrons to the K shell in the presence of any number of L spectator electrons. These satellites cannot be separated with a germanium detector, but the mean energy of the line measured gives the mean number of L electrons present at the time of the decay (Tables I and II). The energy of the Kα line emitted by Fe^{25+} ions is centered on the KL^x satellite (four L spectator electrons, on an average, instead of e.g., five, as observed for argon). This result is in agreement with the observed shape of the Kβ line (whose KL^2 components are more widely separated than for the Kα line), which shows that most of the eight satellite lines (except maybe the KL^8 and KL^7) are present. In the case of Kr^{35+} the Kα line is centered on a KL^x satellite, with a mean value for x of 2.7. It clearly appears from the Kβ spectrum that only the (first) few $KL^?$ lines are emitted.

One of the most visible features of these spectra is the very large (unusual) intensity of the Kβ lines as compared to the Kα lines: 38% and 42% for iron and krypton, respectively (Table II). Since the transition rates for the Kβ lines are compared to the Kα lines are for an equal number of p electrons in the n = 2 and 3 shells, for e.g. krypton between 15% and 26%, these results mean that the mean number of M electrons (of the 3p state at least) is always about two times as large as the number of electrons in the L shell. Like in the case of Ar, the M shell is then roughly closed when the L shell is empty. These results also mean, like in the case of argon, that the ion is quickly fed to reach its equilibrium charge state, which corresponds at the given kinetic energy (7 kV/q) to charges ~3+, before or at the beginning of its radiative decay.

We present in Tables I and II the energies and number of spectator electrons deduced from the Kα lines observed for Fe^{25+} and Kr^{35+}. The first interesting result of these tables, compared to previous ones on argon ions is the decrease of the number of L spectator electrons present at the time of the K hole filling as a function of the atomic number of the ion: 5, 4.2 and 2.7 for argon, iron, and krypton hydrogenlike lions, respectively. In any case, the ions are quasineutralized, i.e., have comparable L shell filling rates for an equal number of electrons. The L shell filling rate is, however, also faster, owing to the larger number of outermost shell electrons for the ions of larger Z atomic numbers (a factor of approximately

2 between Ar and Kr). This result shows clearly the effect of the fast decrease of the K shell lifetime as a function of Z (the radiative lifetime $T_k \sim Z^{-4}$), which leads to a relatively faster filling rate for the K shell than for the L shell for increasing atomic numbers.

The second interesting result is obtained by comparing the numbers of L spectator electrons for e.g., Fe^{25+} and the first K transition (hypersatellite) for Fe^{26+}, which is found to be 3.8 for Fe^{26+} and 4.2 for Fe^{25+}. This result can be explained by considering that the lifetime of the K hole is abut two times shorter when two K holes are present instead of one. Since the L shell filling rate in this case is roughly the same for Fe^{26+} and Fe^{25+}, this means that the Kα line is emitted in a shorter time for Fe^{26+} than for Fe^{25+} and then for fewer L electrons. A similar effect is also observed with Kr^{35+} and Kr^{36+} ions ($0.7e_L$ for Kr^{35+} than for Kr^{36+}).

A third results that can be extracted from the data presented in Table II is the mean time for the filling of an L hole, which can be deduced from the energies of the satellite and the hypersatellite lines for a given element. In this case we used bare ions Fe^{26+} and Kr^{36+} whose two K vacancies are sequentially filled through the hypersatellite lines at the times of the filling of the two K holes (the KL^2 satellite structure of the Kα hypersatellite and of the satellite) it is possible to observe separately two steps of the time evolution of the electronic configuration of the hollow atoms, the two lines being emitted one after the other. A completely different KL^2 distribution was observed, where more L electrons are present on the satellite spectrum than on the hypersatellite one, which demonstrates clearly the stepwise filling of the L shell.

Reference:
1. J.P. Briand et al. Phys. Rev. A 53, 4 (1996).
J.P.B and B.d.B. would like to express their gratitude to D. Schneider and the Lawrence Livermore National Laboratory for their kind welcome to carry out this experiment on the EBIT ion source.

Table I. (a) Experimental energies of the KL^x satellite lines for $Fe^{25+,26+}$ and $Kr^{35+,36+}$ and (b) theoretical values

Line	Fe^{25+}	(a) Expt. energy (eV) Fe^{26+}	Kr^{35+}	Kr^{36+}
$K^X\alpha$	6555	6535	12935.5	12917.4
$K^H\alpha$		6867		13389

Line	(b) Theor. energy (eV) Fe	Kr
$K\alpha S_2$ neutral	6392 (E) $K^1L^8M^X$=6397.5	12605 (E) $K^1L^8M^X$=12631
$K\alpha S_1$ neutral	6404	12657
$K\alpha H_2$ neutral	6558 (E) $K^0L^8M^X$=6668	12990 (E) $K^0L^8M^X$=13018
$K\alpha H_1$ neutral	6678	13047
He-like $^3P_1$	6667 (E) $K^1L^1M^0$=6684	13023 (E) $K^1L^1M^0$=13068
He-like $^3P_1$	6701	13114
He-like Ly-α_2	6952.5 (E) $K^0L^1M^0$=6965	13431 (E) $K^0L^1M^0$=13483
He-like Ly-α_1	6971.2	13431

Table II. Mean numbers of L spectator electrons for Ar^{17+}, Fe^{25+}, and Kr^{35+}, Kα, Kβ, and γ line relative intensities (values for argon are corrected from fluorescence yields); and changes in mean numbers of L spectator electrons during the hypersatellite-satellite cascade.

Ions	Ar^{17+}	Fe^{25+}	Kr^{35+}
$K\alpha L^x$	$K\alpha L^{(5)}$	$K\alpha L^{(4.2)}$	$K\alpha l^{(2.7)}$
I(Kβ)11(Kα)	0.3	0.38 (No.e⁻M> No. e⁻L)	0.42 (No.e⁻M> No.e⁻L)
I(Kβ)11(Kα)			(No.e⁻N> No.e⁻L)
Ions	Ar^{17+}	Fe^{26+}	Kr^{36+}
$K\alpha L^x$	$K\alpha K^{(5.4)}$	$K\alpha L^{(5.3)}$	$K\alpha L^{3.2)}$
$K\alpha L^x$	$K\alpha L^{(3.8)}$	$K\alpha L^{(3.8)}$	$K\alpha L^{(2.2)}$
No. of additional Le-	2.6	2.5	2.2

References:
1. J.P. Briand et al., NIM 87, 138 (1994).

Interaction of Slow $Ar^{(17,18)+}$ Ions with C_{60}: An Insight Into Ion-surface Interactions

J.P. Briand and L. deBilly
University Pierre et Marie Curie, Paris, France
J. Jin, H. Khemliche, M.H. Prior, Z. Xie and M. Nectous
Lawrence Berkeley National Laboratory, Berkeley, CA
D.H. Schneider
Lawrence Livermore National Laboratory, Livermore, CA

The interaction of $Ar^{(17,18)-}$ ions with C_{60} has been studied by observing coincidences between Ar K x rays and the fullerene ions and fragments. At large distances the capture of electrons from C_{60} into excited states of the ion has been observed and compared to the interaction of the same ions with surfaces. Most of the observed events correspond to the capture of many electrons by the ion and the loss of all but one. These results show clearly the same characteristic behavior of ions flying over a surface without any contact.

The Ar^{17+} and Ar^{18+} ions were produced by the AECR ion source of the 88-inch cyclotron of the Lawrence Berkeley National Laboratory at an energy of 10 keV/q. They were mass and charge analyzed on the joint Lawrence Berkeley National Laboratory-Lawrence Livermore National Laboratory (LBNL-LLNL) ion beam facility by two dipoles and sent into a vapor beam produced by heating C_{60} power to 430°C in an oven. The ion x rays were analyzed with a Si(Li) detector with a resolution of 147 eV (full width at half maximum) at 6 keV, and the charged fullerene ions, or fragments were analyzed by a time-of-flight apparatus.

Some events that show the very specific behavior of an ion interacting with a surface without contact (grazing incidence conditions) have been observed. It is found that capture occurs into large-n states of the ion in an original situation where there is no essential dynamical screening of the ion (large "parallel" velocity, the ion flies over a large fraction of the surface). We have then observed what happens when an ion captures many electrons and cannot be easily refed (it escapes from the capture area much faster than it loses electrons through Auger decays). This specific behavior where an ion captures and loses many electrons in a very short time will certainly be of interest for studying the interaction of highly charged ions with insulators where one can expect to observe some ion backscattering.

This work was supported in part by the Office of Energy Research, Office of Basic Energy Science, Chemical Science Division under contract no. DE-ACO3 76S100098 and Center National de la Recherche Scientifique. The authors would like to express their gratitude to C. Lyncis of the Nuclear Science Division for his support.

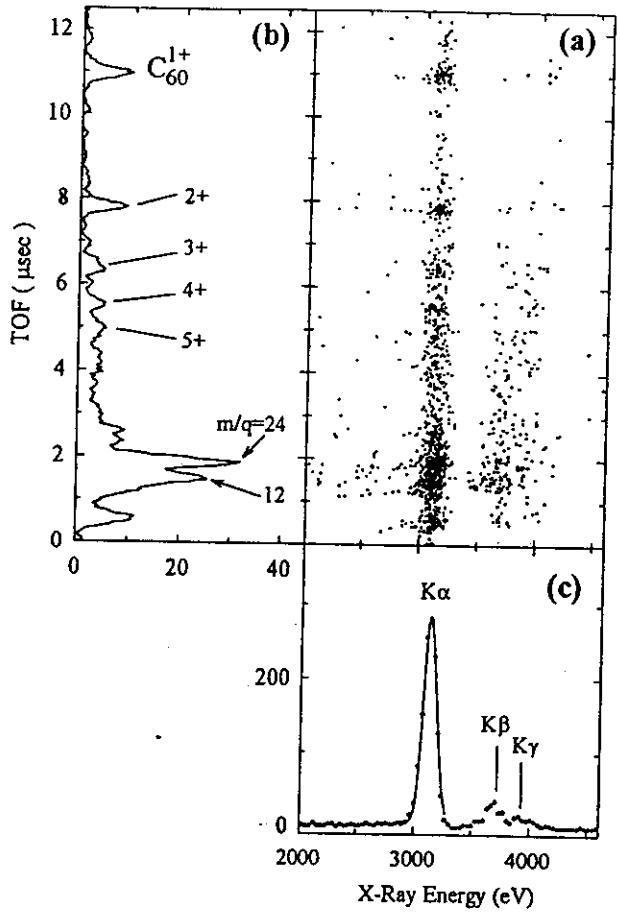

Fig. 1. Ar K x-ray-recoil ion coincidence data from Ar^{17+} (170 eV) collisions with C_{60}. (a) C_{60} product ion time-of-flight vs. x-ray energy, (b) projection of (a) on the time-of-flight axis, (c) projection of (a) on the x-ray energy axis.

Fragmentation of Biomolecules Using Highly Charged Ions

C. Ruehlicke, D. Schneider, T. Schenkel and R. Balhorn
Lawrence Livermore National Laboratory, Livermore, CA 94550

Studies of the interaction of highly charged ions (HCI) with biomolecules, i.e. DNA and protein, are a new application of HCI extracted from LLNL-EBIT. As slow, highly charged ions carry a high potential energy compared to their kinetic energy and deposit the energy in a fairly localized region of the target, fragmentation effects and mechanisms different from those observed with photons, electrons or neutrons, e.g. are expected. First experiments on fragmentation and secondary ion emission from biomolecules upon impact of Xe^{44+} have been performed.

The target was a polypeptide (RRRVAC), dried on a SiO_2 substrate and stored in air previous to being brought into the high vacuum (ca. 10^{-9} T) . A pulsed beam of Xe^{44+} ions extracted at 7keV/q with a flux of ca. 600/s was directed at the target. Secondary ions were detected with a time-of-flight secondary-ion-mass-spectrometer (TOF-SIMS), which has been designed for studies of ion interaction with solid surfaces. Start and stop signals, which determine the flight time of secondary ions are taken on one channelplate, towards which the ions are accelerated by a voltage of +3kV or -3kV, depending on the secondary ions of interest, between the target and the detector.

Secondary ions with flight times up to 10us were recorded, which corresponds to a mass range of ca. 1000 - 2000 amu, depending on the actual accelerating voltage. The negative ion spectrum shows a number of peaks of mass < 100, which consist of combinations of mostly C, O, and H. In addition there are strong mass contributions at masses up to 1000 amu, which are not seen in spectra obtained from SiO_2 only. The resolution of the current system is ca. 60-70 m/Δm, therefore only approximate values can be given for high masses.

Fragmentation studies of greater detail involving a wide range of ions are currently underway.

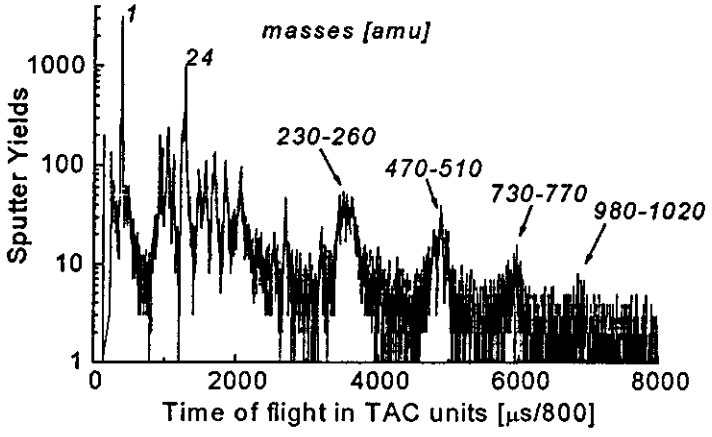

Fig. 1:
Negative secondary ions sputtered off the polypeptide RRRVAC by Xe^{44+}.

IV. Electron-Ion Interactions Studies

Measurement of the Resonance Strengths of High-n Dielectronic Satellites to the Kβ Lines of He-like Ar^{16+}

A. J. Smith[1], P. Beiersdorfer[2], V. Decaux[2], K. Widmann[2], K. J. Reed[2], and M. H. Chen[2]
[1]*Department of Physics, Morehouse College, Atlanta GA 30314*
[2]*Lawrence Livermore National Laboratory, Livermore, CA 94550*

X-ray emission from intermediate-Z atoms such as Ar^{16+} is used extensively as electron temperature (T_e) and electron density (n_e) diagnostics for inertial confinement fusion (ICF) plasmas. The argon is usually added as dopant (0.1 atomic %) to the solid fuel. The electron temperature is deduced from the intensity ratio of transitions between n = 3 and n = 1 levels in hydrogenic and heliumlike ions, Lyβ/Kβ ; the electron density is derived from Stark broadening of the Kβ line. In considering the Kβ line profiles, one must take into account contributions from Li-like satellite lines of the form $1s3lnl' - 1s^2nl'$ for $n \geq 2$. These satellite contributions are usually derived from theory and so far only the n = 2 and 3 satellites have been included in the modeling of the ICF data.

We have used EBIT to measure the resonance strengths on high-n lithiumlike satellites to the Kβ lines of heliumlike Ar^{16+} [1]. In particular, we have measured line positions relative to Kβ1 and the contributed intensities from transitions of the type $1s3lnl' - 1s^2nl'$ for n =3-5 and $n \geq 6$. For these measurements we used a high resolution Bragg-crystal spectrometer in the von Hámos geometry. A LiF(200) crystal with a spacing of 2d = 4.027 Å and bent to a radius of 75 cm was used. The crystal was centered at 3.4 Å, corresponding to a Bragg angle of 57.6° and a nominal resolving power $\lambda/\Delta\lambda = 12300$. The electron beam was first maintained at about 4 kV (above the ionization potential of Ar^{16+}) to produce mostly Ar^{16+} ions. The beam was then quickly swept from 4.0 kV which is well above the threshold for direct excitation of the Kβ lines to 2.4 kV which is just above the KLL resonance, and back again. The duration for each back and forth sweep was 16 ms, which is fast enough so that the charge balance was not appreciably changed. This range of electron beam energies ensures the production of the Kβ lines by direct excitation as well as the production of the associated dielectronic recombination satellite lines from the KLM, KMM, KMN, KMO, and KMP resonances, but not from the KLL resonance.

From our measurements we find the resonance strengths $S = (4.65 \pm 0.65) \times 10^{-21}$ cm^2 eV for $1s3l3l' - 1s^23l'$ resonance, $S = (5.80 \pm 0.82) \times 10^{-21}$ cm^2 eV for $1s3l4l' - 1s^24l'$ resonance, $S = (4.32 \pm 0.73) \times 10^{-21}$ cm^2 eV for $1s3l5l' - 1s^25l$ resonance', and $S = (5.87 \pm 0.63) \times 10^{-21}$ cm^2 eV for $1s3lnl' - 1s^2nl'$, $n \geq 6$ resonances [1]. This means that the resonance strength for the n = 4 satellites is larger than that of the n = 3 satellites, and that the strength of the n = 5 satellites is nearly equal to that for the n = 3. The n^{-3} dependence of resonance strengths expected from the n-scaling of the Auger rates is thus shown not to be valid for the satellites studied in our measurements. Our measurements therefore show that satellites with $n \geq 4$ should also be included in the modeling of the ICF data.

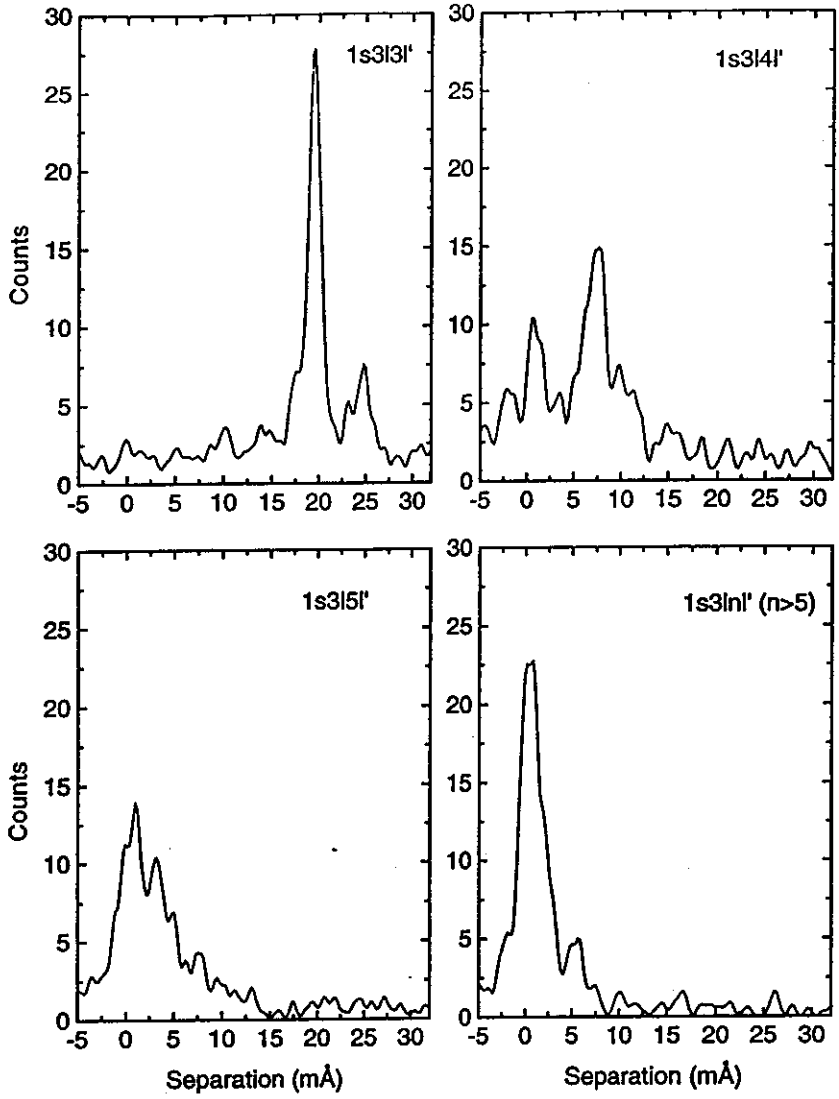

Fig.1. Intensities of high-n satellites to Kβ1 and Kβ2 transitions of Ar^{16+}. Shown in (a), (b), (c) and (d) are contributions from the satellites 1s3lnl', for n = 3, 4, 5 and n ≥ 6, respectively. The satellite positions are given relative to that of Kβ1.

References

[1] A.J. Smith, P. Beiersdorfer, V. Decaux, K. Widmann, K.J. Reed, and M.H. Chen, Phys. Rev. A**54**, 462(1996).

This work was supported in part by the Lawrence Livermore National Laboratory Research Collaborations Program for Historically Black Colleges and Universities.

Measurement of the Linear Polarization of the X-ray Line Emission Heliumlike Fe^{24+} Excited by an Electron Beam

P. Beiersdorfer[1], D. A. Vogel[1,*], K. J. Reed[1], V. Decaux[1], J. H. Scofiled[1], K. Widmann[1], G. Hölzer[2], E. Förster[2], O. Wehrhan[2], D. Savin[3], and L. Schweikhard[4]

[(1)]Lawrence Livermore National Laboratory, Livermore, CA 94550
[(2)]Schiller Universität, D-07743 Jena, Germany
[(3)]University of California, Berkeley, CA 94720
[(4)]Gutenberg Universität, D-55099 Mainz, Germany

Excitation by unidirectional electrons produces polarized line radiation. As a result, the presence of electron beams in high-temperature plasmas can be ascertained by analyzing the degree of polarization of the emitted radiation. For this purpose, polarization spectroscopy of x-ray lines from highly charged ions is especially useful, because such lines are typically less susceptible to the effects of magnetic and electric fields than, for example, optical lines from low ionization stages that could mask the polarizing effects of beam excitation. Polarized x-ray emission has been used to diagnose directional electrons in laser-produced plasmas, and the Sun; it may also be used to diagnose runaway electrons, for example, during tokamak startup. Polarization spectroscopy is, thus, a useful diagnostic of conditions for a large number of plasma sources.

X-ray line polarization is maximized in electron beam x-ray sources, such as an electron beam ion trap, where highly charged ions are excited by a monoenergetic electron beam. Such sources are, therefore, ideal for testing theory and developing plasma-polarization spectrometers. Using the Livermore EBIT, we performed measurements of the polarization of the x-ray line emission from heliumlike Fe^{24+} [1], i.e., the four lines commonly denoted w, x, y, and z, which correpsond to the decay from the upper levels $1s2p\ ^1P_1$, $1s2p\ ^3P_2$ $1s2p\ ^3P_1$, and $1s2s\ ^3S_1$ to the $1s2p\ ^1P_1$ ground state, respectively. This is the first such measurement of a highly charged heliumlike ion where the hyperfine interaction is absent. It thus complements an earlier measurement of heliumlike Sc^{19+} [2], where the hyperfine interaction destroys most polarization effects in the case of the triplet lines.

In our measurements, we relied on the use of two analyzing crystals with different lattice spacings to determine the line polarization. This experimental arrangement made use of the polarization sensitivity of different analyzing crystals, which varies as a function of Bragg angle. With each crystal, the K-shell spectrum of heliumlike Fe^{24+} generated in EBIT by excitation with a monoenergetic electron beam just above threshold for electron-impact excitation was recorded in a dispersion plane perpendicular to the beam direction. One crystal analyzes the emission near 28°, the other near 45°. The result of these measurements are shown in Fig. 1. Very different line ratios are obtained in the two measurements that illustrate the use of the two-crystal technique for polarization spectroscopy.

---

*Present address: Langley AFB, VA 23665

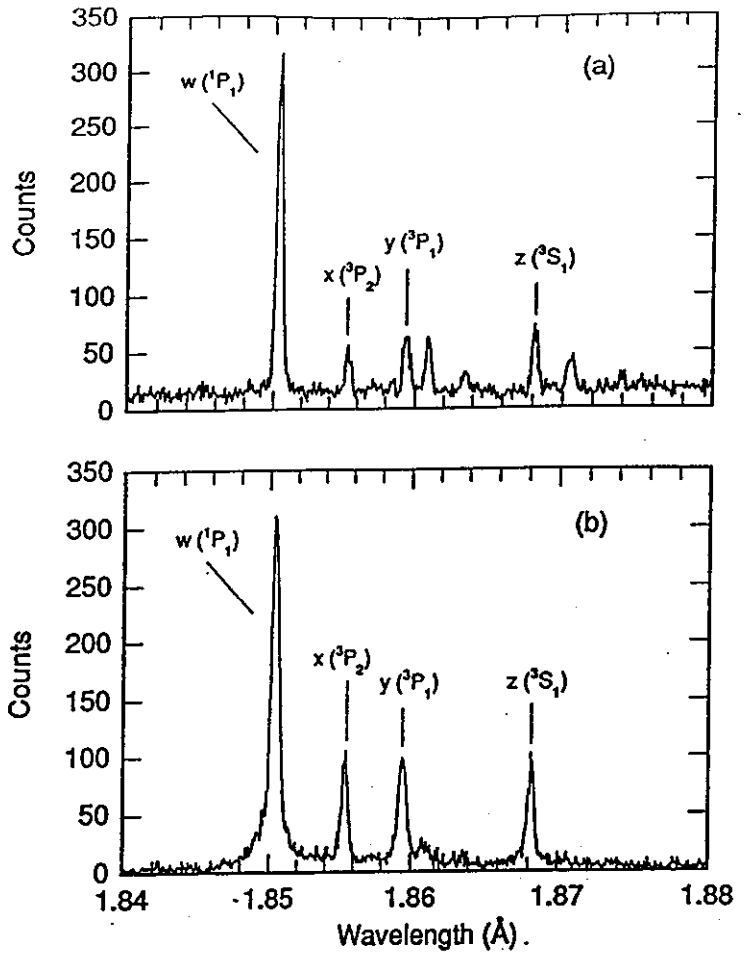

Fig. 1. Crystal-spectrometer spectra of lines w, x, y and z in heliumlike Fe^{24+} excited by a 6800-eV electron beam: (a) spectrum obtained with a Quartz(203) crystal at a Bragg angle of 42.5°; (b) spectrum obtained with a LiF(200) crystal at a Bragg angle of 27.5°. Unlabled features are from transitions in Fe^{22+} and Fe^{23+} formed by innershell excitation.

The values of the line polarization inferred from our measurements are $P_W = 0.56$, $P_X = -0.53$, $P_Y = -0.22$, and $P_Z = -0.076$. These values agree very well with those calculated using the distorted-wave approach [1]. This agreement is shown in Fig. 2. By contrast, the measured values disagree markedly with those calculated with the Coulomb-born method without exchange [1].

Experiments are now in progress to measure the polarization of the satellite transitions of Fe^{24+}. These include both dielectronic and collisional satellites and are important diagnostics of charge balance and electron temperature of high-temperature plasmas. Understanding their polarization behavior will not only test very complex theoretical models, but will also open up the entire K-shell emission spectrum for polarization diagnostics.

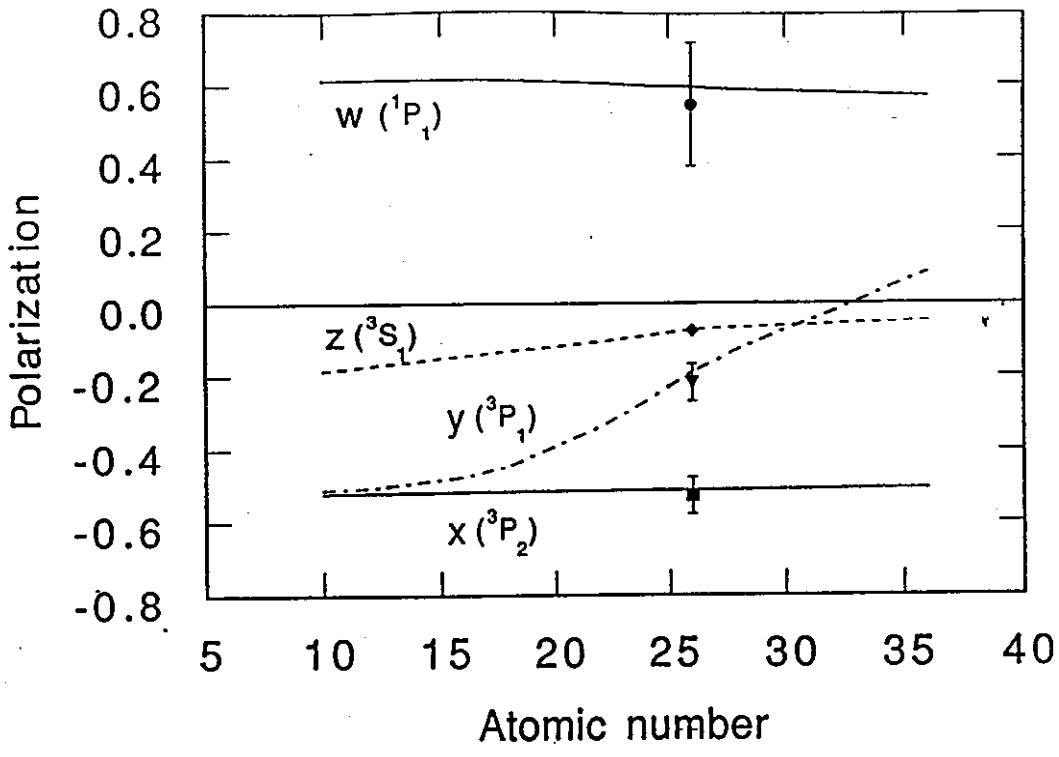

Fig. 2. Predicted polarizations of the resonance linew, the intercombination lines x and y, and the forbidden line z in heliumlike ions between Ne^{8+} and Kr^{34+}. The predictions are for nuclei without a magnetic moment. Strong hyperfine interaction with the nucleus results in vanishing polarizations for the triplet lines. The values measured for Fe^{24+} are shown for comparison. Also shown is the measured value for the singlet line in Sc^{19+} (open circle) from Ref. [2].

References:

[1] P. Beiersdorfer, D. A. Vogel, K. J. Reed, V. Decaux, J. H. Scofield, K. Widmann, G. Hölzer, E. Förster, O. Wehrhan, D. W. Savin, and L. Schweikhard, Phys. Rev. A **53**, 3974 (1996).

[2] J. R. Henderson, P. Beiersdorfer, C. L. Bennett, S. Chantrenne, D. A. Knapp R. E. Marrs, M. B. Schneider, K. L. Wong, G. A. Doscheck J. F. Seely, C. M. Brown, R. E. LaVilla, J. Dubau, and M. A. Levine, Phys. Rev. Lett. **65**, 705 (1990).

This work was supported by NASA High Energy Astrophysics X-ray Astronomy Research and Analysis grant NAGW-4185.

Effect of DR Resonances on the Equilibrium Abundances of H-, He and Li-like Fe Ions Trapped in a Plasma

J. Tanis*, D. Schneider, D. DeWitt, M. Chen, J. McDonald
Lawrence Livermore National Laboratory, Livermore, CA 94550
**Western Michigan University, Kalamazoo, MI 49008*

The excitation function for dielectronic recombination (DR) for H-, He- and Li-like ions has been measured in the EBIT by detecting simultaneously K X rays and extracted ions at a given charge state. This work is an extension of earlier work by Knapp et al.[1]

The H-, He- and Li-like ions were produced via electron impact ionization in EBIT and the DR excitation function was measured by detecting Fe K X rays emitted at 90° to the electron beams[1] and by detecting ions in a given charge state after they were extracted and momentum analyzed.[2] An electron beam energy timing pattern was used to first ionize the Fe ions and achieve a steady-state condition for the H-, He- and Li-like ions in the trap (1 sec). The ions were then probed with a variable energy electron beam for a short time interval (20 msec). Maximum electron beam energy resolution was achieved by lowering the electron beam current to about 20 mA. After that the ions were extracted in a short pulse (20 msec) while the electron beam was turned off in order to avoid changing the extracted ion charge-state balance. The extraction potential was held constant to avoid variations in the extraction efficiency. After the extraction pulse, the electron beam energy was set back to the ionization energy for a time long enough to reach the steady state condition.

In the isolated resonance approximation the energy-averaged DR cross section from an initial state i to an intermediate state d with energy bin width ΔE can be expressed in atomic units by

$$\sigma_{DR}(i \rightarrow d) = \frac{\pi^2 g_d A_A(d \rightarrow i) \sum_f A_R(d \rightarrow f)}{\Delta E E_d 2 g_i \sum A_A(d \rightarrow j) + \sum_k A_R(d \rightarrow k)}$$

where g_d and g_i are statistical weight factors for the states d and i, respectively, $A_A(d \rightarrow i)$ is the Auger rate from state d to i, and $A_R(d \rightarrow f)$, $A_R(d \rightarrow k)$ are the radiative rates from states d to f and d to k, respectively. E_d is the energy of the state d with respect to state i in the rest frame of the ion.

The analysis of the Fe^{24+} and Fe^{23+} systems follows the following scheme:[3] In equilibrium, the Fe^{24+} charge state is fed by ionization from Fe^{23+}, while it is destroyed by DR and radiative recombination (RR) on Fe^{24+}, and by capture collisions with the residual gas in EBIT. The rate equation is

$$n_{23}\sigma_i J_e / e = n_{24}\left[(\sigma_{RR} + \sigma_{DR})J_e / e + \sigma_c n_0 \bar{v}\right].$$

where n_{23} and n_{24} are the numbers of ions in the 23+ and 24+ charge states, respectively, σ_i is the ionization cross section, J_e the electron current density, e the electronic charge, σ_{RR} and σ_{DR} the radiative and dielectronic recombination cross sections, σ_c the capture cross section in the residual gas, n_0 the number density of residual gas atoms, and $\bar{v}$ the average electron velocity. Solving for σ_{DR} in terms of the ratio n_{23}/n_{24} gives

$$\sigma_{DR} = \sigma_i n_{23} / n_{24} - \left[\sigma_{RR} + \sigma_c n_0 \bar{v} e / J_e\right]$$

For the actual comparison of the measured spectrum with theoretical calculations the theoretical resonance strength needs to be folded into the experimental resolution function for E and summed over all resonances as

$$\sigma_{DR} = \sum\left(\left(A_i - \sqrt{2\pi}\sigma\right)\exp\left[-E_e - E_i\right]^2 / 2\sigma^2\right)$$

where σ is the width of the resonance. The width of the measured resonances and the relative intensities can then be compared to theoretical cross sections for dielectronic recombination derived from MCDF calculations.

The KLL DR intensity can also be compared to results[4] for resonant transfer excitation (RTE) in an ion-atom collision, a process analogous to DR. For a comparison with data for the RTE process, the following consideration is necessary: the total RTEX (RTE by x-ray emission) cross section $\sigma^x_{RTE}(i)$ in the impulse approximation can be obtained from the DR cross section by convolution with the Compton profile of the target atom, i.e.,

$$\sigma^x_{RTE}(i) = \sum_d (M/2E)^{1/2} \Delta E \bar{\sigma}_{DR}(i \rightarrow d) J(Q)$$

where $Q = (E_r - Em/M)\ (M/2)^{1/2}$, E is the projectile energy in the laboratory frame, E_r is the resonance energy, and M and m are the masses of the projectile and the electron, respectively; J(Q) is the Compton profile of the target atom.

References

1. D.A. Knapp, R.E. Marrs, M.A. Levine, C.L. Bennett, M.H. Chen, J.R. Henderson, M.B. Schneider, and J.H. Scofield, Phys. Rev. Lett. 62, 2104 (1989).

2. D. Schneider, D. DeWitt, M.W. Clark, R. Schuch, C.L. Cocke, R. Schmieder, K.J. Reed, M.H. Chen, R.E. Marrs, M. Levine, and R. Fortner, Phys. Rev. A42, 3889 (1990).

3. D.R. DeWitt, D. Schneider, M.H. Chen, M.B. Schneider, D. Church, G. Weinberg, and M. Sakurai, Phys. Rev. A47, R1597 (1993).

4. M.W. Clark, J.A. Tanis, E.M. Bernstein, N.R. Badnell, R.D. DuBois, W.G. Graham, T.J. Morgan, V.L. Plano, A.S. Schlachter, and M.P. Stockli, Phys. Rev. A45, 7846 (1992).

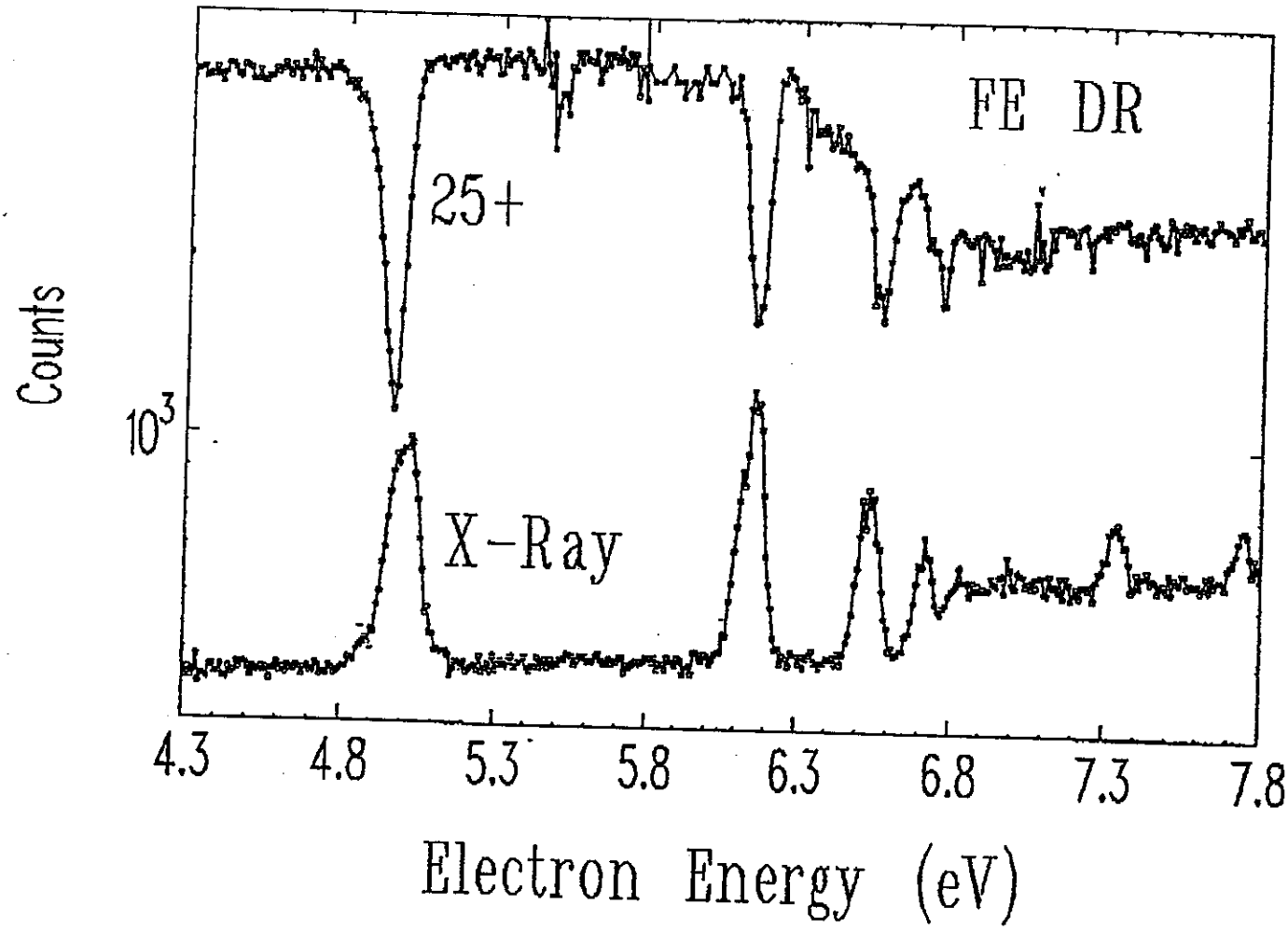

Fig. 1 Typical DR spectrum obtained from EBIT for Fe^{25+} ions. The upper plot, showing the charge-state fraction of extracted 25+ ions as a function of the electron probe energy, indicates the depletion of the charge fraction at the position of the DR resonances. The lower plot, showing the x-ray emission as a function of probe energy, exhibits a corresponding enhancement at each DR resonance.

J.A.T. was supported in part by the U.S. Departmento Energy, Office of Basic Energy Sciences, Divison of Chemical Scineces

Dielectronic Recombination of Lithiumlike Krypton

D.R. DeWitt
Stockholm University, Stockholm, Sweden
D. Schneider, M.H. Chen, G. Weinberg
Lawrence Livermore National Laboratory, Livermore, CA

We have measured relative dielectronic recombination cross sections for the $\Delta n = 1$ resonances of Kr^{33+}. The electron beam ion trap (EBIT) was used to scan the resonances, which lie in the energy range 0.5-2.6 keV. The spectrum also includes the $4\ell 4\ell'$ and $4\ell 5\ell'$ $\Delta n = 2$ resonances. The cross sections were measured by observing the decay rate of the ion population as a function of electron energy. By using an ultra low electron beam current of 3 mA, an energy resolution of 9.6 eV FWHM was achieved. The experimental results are compared to theoretical calculations performed using an MCDF model. The effective electron beam current density is obtained as a normalization parameter from a fit of the calculated resonance strengths to the experimental data.

The overall agreement is good. However, the total calculated 4l5l' $\Delta n = 2$ resonance strengths are 21% smaller than the measured total.

Figure 1 shows the experimental and convoluted theory for the $3\ell 3\ell'$ n > 3 $\Delta n = 1$ and $4\ell n\ell'$ n = 4,5 $\Delta n = 2$ resonances. The $4\ell 4\ell'$ resonances fall below the $\Delta n = 1$ series limit and are not resolved in the data. The $4\ell 5\ell'$ resonances are centered at 2514 eV. The $3\ell 4\ell'$ resonances cannot be separated into resolved terms despite the resolved structure; however, the experimental data for this group is uniformly more intense than the calculated curve, and has a total intensity 22% higher than theory. Another interesting trend is the consistently higher intensity of the calculated 3snl resonances, (n = 5,6,7,8 resolved). The measured intensities are 12 to 26% lower.
Finally, the total experimental intensity of the $4\ell 5\ell'$ resonances is 21% higher than calculated. This difference is smaller than the >50% higher experimental intensity over calculations for the $\Delta n = 2$ resonances of the He+ case (1), but the trend of smaller calculated $\Delta n = 2$ strengths is clear. The discrepancies between DR strengths in theory and experiment are probably in part due to the inadequate treatment of electron correlation.

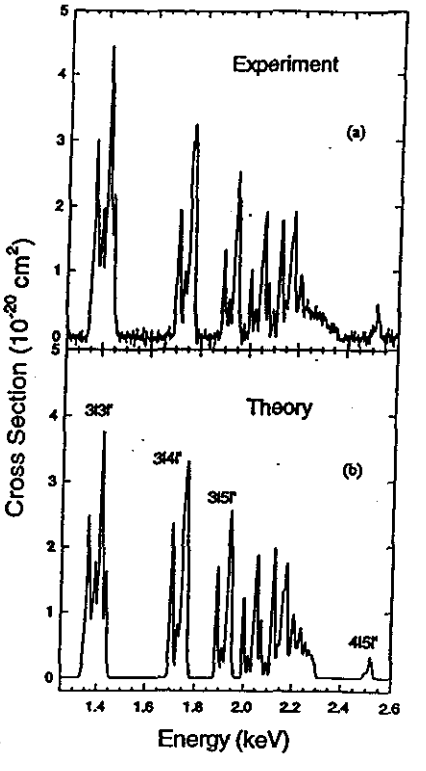

Figure 1 (a) Experimental $3\ell n\ell'$ cross sections for n > 3. (b) convoluted theoretical cross sections. The peak near 2500 eV contains $4\ell 5\ell'$ $\Delta n = 2$ resonances. The $4\ell 4\ell'$ resonances are blended with the $3\ell 3\ell'$ resonances near 220 eV.

Reference:
1. D.R. DeWitt et al. J. Phys. B 28, L147 (1995).

The technical assistance of D. Nelson and E. Magee in the performance of this experiment is gratefully acknowledged.

Ionization Cross Sections for Highly Charged Uranium Ions

R. E. Marrs, S. R. Elliott, K. J. Reed, and J. H. Scofield
Lawrence Livermore National Laboratory, Livermore, CA 94551
Th. Stöhlker
Gesellschaft fur Schwerionenforschung, D-64220 Darmstadt, Germany

The electron impact ionization cross sections for highly charged uranium ions are an excellent test bed for our understanding of relativistic and QED effects in the ionization process. Unfortunately, these cross sections are extremely small and difficult to measure. In fact, there were no direct measurements of any ionization cross sections for very highly charged ions until we introduced a new technique based on x-ray measurements with Super EBIT. Even the approximate size of these cross sections was previously in doubt due to large discrepancies between stripping measurements of accelerator beams and theoretical calculations [1]. Our Super-EBIT measurements, combined with recent theoretical calculations, have settled the issue of the correct size of the ionization cross sections for highly charged uranium ions.

After our previous measurement of the ionization cross sections for hydrogenlike and heliumlike uranium [2], we turned our attention to the uranium L shell [3]. We have now completed ionization-cross-section measurements for the uranium ions from lithiumlike to fluorinelike at three different electron energies. As described previously, our approach uses a steady-state ionization-balance technique in which radiative recombination is used for normalization [3]. Results for berylliumlike uranium at 45, 60, and 70 keV electron energy are shown in Fig. 1 along with the results of a recent relativistic distorted wave calculation [4]. The two curves show the effect of the (relativistic) Moeller interaction with exchange terms compared to the (nonrelativistic) Coulomb interaction. Interestingly, calculations that include the Moeller interaction without exchange give almost the same result as those with the Coulomb interaction alone. Our results favor the Moeller interaction with exchange. The difference between the two types of calculations is even larger for K-shell ionization [4].

References

[1] N. Claytor, B. Feinberg, H. Gould, C. E. Bemis, J. G. Campo, C. A. Ludemann, and C. R. Vane, Phys. Rev. Lett. 61, 2081 (1988).
[2] R. E. Marrs, S. R. Elliott, and D. A. Knapp, Phys. Rev. Lett. 72, 4082 (1994).
[3] EBIT 1994 Annual Report, pg. 67.
[4] D. L. Moores and K. J. Reed, J. Phys. B 28, 4861 (1995).

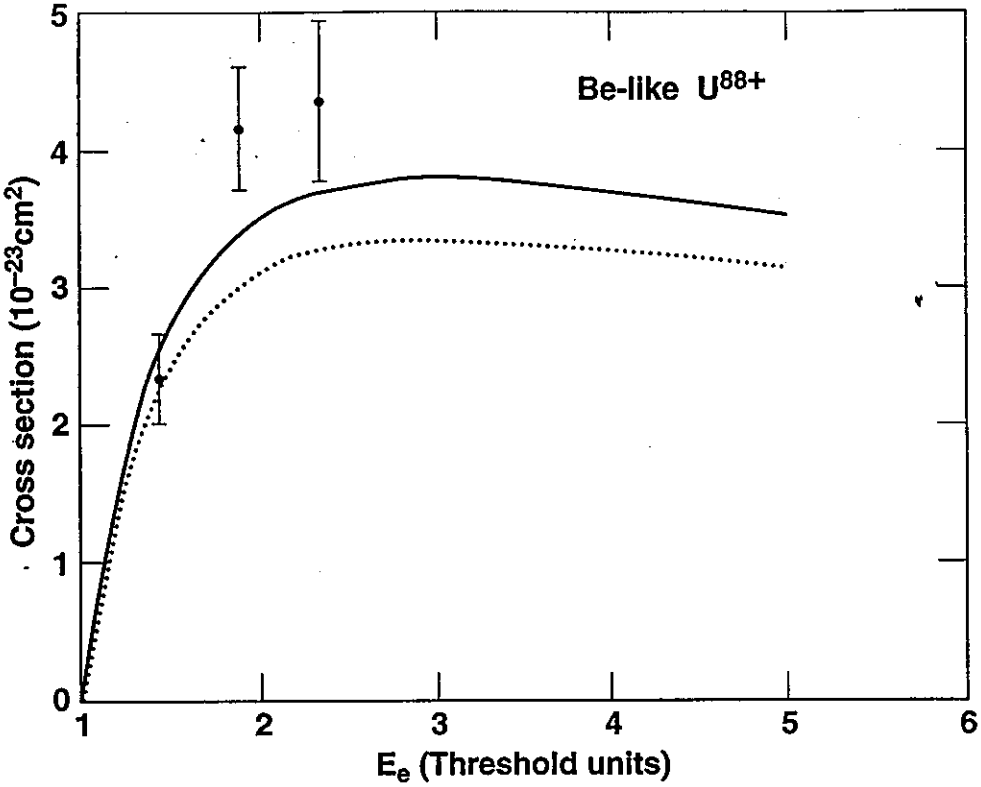

Fig. 1. Electron impact ionization cross section of berylliumlike U^{88+} vs. electron energy in threshold units. The data points are Super EBIT measurements. The upper (solid) curve is theory with the Moeller interaction; the lower (dashed) curve is theory with the Coulomb interaction.

V. Retrap and Ion Collisions

Double Electron Capture in Low-energy Fe^{17+} + He Collisions

R. Bruch and P.L. Altick
University of Nevada, Reno, NV 89557
D. Schneider
Lawrence Livermore National Laboratory, Livermore, CA 94550
M.H. Prior
Lawrence Berkeley National Laboratory, Berkeley, CA 94720
S. Bliman
Universite de Marne La Vallee, 93166 Noisy le Grand, France

Double electron transfer processes for the system Fe^{17+} + He have been studied utilizing high-resolution Auger electron spectroscopy. In recent years great efforts both experimentally and theoretically have been made to understand the collision dynamics in double electron transfer from total spin S=0 targets to highly ionized projectile beams in the low collision velocity regime. Among the many open problems to be addressed, one is the identification of the observed highly excited states and their stabilization via autoionization and radiative decay. In the case of Li-like core-excited states, several collision systems have been carefully analyzed, giving detailed insight in the dominant channels and their decay. In the case of collision of fluorinelike ($2p^5$) projectiles with He sodiumlike core-excited states are created.

In this study we address the excitation and deexcitation mechanisms of Na-like core excited Fe^{15+} ($2p^5$ nln'l') states produced in $Fe^{17+}(2p^5)$ + $He(1s^2) \rightarrow Fe^{15+}$ ($2p^5$nln'l') + He^{2+} collisions at 3 keV/amu. A beam of Fe^{17+} ions delivered by the Lawrence Berkeley Laboratory electron cyclotron resonance ion source with a kinetic energy of 170 keV was mass and charge analyzed. The Fe^{17+} beam was carefully selected by two stages of magnetic charge to mass analysis. The distance from the second magnet exit port tot he entrance of the target chamber was about 1 m and the vacuum in the beam transport system is $<5\times10^{-8}$ Torr.

The collimated ion beam is focused onto a differentially pumped gas cell and electron emission within the gas cell (prompt decays) and after the gas cell (time-delayed transitions) can be studied by means of a tandem-type electrostatic analyzer. The interaction region is comprised of two coaxial cylinders electrically insulated from each other, which allows one to isolate time-delayed spectra. The gas pressure in the target cell was regulated to a pressure of 3×10^{-5} Torr and controlled by an absolute Baratron gauge. The collision cell is 4 cm long. Experimentally we studied the formation and Auger decay of $Fe^{15+}(2p^53lnl')$ states by means of the high-resolution 0° electron spectroscopy technique.

In Figs. 1(a) and 1(b) we present typical high-resolution projectile electron spectra produced in a 170 keV Fe^{12+} + He collision. Our identification of most of the pronounced autoionization line structures is based mainly on the comprehensive theoretical calculations of excitation energies of Na-like ions by Zhang et al. In these calculations both configuration mixing and intermediate-coupling mixing among all states having the same set of n values, parity, and l values have been included. For comparison, we also list some of the earlier multiconfiguration Dirac-Fock results of Chen. Most of the observed peaks arise from several initial states associated with the $2p^53s3p$, $2p^53p3p$, $2p^53s3d$, and $2p^53p3d$ configurations.

As can be seen, the lowest line labeled 1 originates from $(2p^53s^2)^2P^0_{3/2} \rightarrow (2p^6\varepsilon p)^2P^0_{3/2}$ Coulomb allowed Auger transition. The most prominent lines in the spectrum (labeled 2 and 3) are due to spin-induced Auger decay of the $(2p^53s3p)^4D_J$ and $(2p^53s3p)^4P_J$ levels. Biasing between the inner cell and the outer cell of the gas target allows

discrimination between "prompt" and "time-delayed" Auger transitions. We have isolated the $(2p^53s3p)^4D_{7/2} \rightarrow (2p^6\varepsilon g)^2G_{7/2}$ transition (line 2). In fact, the predicted line energy of 253.5 eV for the $(2p^53s3p)^4D_{7/2} \rightarrow (2p^6\varepsilon g)^2G_{7/2}$ transition is in excellent agreement with experiment. Since the excitation of the $4D_{7/2}$ states results from radiative cascade population from higher-lying states, the question of possible spin-flip mechanisms is raised.

Several of the higher-lying quartet states such as $(2p^53s3d)^4F^0_{9/2}$ are not metastable with respect to electric transitions and contribute to the population of the lowest quartet state via cascade feeding. The most prominent Auger features above 500 eV, labeled 14-17, are mainly associated with the $2p^53snl$, n=5-8, Rydberg series.

LS coupling fails to describe properly the excitation and deexcitation of the most dominant states. Therefore the total spin quantum number of these states is not a good quantum number any more and in that sense the Wigner spin-conservation rule is violated in our experiment. Our analysis has shown clearly that a possible content of metastable states in the incident ion beam does not account for this pronounced population of spin-flipped states. Our theoretical model using time-dependent perturbation theory predicts that spin-flip processes are as likely as no flip for conditions of our experiment. Finally, there is a need for further experiments where different isotopes of the same ion species (high Z) with I=0 and I=0 would be observed to support this conclusion.

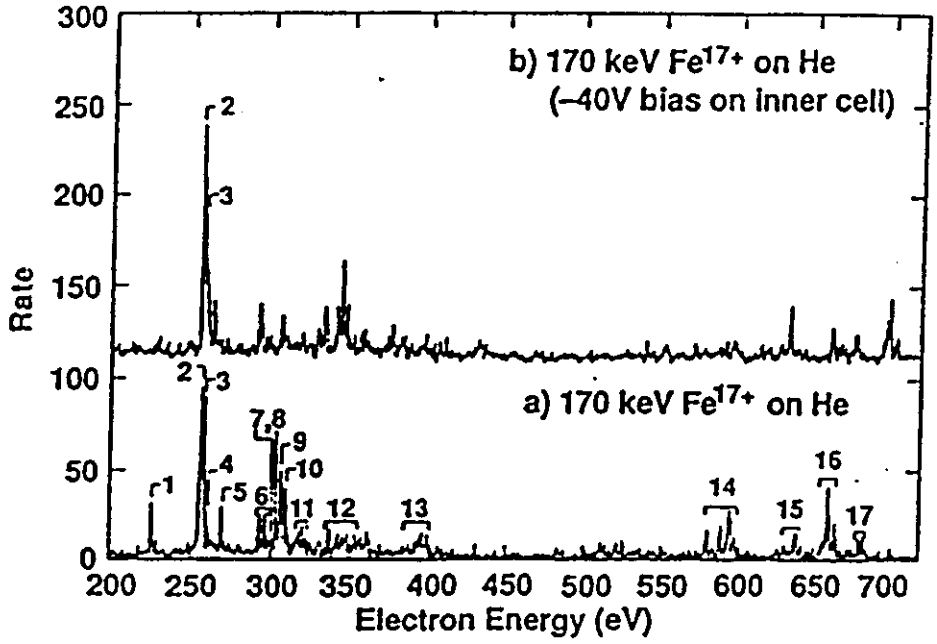

Fig. 1. (a) Fe^{15+} $(2p^53\ell n\ell')$ L Auger spectrum following 170-keV Fe^{17+} + He collisions in the energy range from 200 to 700 eV. The electron energies are given in the projectile emitter frame. (b) Separation of long-lived metastable autoionizing states from prompt Coulomb autoionizing states.

Measurement of Charge Exchange Between H_2 and Low-Energy Ions with Charge States $35 \leq q \leq 80$

B. R. Beck, J. Steiger, G. Weinberg*, D. A. Church*, J. McDonald, and D. Schneider

Lawrence Livermore National Laboratory, Livermore, CA 94550
*Physics Department, Texas A&M University, College Station, TX 77843-4242

Charge exchange between H_2 and highly-charged ions of Xe (Xe^{35+}, Xe^{43+} to Xe^{46+}) and Th (Th^{73+} to Th^{80+}) has been measured [1] at very low center-of-mass energies of about 6 eV. The experimental total electron-capture cross-sections in this energy range have been compared to predicted cross-sections that employ the absorbing-sphere model [2]. This model is expected to be most valid for high charge, and predicts a cross-section that scales slightly-less-than-linearly with charge state q. On the other hand, the cross-section for double-electron capture versus q is not well estimated, and is a matter of continuing investigation. True double capture occurs when both electrons remain on the ion. The present measurements, averaged over the charge states indicated above, are consistent with a total cross-section that scales linearly with q to q = 80+. The true double-capture cross-sections at intermediate q (44+) and high q (80+) are about 25% of the total cross-sections.

The present measurements were performed at Lawrence Livermore National Laboratory (LLNL), using the LLNL Electron Beam Ion Trap (EBIT) and RETRAP systems [3]. The highly-charged ions were produced in EBIT, extracted, analyzed, and transported to the cryogenic Penning trap of RETRAP, where the charge-exchange measurements were performed. The time evolution of the numbers of ions in sequential charge states was determined using a non-destructive technique, and the data were fitted to rate equations to determine the charge-exchange rates. From the rates, the ratio of the true double-capture cross-section to total cross-section was obtained without further analysis. However, a determination of an absolute cross-section requires knowledge of ion velocities and the density of H_2. The ion velocities were determined from ion signals and storage properties, and the density of H_2 was determined from measurements performed on Ar^{11+}, for which the electron-capture cross-section had previously been measured [4].

The absorbing-sphere model predicts a total cross-section that varies nearly linear with q as shown by the dot-dashed line in Fig. 1. In the calculation, the Franck-Condon factor for H_2 was chosen as 0.1, in accord with earlier work [2], and a correction to account for the polarization of H_2 by the high charges was included. The data in figures 1 and 2 are plotted in a simplified way by averaging the measurements for 10% ranges of charge states (i. e. Xe^{43+} to Xe^{46+} and Th^{73+} to Th^{80+}) since variations with charge in these ranges are not significant relative to the measurement uncertainties. The data lie well above the theory, especially at high q, although it should be noted that the normalizing Ar^{11+} cross-section also lies above the calculation.

The ratios of the true double-capture cross-section to the total cross-section are plotted versus q in Fig. 2. This ratio agrees with the published result for Ar^{11+}, and rises with q. This is consistent with the expectation that double capture preferentially occurs into radiatively-stabilized states for large q. There is no apparent increase of the mean values for $q \geq 35+$, indicating that transfer ionization, in which one captured electron is lost during the collision or through an Auger process, may be minimal. Transfer ionization is theoretically largest at low q, and contributes to the single-capture fraction in the present measurements.

1) B. R. Beck, J. Steiger, G. Weinberg, D. A. Church, J. McDonald, and D. Schneider, Phys. Rev. Lett, **77**, 1735 (1996)
2) R. E. Olson and A. Salop, Phys. Rev. A **14**, 579 (1976).
3) D. Schneider, et al., Rev. Sci. Instrum. **65,** (11) 3472 (1994).
4) S. Kravis, H. Saitoh, K. Okuno, K. Soejima, M. Kimura, I. Shimamura, Y. Awaya, Y. Kaneko, M. Oura and N. Shimakura, Phys. Rev. A **52**, 1206 (1995).

This work was performed under the auspices of the U. S. Dept. of Energy by the Lawrence Livermore National Laboratory under contract #W-7405-ENG-48.

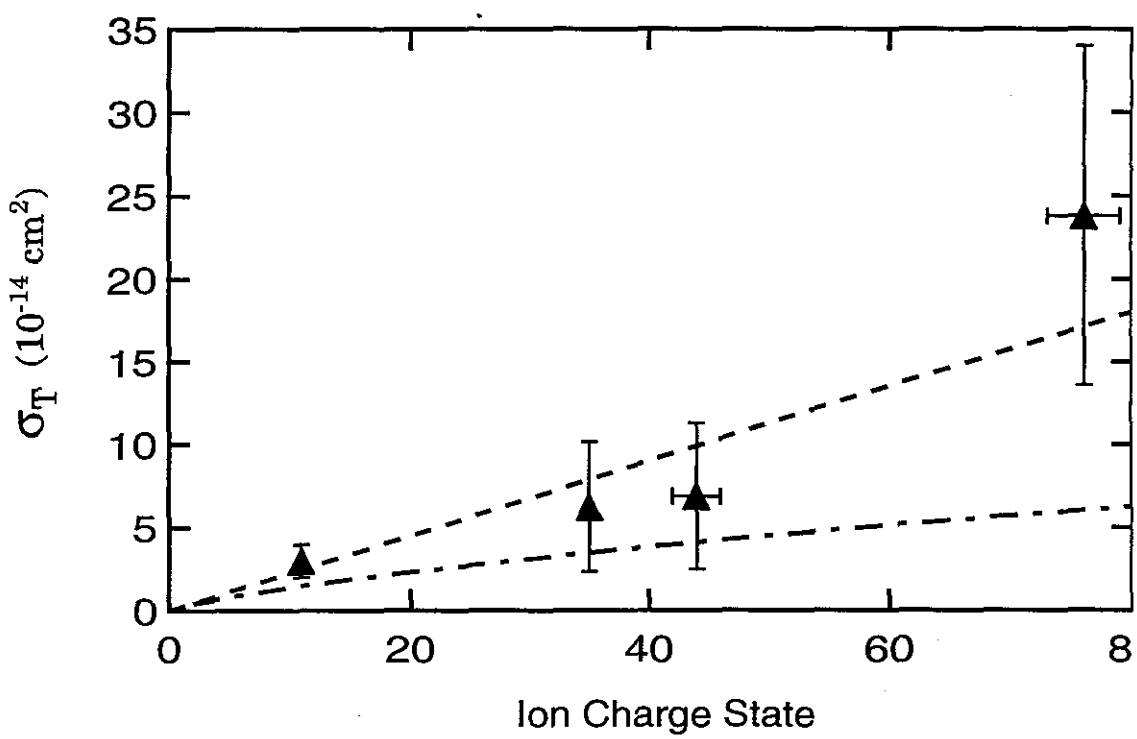

Fig. 1 Plots of the total cross-section for different highly-charged ions as a function of ion-charge state q. The dashed line is a linear fit to the data, and the dot-dashed line is a plot of the absorbing sphere model.

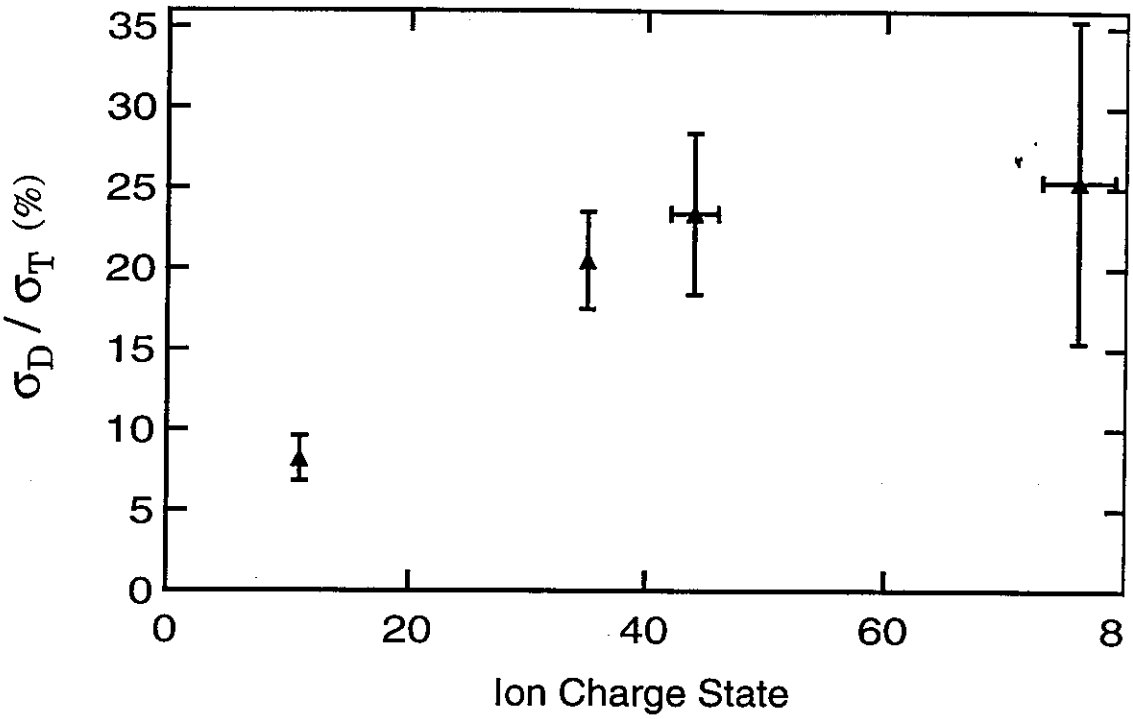

Fig. 2 Plots of the ratio of true double-capture cross-section to total cross-section for different highly-charged ions as a function of ion-charge state q.

Observation of Sequential Electron Capture to Individual Highly-Charged Th Ions

J. Steiger, D.A. Church*, G. Weinberg*, B. R. Beck, J. McDonald, D. Schneider

Lawrence Livermore National Laboratory

*Texas A&M University

Electron capture from neutrals is an important collision process that reduces ion charge in laboratory and astrophysical plasmas. A question of current interest is the fraction of "true double-electron-capture" collisions that occur when ions with charge q collide with two-electrons atoms or molecules [1]. When two electrons are captured in the same collision, autoionization of one electron with stabilization of the other may occur, leading to apparent single electron capture (transfer ionization). True double capture occurs when both electrons stabilize radiatively.

We applied a novel technique to measure the ratio of true double capture to the sum of true single capture and transfer ionization (which are not distinguished) for very low energy Th^{79+} ions. One or a few ions in a single charge state were captured and confined in a Penning ion trap. Their signals, dependent on charge to mass ratios, were periodically and non-destructively observed. The measurements were carried out with the following procedure. Very highly-charged ions were produced in an Electron Beam Ion Trap (EBIT) [2]. The ions were then extracted [3] from EBIT, mass-to-charge selected, and transported to RETRAP [4]. The captured ions typically have a wide range of axial energy, which was reduced by a temporary decrease in the trapping potential to release the highest energy ions. The remaining ions reside in a nearly axial harmonic well, and oscillate axially with frequency $\omega = \sqrt{\frac{qeU_0C_2}{md^2}}$. These ions were detected by their interaction with a high impedance, parallel, tuned circuit consisting of the capacitance between the compensation electrodes of the trap and a large external inductance. When the ion axial oscillation frequency was swept through the tuned circuit resonance by a linear ramp of the trapping potential, signals due to the motions of individual or multiple ions appeared at ramp potentials determined by their charge state, as shown in Figure 1. Periodic ramps of the potential produced snapshot signals which showed the development of the charge of the particles throughout the storage interval of about 100 s.

The storage duration of the particle provided information from which the total charge transfer rate coefficient and true double capture rate coefficient were derived. The data were analyzed by simply counting the number of ions remaining in each charge state as a function of time, for many measured sequences. Figure 2 shows plots of such measurements for the primary and the first product charge state. These plots

were fitted to the solution of the rate equations for this process [5]. The result is $\sigma_D/\sigma_T = 0.21 \pm 0.11$ where σ_D is the cross section for true double capture whereas σ_T is the total cross section for electron capture.

In summary, a new measurement technique has been used to study electron transfer collisions, and to follow the charge state development of individual particles stored in a Penning trap, due to their collisions with neutrals. This technique is potentially applicable to all ions with sufficiently high charge to produce well-defined signals. Our current data do not indicate a major increase in the true double capture probability when q is increased from 44+ to 79+.

References

1.) H.Cederquist, H. Andersson, E.Beebe. C.Biedermann, L. Broström, Å. Engström, H.Gao, R.Hutten, J.C.Levin, Liljeby, M.Pajek, T.Quinteros, N.Selberg, P.Sigray, Phys. Rev. **A46**, 2592 (1992)

2.) R.E.Marrs, M.A. Levine, D.A.Knapp, J.R.Henderson, Phys. Rev. Lett. **60**, 1715 (1988)

3.) D.Schneider, M.Clark, B.Penetrante, J.McDonald, D.DeWitt, J.Bardsley, Phys. Rev. **A 44**, 3119 (1991)

4.) D.Schneider, D.A.Church, G.Weinberg, J.Steiger, B.Beck, J.McDonald, E.Magee, D.A.Knapp, Rev. Sci. Instrum. **64**, 3472 (1994)

5.) S.E.Barlow, J.A.Luine, G.H.Dunn, In. J. Mass Spectrom. Ion Processes **74**, 97 (1986)

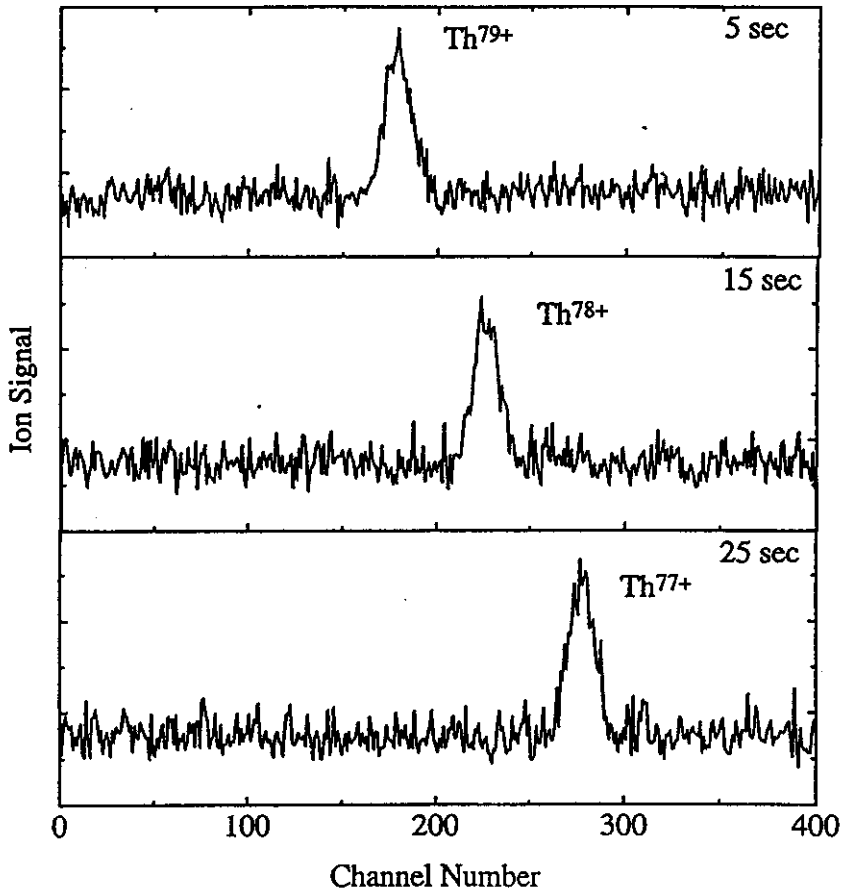

Figure 1: Noise of the tuned circuit as a function of endcap electrode potential (ion charge) at different times. The peaks are due to one Th ion. It successively catches electrons from H_2 molecules, thereby reducing its initial charge from 79+ to 77+.

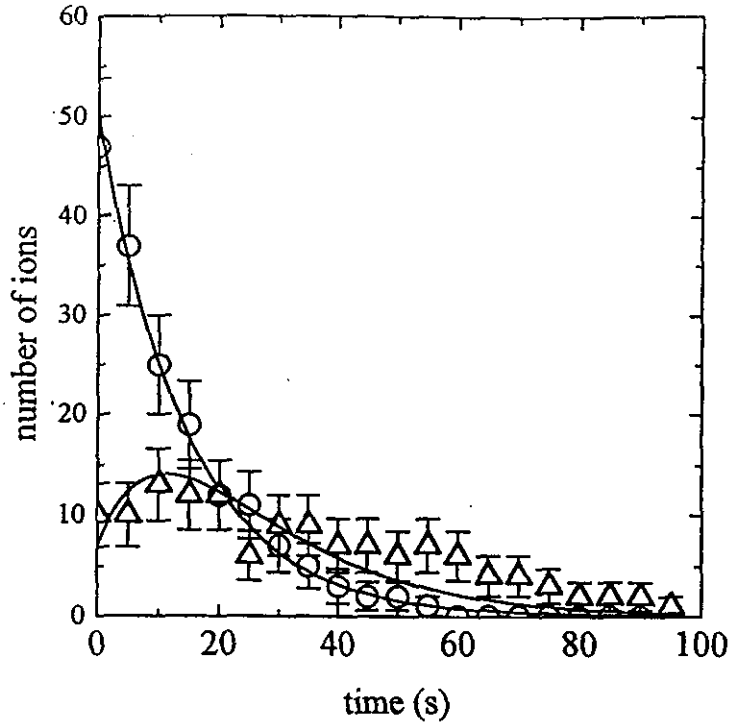

Figure 2: Number of Th^{79+} (circles) ions (injected from EBIT) and Th^{78+} (triangles) product ions plotted versus storage time. The number of Th^{79+} ions decays exponentially whereas the number of Th^{78+} ions first increases due to the decay of Th^{79+} to Th^{78+}. The solid lines are fits of the solutions of the rate equations for this process to our data. The lifetime for Th^{79+} is 14.5 s in this case

Testing the Performance of a Hyperbolic Trap-Assembly

L. Gruber, J. Steiger, B. Beck, D. Schneider
Lawrence Livermore National Laboratory
D. Church
Texas A&M University

In order to sympathetically cool highly charged, high Z ions (HCHZI) it was necessary to design a trap assembly consisting of at least two hyperbolic Penning traps. This assembly has been machined and tested. Two non hyperbolic traps have been added to the assembly (see Figure 1) so that stacking of ions is possible.

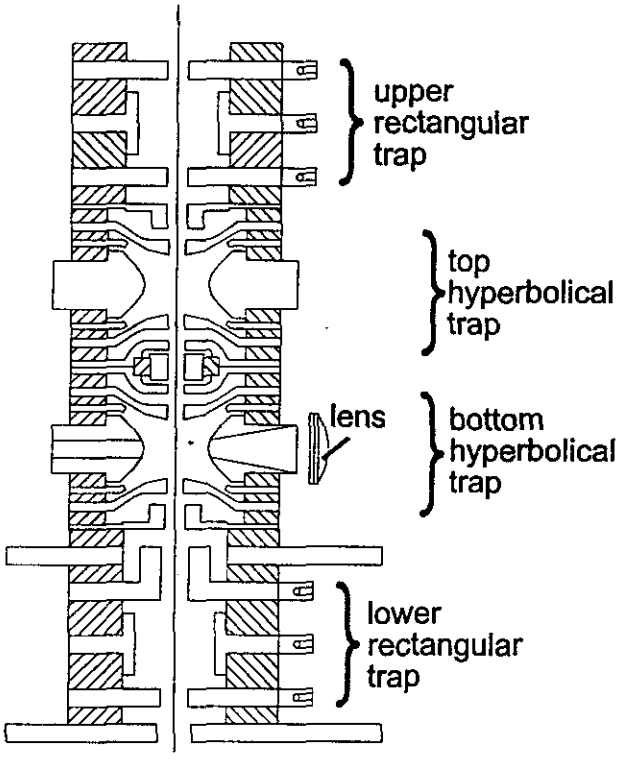

Figure 1: Trap assembly consisting of two "rectangular" traps and two hyperbolical traps. The lens increases the solid angle when fluorescence light is observed.

An initial test of the properties of the tuned circuits attached to the endcaps yielded a quality factor of $Q_B = 33$ for the bottom trap and $Q_T = 45$ for the top trap at room temperature. The quality factor decreased when the trap was cooled to liquid Helium temperature. By a modification of the amplifiers combined with a better decoupling of the tuned circuits (rearrangement of the coils and raising the resonance frequency of the top circuit by 10%) it was possible to reach values as high as $Q_B = 290$ and $Q_T = 202$ at 4 K. The resonance frequencies are $f_T = 2.515$ MHz and $f_B = 2.271$ MHz.

The trapping of highly charged Xenon ions was improved from 1-2 ions to 4-5 ions per cycle with a lifetime of about 700 ms. The Beryllium trapping time increased from only a few seconds to about a 1000 seconds for Be^{2+} in the bottom trap and the lifetime of the Be^{+} was too long to being measured.

Excitation of the cyclotron motion of the Be^{+} and Be^{2+} was demonstrated by applying a sine wave with a certain frequency on two opposite segments of the ring electrode and detecting the noise signal of the tuned circuit. Since cyclotron and axial motion are coupled collisionally is was possible to increase (heating) or to decrease (driving the ions out of the harmonic region of the trap) the noise depending on the excitation amplitude (see Figure 2). The following resonance frequencies were observed:

modified cyclotron frequency	$\nu_{+,Be+}$	=	6.910 MHz
cyclotron frequency	$\nu_{C,Be2+}$	=	14.534 MHz
modified cyclotron frequency	$\nu_{+,Be2+}$	=	14.747 MHz.

Schemes to transfer ions from one trap into an other have been tested. Some of them were found to have an efficiency close to 100%. The next experiments in this trap will focus on the laser cooling of Be^{+}-ions and the sympathetic cooling of HCHZI.

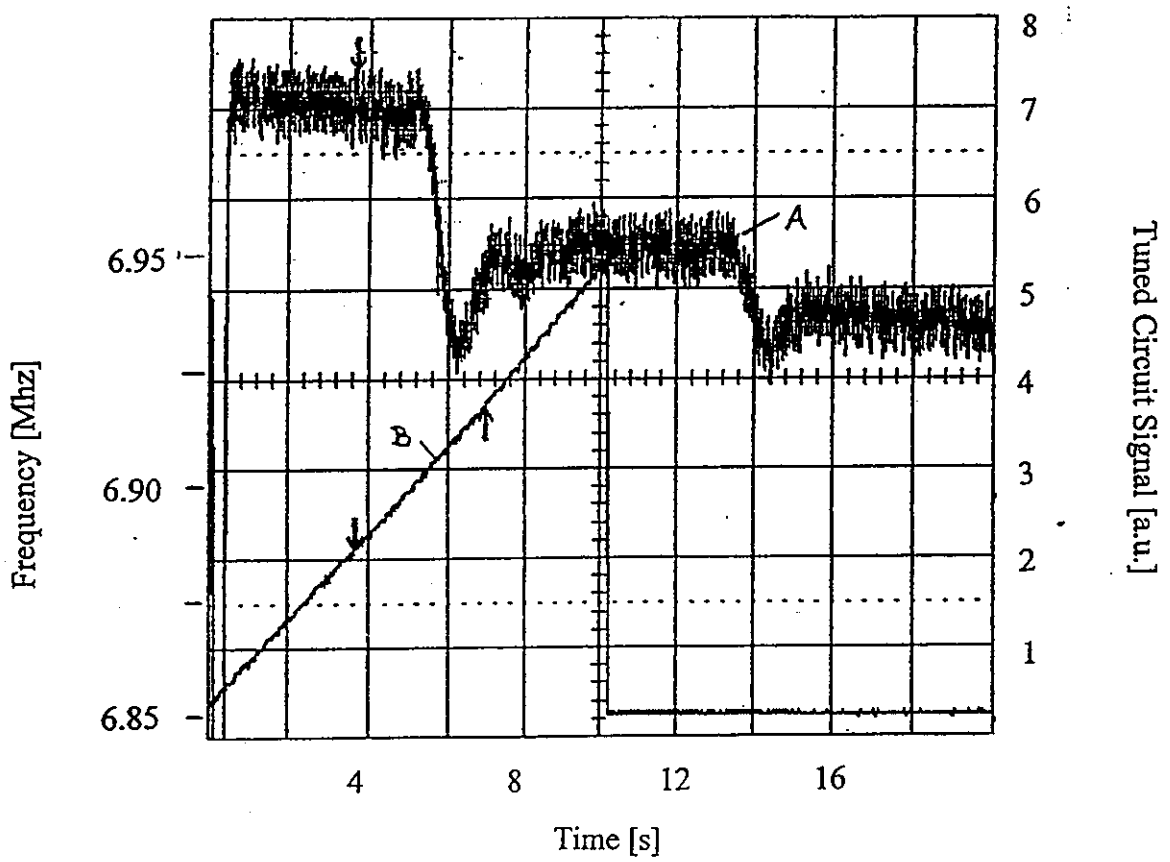

Figure 2: Tuned circuit signal (A) as the excitation frequency (B) is changed over time. The frequency was also ramped down linearly from 6.95 MHz to 6.85 MHz. The figure shows only one ramp.

Laser Stimulated Emission of Soft X-rays from Ti^{18+} in EBIT

Matthew C. Cook*, John Farley*, Joachim Steiger,
David Church** and Dieter Schneider

Lawerence Livermore National Laboratory, Livermore, CA 94566
**University of Nevada, Las Vegas, NV 89154*
***Texas A&M University, College Station, TX 77843*

Studies of fine-structure splitting improve our understanding of electron-electron interactions and QED effects in atoms and ions. Usually fine-structure splitting is a minor effect, and transitions between these levels in neutral atoms take place in the microwave regime. In few-electron highly-charged ions, the increased nuclear charge draws the electrons closer to the nucleus, amplifying such splittings into the visible region of the spectrum and beyond, allowing laser measurements of transition frequencies in certain ions. Further, the ability to induce emission of soft X-rays in response to a visible laser pulse shows promise in the field of X-ray laser technology.

We are in the planning stages of an experiment to measure such splitting in Be-like Ti^{18+}. The $1s^2 2s2p\ ^3P_0$ excited state of this ion has a nearly infinite lifetime due to the lack of a rapid relaxation route to the ground state (an E1M1 two-photon transition). The $1s^2 2s2p\ ^3P_1$ lies 604-609 nm above the metastable state, and relaxes very quickly to the ground state through an intercombination E1 transition.

Ions of the aforementioned charge state will be produced in the EBIT, with some fraction (about 1%) being in the metastable $^3P_0$ state. Because the electron beam energy needed to produce Ti^{18+} is close to the energy that produces Ti^{17+} and Ti^{19+}, a mixture of charge states will exist and an equilibrium will thus be set up among those three charge states, with Ti^{19+} recombining with beam electrons and electrons captured from neutral background gas, Ti^{18+} being ionized by beam electrons to Ti^{19+}, and similar processes occurring between Ti^{18+} and Ti^{17+}. Each of the processes that produces Ti^{18+} will produce some fraction in the metastable state. This, along with a small contribution from direct excitation of Ti^{18+} by beam electrons, will create a population of metastable Ti^{18+} ions in the EBIT trap. Beam energy and other conditions can be varied to optimize this population. Since electron-ion recombination and collisional de-excitation are the only processes that decrease this population, it may form a considerable fraction of the total Ti^{18+} present in EBIT, which is expected to be around 50,000 ions.

A laser beam will be sent into EBIT and focused on the ions. When the laser frequency is coincident with the transition frequency between the metastable state and the $^3P_1$ state (about 604 nm), the ions will be promoted to the higher state from which rapid decay to the ground state occurs with the release of a photon in the VUV-soft X-ray region at 38±.3 eV. Detection of an increase in the number of such photons will indicate absorption of the laser frequency. These photons will be detected by use of a CsI coated

The rate of absorption of laser light is the rate of depletion of the lower level population:

$$-\frac{dN_0}{dt} = B\rho N_0$$

in which ρ is the spectral density given by energy/(volume x bandwidth). The laser will be focused by a cylindrical lens to cover the entire ion volume. The minimum focal width is assumed to be 0.25 mm,

Energy=15 mJ/pulse
Laser pulse length = 10 ns
Bandwidth=3 GHz
Volume=0.25mm x 60μm x 2.5cm=$3.75\text{x}10^{-10}\text{m}^3$
Ion Doppler width=$6\text{x}10^{10}$ Hz

The power produced by the laser is $1.5\text{x}10^{6}$ Watts during a pulse. It takes $2\text{x}10^{-13}$ s for each photon to traverse the 60 μm diameter of the ion volume, so $3\text{x}10^{-7}$ Joules are contained within the reaction volume at any given instant during the pulse. Thus:

$$\rho = \frac{3x10^{-7}}{3.75x10^{-10}x3x10^{9}} = 2.67x10^{-7}\ \text{Js}/\text{m}^3$$

and:

$$-\frac{dN}{dt} = 5.09x10^{8}\,\text{N}\ s^{-1}$$

in which N_0 represents the number of ions within the reaction volume of the proper charge state and in the metastable excited electronic state before the pulse. Further, it only includes those ions whose Doppler shift puts their transition energy within the frequency envelope of the laser. It will take 9 ns to deplete the population by 99%, thus the laser power is just enough to saturate the transition during one pulse.

The total number of titanium ions in EBIT is expected to be around 10^5. Of this number, the quantity in the charge state of interest is expected to total about 50,000. The thermal energy of the ions in EBIT gives them an average velocity of $2.69\text{x}10^{4}$ m/s, which means that half of them fall within a $6\text{x}10^{10}$ Hz Doppler envelope. The laser bandwidth is about 3 GHz, so only 2• % of the total number of suitable ions is within Doppler range of the laser at any given time. The number of suitable ions within Doppler range is about 12 assuming 1% metastable fraction. Ion cyclotron motion varies the Doppler shift of the ions through the entire envelope approximately every $5.77\text{x}10^{-7}$ s in a 3 Tesla field, so an additional 20% of the ions will enter the N population at a steady rate and become capable of absorbing photons within one pulse. Further, there will be some rate of reactivation of

microchannel plate, which has about 50% efficiency at that frequency. Photons of other frequencies will be attenuated by placing a thin (1000 A) aluminum foil between the MCP and EBIT. That thickness should allow 90% transmission of the X-rays emitted, and is supported on an 80% transmittance mesh. The laser will be pulsed (or a cw laser will be chopped), and a lock-in amplifier can be used for detection, or detection can be gated to the laser pulse.

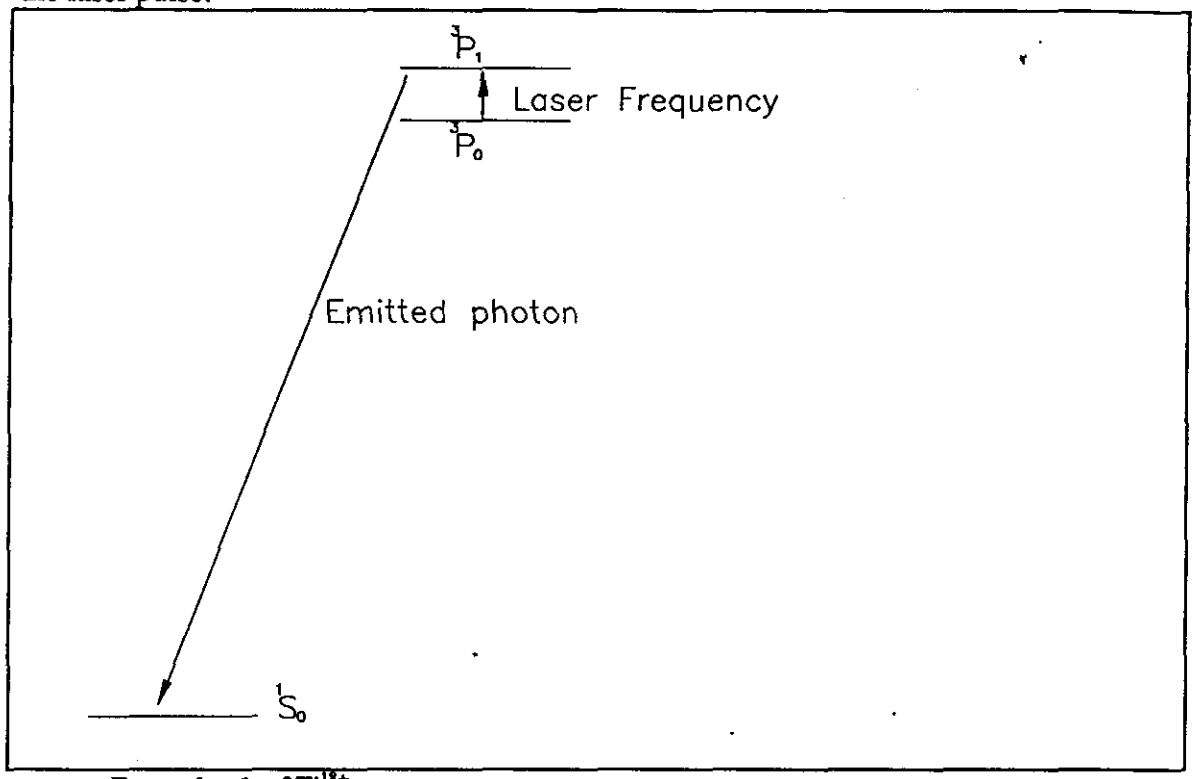

Energy levels of Ti^{18+}.

The Einstein A coefficient for the reverse of the laser transition ($A_{1\text{-}0}$) is 49 s^{-1} [1] to 78.1 s^{-1} [2]. Assuming a worst case of 49, the Einstein B coefficient for that process is found from the formula:

$$B_{1\text{-}0} = \frac{A_{1\text{-}0}c^3}{8\pi h \nu^3}$$

λ=600 nm = $6\text{x}10^{-7}$ m
ν=c/λ = $5\text{x}10^{14}$ Hz

$$B_{1\text{-}0} = \frac{49x(3x10^8 ms^{-1})^3}{8\pi(6.626x10^{-34} Js)x(5x10^{14} s^{-1})^3} = 6.355x10^{14}\frac{m^3}{Js^2}$$

$$B_{0\text{-}1} = B_{1\text{-}0}\frac{g_1}{g_0} = 3B_{1\text{-}0} = 1.91x10^{15}\frac{m^3}{s^2 J}$$

the ground state ions during this time, increasing the signal rate by an unknown amount. Assuming no significant increase in signal due to this effect, the population N_0 of metastable ions will absorb at a rate of about 112/pulse, or 1.1×10^{10} s^{-1} during a pulse.

The detector has a circular active area 5 cm in diameter, and is positioned 33 cm from the ions, giving it a collection angle of about 0.14%. Taking into account the efficiency of the detector, the count rate should be about 0.05/pulse or 5/sec at 100 Hz laser pulse rate. With detection gated to the laser pulse, this should easily be detectable above the estimated background rate of 10^5/s.

---

[1] J.P. Marques, F. Parente, and P. Indelicato, Phys. Rev. A 47(2) 929 (1993).
[2] *Spectroscopic Data for Titanium*, W.L. Wiese and A. Musgrove, ed. (1989).

VI. Instrumental Development

Charge State Dependence for Direct Highly Charged Ion Detection with a CCD Chip

D. Schneider, B. Beck, J. McDonald, J. Steiger, G. Weinberg, M. Chen
Lawrence Livermore National Laboratory, Livermore, CA 94550

Abstract

We measured the response function of a CCD chip for slow highly charged ion detection as a function of incident ion charge states q ranging from q = 30 + to 70+ and ion energies varied between 4 keV/q and 7 keV/q. The detection efficiency per ion was found to increase significantly with charge state. A possible physical reason for the q dependence of the response function is an enhanced low energy photon emission which is consistent with an earlier reported results indicating a strong q-dependence of low energy photon emission following highly charged ion impact on surfaces.[1,2]

De-excitation of the outer shells of "hollow" atoms can occur via autoionization or radiative de-excitation, the radiative de-excitation in high Z highly charged ions is expected to be a significant decay channel. If it can be verified that the radiative de-excitation of high n states in "hollow" atoms is the responsible process, that could be useful for developing imaging devices involving highly charged ion beams. These issues motivated the experiment to measure the response function of a photon sensitive CCD for direct highly charged ion exposure as function of charge state.

The experiment was carried out at the LLNL "Electron Beam Ion Trap" (EBIT) using low energy beams (4 and 7 kV • q) of very highly charged Xe and Th ions ranging in charge q from 30+ to 70+.

In the experiment, highly charged ions were directly impacted onto a backthinned TEK512 CCD chip. The chip's pixel size is $(27\ \mu m)^2$ and it has a 10 to 15 μm Si/SiO_2 cover layer. The integrated intensities in the pixels were summed and the sum was normalized to the incident number of particles. The photon quantum efficiency vs. photon energy for the chip maximizes for photon energies less than 50 eV.[2]

Figure 2 represents the response function for highly charged ion impact on the CCD chip plotted as function of ion charge states, the different ion species (Xe and Th) are indicated. The yield curves are arbitrarily normalized at 30+ ion charge. The photon emission yield deduced from previous measurements (MCP) show a q^4 dependence and for Xe^{50+} ions it was reported that close to ten low energy photons (>50 eV) are emitted per ion. Although the strong charge state dependence of the CCD detection efficiency for highly charged ions is presently not understood one may, based on previous results assume that radiative recombination causing low energy photon emission could be responsible for the strong charge state dependence. In order to verify the photon emission a 100 Å thick carbon absorber was mounted in front of the CCD chip. The absorber has a transmission of about 60% for photons between 40 and 200 eV. The intensities measured in the CCD chip behind the absorber agree to within 40% with the quoted transmission. This could be evidence for the photon energies to be in that range and that the signal in the CCD chip could be that produced by photons.

References:
1) D. Schneider, M. Brier, Physica Scripta 53, 228 (1996).
2) G. Schiwietz, et al. Rad. Effects and Defects in Solids 127, 1, 111 (1993).

Fast Ion Extraction from EBIT

J. W. McDonald and D. H. G. Schneider
Lawrence Livermore National Laboratory, Livermore, CA 94550

The EBIT at LLNL has been used to study the pulsed extraction of highest charge state ions as function of the rise time of the extraction pulse.
The extraction of highly charged ions from an EBIT has been described in detail in Ref. 1. There the extraction is performed In an adiabatic mode. The ions are produced in the center tube of a confining symmetric three drift tube trap assembly. This assembly is held at high potential with an electron beam focused through it. Neutrals or low charge state ions are successively ionized by the electron beam with an energy defined by the high potential on the drift tubes. The ions are confined radially by the space charge of the electron beam, which is compressed by a 3 T field in the center drift tube. This gives an electron density of 2-4 kA/cm^2 depending on the electron-beam current The longitudinal confinement is accomplished by a potential (V_{Trap}≈200 V) on the two end drift tubes that is superimposed on the high voltage. The confinement time and electron-beam energy can be varied to optimize the desired ion charge state. Typical values for confinement time and electron beam energy are 500ms at 9 keV with a 100mA electron current to produce $^{136}Xe^{44+}$. The extraction of ions in the adiabatic mode is accomplished by ramping the center drift tube potential above the potential of the top drift tube. The usual time for this ramping is about 100 ms. In the adiabatic extraction mode the trapped ions, which have an energy distribution of about 10 V*q, emerge over the time interval defined by the slope of the ramp. This gives a detector pulse rate which is generally low enough to determine the actual number of extracted ions.
In order to capture highly charged ions in a secondary trap (RETRAP), a short spatial ion pulse is required. To obtain this short spatial ion pulse the center drift tube is ramped up in 5ms this mode is termed "fast extraction". A typical ion dump pulse is shown in fig. 1. Fig. 2 shows a comparison of charge state distributions of extracted Xe ions in the adiabatic or "slow" mode a) and the "fast extraction mode b). In addition, the electron-beam current was decreased from 127 mA a) to 47 mA b) during the fast extraction in order to reduce ion heating by the electron beam in the trap. It is clearly demonstrated by the relative line widths of Fig. 2(a) and (b) that the momentum spread of extracted ions is greatly reduced for the lower electron-beam. Two different Xe isotopes are separated in Fig. 2(b) showing the presence of ^{134}Xe in the ^{136}Xe gas. The number of ions decreased by a factor of 10^2 when going from the "slow" to "fast" extraction mode. When comparing line widths for different parameters using fast extraction, it is also observed that the FWHM (full width at half maximum) of the charge-to-mass ratio peaks increases with decreasing extraction pulse width. It can be inferred from these observations that in a fast dump preferentially ions which lie very close to the electron beam axis with higher temperature are extracted. Their higher temperature (momentum spread) can be decreased by a reduction of the electron-beam current. These measurement infer that in the adiabatic mode the ion cloud can equilibrate to lower temperatures and a larger fraction of the ions can be extracted.

References:

1) D. Schneider, M. Clark, B. Penetrante, J. McDonald, D. DeWitt, N. Bardsley, Phys. Rev. A, **44**, 3119 (1991).
2) D. Schneider, et al., Rev. Sci. Inst. **65** (11), 3472 (1994).

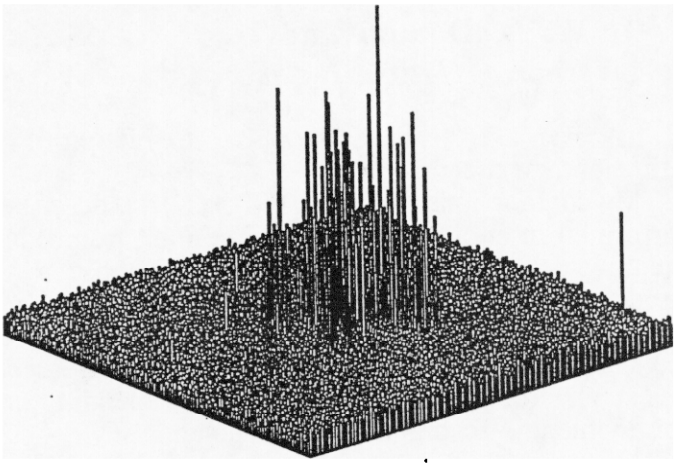

Fig. 1 Ion beam image from a CCD chip following impact of Xe^{44+} ions onto the chip's backthinned surface of Si/SiO_2. About 10^4 ions impacted the CCD chip that contains $(512)^2$ pixels. Each spike relfects the impact of at least one ion.

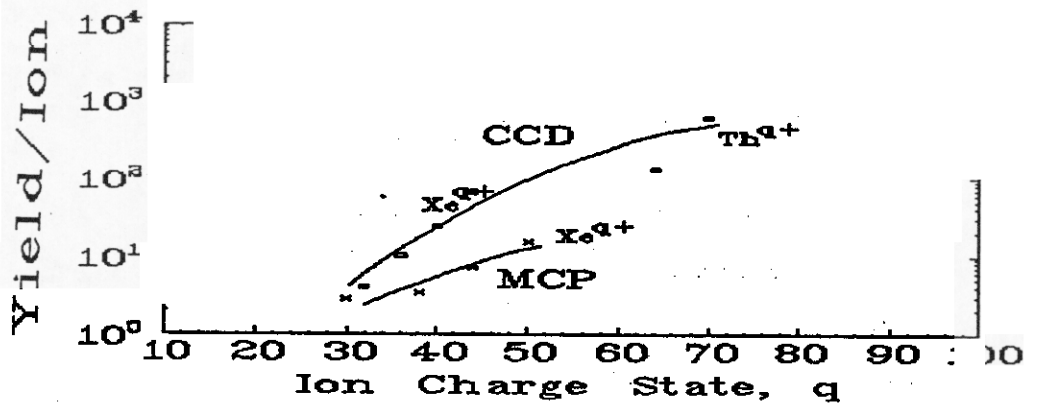

Fig. 2 Photon emission yield as function ion charge states from measurements with a CCD chip (labeled CCD) and multi-channel plate (labeled MCP) from Ref. 2. Curves are arbitrarily normalized at 30+ ion charge.

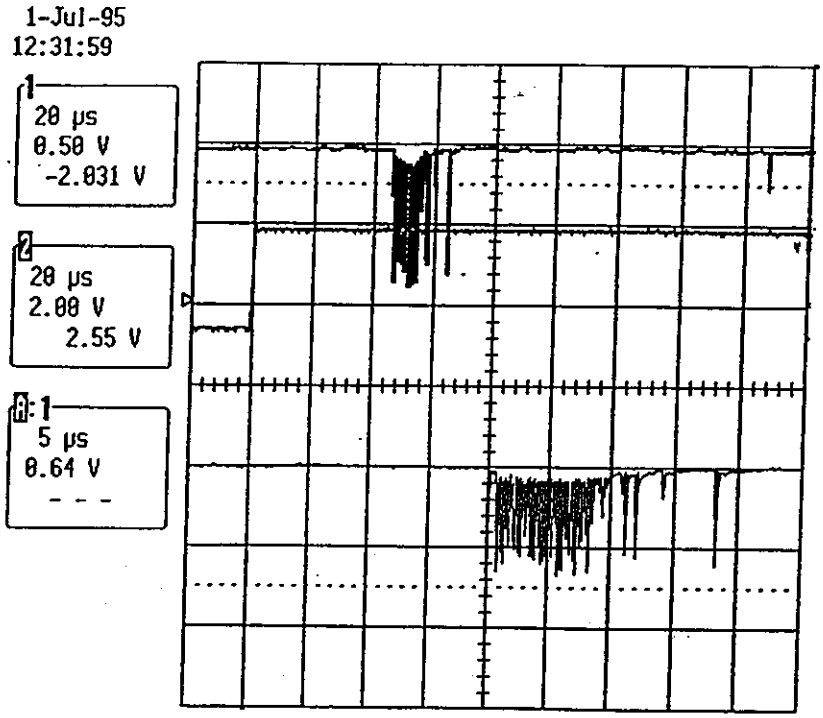

Figure 1 Typical "fast mode" dump

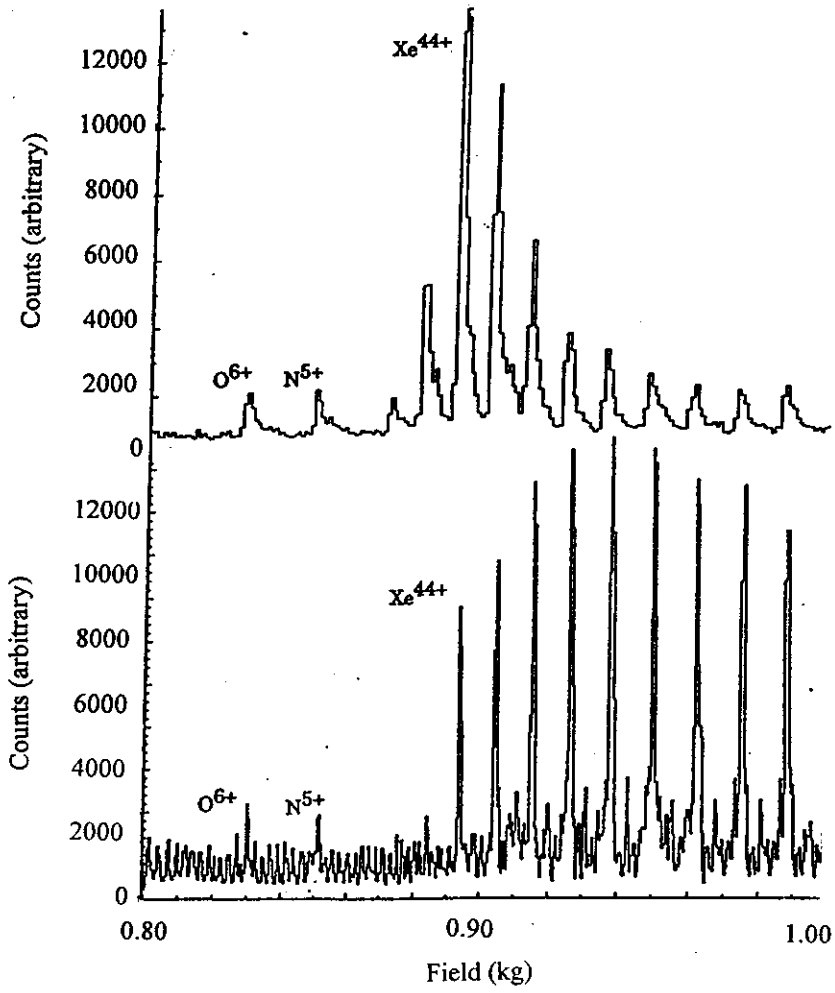

Figure 2 Magnet scans

Extraction of Highly Charged Ions from Super EBIT

J. W. McDonald, D. Nelson and D. H. G. Schneider
Lawrence Livermore National Laboratory, Livermore, CA 94550

We performed the first highly charged ion extraction tests on the LLNL Super EBIT where fully stripped Xenon ions and Uranium ions with charge states up to 90+ have been extracted. Super EBIT was originally designed from the first operational Electron Beam Ion Trap (EBIT), it has been extensively modified to achieve higher voltages (i.e., 220 kV) and ion extraction. The high voltage modification consisted of placing the electron gun and collector on a high negative potential (i.e., -180kV) which when combined with the high positive potential (i.e., +40kV) of the drift tubes yields the effective electron beam energy. The operation of an EBIT is based on sequential ionization of atoms and ions nearly at rest by an energetic electron beam that has been compressed to a small radius (≈ 60 mm) and a very high current density by the superconducting magnets. The electron bean radialy attracts the positively charged ions. The electron beam is focused through three drift tubes that form a longitudinal trap four cm in length. The source of the electron beam is a Pierce type electron gun located about 50 cm below the trap and has a magnet wound around it to zero the field of the super conducting magnets. At the present time the maximum current recorded is 240 mA. The electron beam dump is a kerosene cooled collector that has a magnet wound around it to partially cancel the magnetic field of the superconducting magnets. The vacuum in the trap region (about 5 X 10^-12 Torr) is due to the cryopumping associated with the superconducting magnets. There are several ways to inject ions into the trap the most widely used are neutral gas injection through one of the two gas leak valves, or a Metal Vapor Vacuum Arc (MEVVA) can spray low charged metallic ions into the trap. In order to produce high Z highly charged ions it is essential to provide cooling to compensate for the heating of the ions by the electron beam. This is particularly critical at high electron beam energies Ref 1. Low Z gases such as Neon or Nitrogen are leaked into the trap to provide evaporative cooling of high Z ions within the trap.

Highly charged ions have been extracted from the low energy (30kV) EBIT since 1989 Ref 2 and since 1994 they have been extracted from Super EBIT. The extraction of highly charged ions at Super EBIT began after the addition of an extraction beam line. The extraction beam line and SEBIT are depicted in figure 1. The major components of the extraction beam line are an electrostatic 90 deg. bender, an einzel lens, an analyzing magnet, and a channel plate detector. Ions are dumped from the trap by raising the middle drift tube potential above that of the top drift tube. The ions then spill out of the trap at the potential of the floating power supply plus the top drift tube potential minus the potential of the space charge. We have extracted $^{136}Xe^{54+}$ ions at 7kV and 20kV and U ions at 7kV. The spectra for ^{136}Xe ions are displayed in the inset of figure 1. ^{136}Xe gas atoms were injected through the gas inlet of SEBIT where they were ionized and trapped utilizing a 73keV electron beam and a 200 V longitudinal trap. These ions were extracted after about 500 ms by ramping the middle drift tube above the top drift tube.

The use of high electrostatic extraction potentials demonstrates a capability to readily produce low emittance highly charged heavy ion beams at MeV energies. It is furthermore noted that the intrinsic characteristic of the EBIT to produce low emittance ion beams (< 1 ¹ mm mrad)

can be improved by designing the top drift tube in such a way that it can act as an einzel lens during extraction.

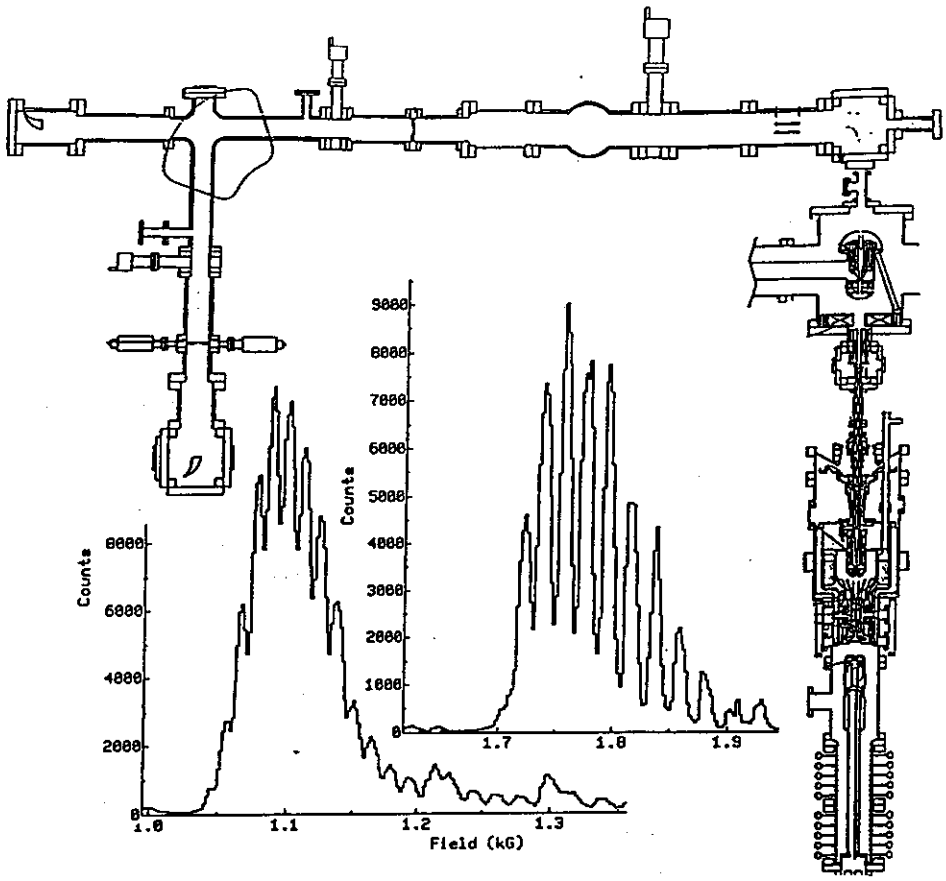

Figure 1 Super EBIT extraction system and typical $^{136}Xe^{q+}$ magnet scans taken at 7kV and 20kV.

References:

1) Bare Uranium in Physics Today, Oct. 1994.
2) D. Schneider, M. Clark, B. Penetrante, J. McDonald, D. DeWitt, N. Bardsley, Phys. Rev. A, **44**, 3119 (1991).

Development of an Intense EBIT

R. E. Marrs, L. Gruber, and E. Magee
Lawrence Livermore National Laboratory, Livermore, CA 94551

Most EBIT experiments are presently limited by count rate, and some very exciting future opportunities in both basic and applied science will not be achievable without a substantial increase in x-ray and extracted ion intensity. To capture these future opportunities, we are building an Intense EBIT with a goal of 100 times more x-ray emission per cm of beam length, and 1000 times more extracted ions. In addition, the maximum electron beam energy will be somewhat higher than that of our Super EBIT, resulting in a further increase in intensity for the highest charge states. The Intense EBIT will replace the Super EBIT in the same location so that all the external electrical and mechanical equipment can be used as is without significant modification.

The x-ray and highly-charged-ion production rate in an EBIT are both determined by the product of the number of ions in the trap and the electron beam current density. We are making several changes to increase both of these parameters: (1) The electron beam current is being increased by a factor of 2 initially and eventually by up to a factor of 50. The number of ions in the beam increases proportionately. The current will be increased by increasing the cathode area in an electron gun design that we developed ourselves. (2) The electron current density is being increased by a factor of roughly 5. This is accomplished by doubling the magnetic field in the trap and increasing the cathode brightness. (3) The trap length is being increased by a factor of 10 (from 2.5 cm to 25 cm). This increases the ion output by the same factor. (4) The cooling gas injection is being reconfigured to avoid degrading the ionization balance through charge exchange recombination.

The conceptual design of the Intense EBIT was completed in 1995. We expect the fabrication of the parts and the assembly of the device to be completed in 1996. A drawing of the Intense EBIT magnet and cryostat are shown in Fig. 1. One of the key components of an EBIT is the electron gun. Our existing EBITs all use a commercial gun in a mounting that we built in house. In order to get the highest level of performance from the Intense EBIT we have designed and built a completely new gun. An example of computer ray tracing calculations for this gun are shown in Fig. 2. A rising magnetic field that starts from zero on the cathode is an important part of the design. This field is produced by a bucking coil and steel shims operating in combination with the fringing field of the superconducting main coils.

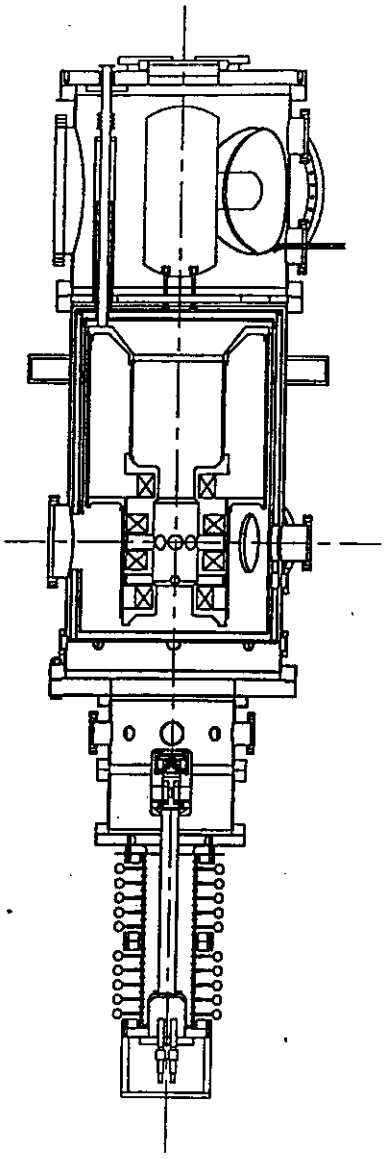

Fig. 1. Layout of the Intense EBIT. The magnet is split into four coils instead of two to provide radial access at two different elevations. The electron beam will be launched from a gun at the bottom of the apparatus, travel along the center line , and terminate in a collector located in the upper section of the vacuum chamber. The vacuum chamber is 24 inches in diameter.

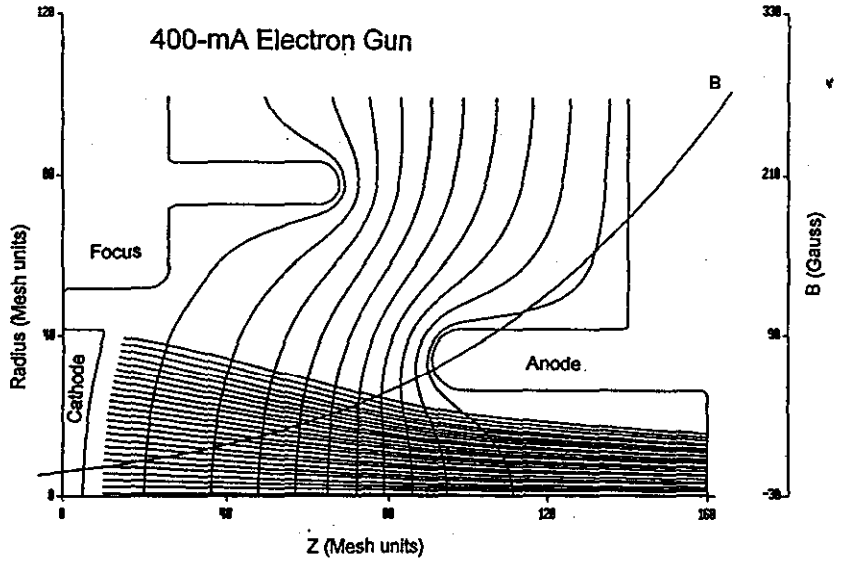

Fig. 2. Computer design of the 400-mA gun being fabricated for initial use with the Intense EBIT. The circular cathode has a 4-mm diameter, and the surface is spherical. The electron beam is represented by multiple rays that converge as they enter the tubular anode. Here they are terminated artificially at 160 mesh units, but the ray tracing was carried much farther down stream

Computer Modeling of Ions Trapped in an EBIT

R. E. Marrs, B. Beck, A. Ullrich, T. Werner, and A. E. Schach von Wittenau
Lawrence Livermore National Laboratory, Livermore, CA 94551

The processes that determine the energy balance and charge state distribution of ions trapped in an EBIT have been known for some time. For the energy balance these processes are: ion heating by the electron beam, exchange of energy between different ion species through collisions, and evaporation (escape) of ions over the radial and axial potential barriers that form the trap. The processes that determine the charge state distribution are: ionization by beam electrons, recombination with beam electrons, and charge exchange recombination with neutral gas in the trap. Several years ago Penetrante et al. developed a very successful time-dependent computer model for the ion temperature and charge state distribution [1]. This model included all the important processes, but it did not calculate the radial distribution of the trapped ions. We are developing an improved model that includes the self consistent radial distribution for all the ion species in the trap.

Understanding the radial distribution, density, and temperature of ions in the EBIT trap is critical for the development of submicron focused ion beams, especially with the new Intense EBIT. The ion radial distribution will also be important for future x-ray experiments in which knowledge of the electron-ion overlap factor is required, or in which the ion temperature must be reduced to minimize the Doppler broadening of spectral lines.

We are pursuing two approaches toward a more complete model of the EBIT trap. In the first approach, we have written a new computer code that finds the steady-state solution for the energy and ionization balance of trapped ions, but omits the (time-dependent) evolution of trap conditions at early times. This code keeps track of the ion radial distribution as an array of density values for each ion species. The radial potential is calculated self consistently from the spatial distribution of ion charges and the fixed electron beam profile. A solution is found by iteration. Results from a typical calculation are shown in Fig. 1. In this case, the calculation predicts a distribution of uranium ions that lies inside the electron beam.

In a second approach, which is just beginning, we are trying to combine the time-dependence and radial-distribution features in one code. This will provide a capability to model more complicated EBIT operating modes such as precooling ions just before extraction by changing the axial trap potential or reducing the electron beam current.

References

[1] B. M. Penetrante, J. N. Bardsley, D. DeWitt, M. Clark, and D. Schneider, Phys. Rev. A 43, 4861 (1991).

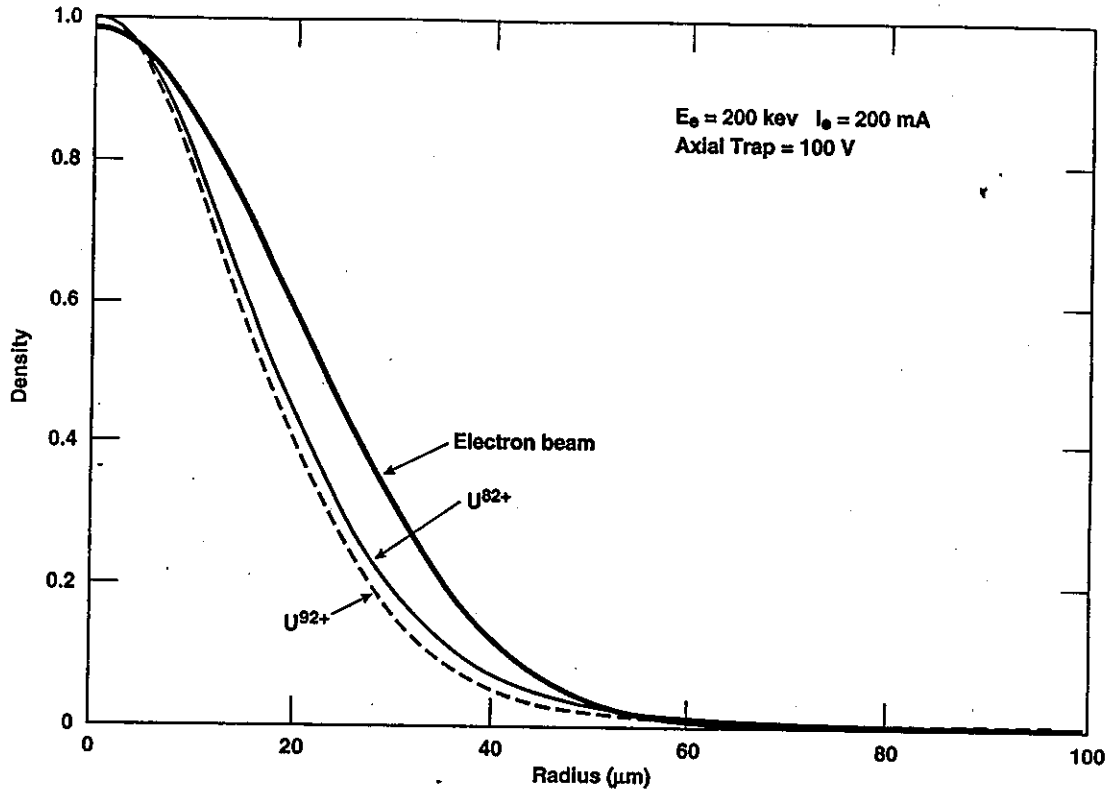

Fig. 1. Calculated radial distribution from the static solution for neon-cooled uranium ions trapped in Super EBIT at 200 keV electron energy.

A Test Stand for Electron Guns

R. E. Marrs, A. E. Schach von Wittenau, and E. Magee
Lawrence Livermore National Laboratory, Livermore, CA 94551

The successful compression of an electron beam to extremely high density is a key requirement for maximizing the performance of an EBIT. Although it is the high magnetic field of a superconducting magnet that compresses the beam in an EBIT, the amount of compression is determined by conditions farther upstream in the electron gun itself. Hence the quality of the upgraded electron guns that we are building for use in the new Intense EBIT will be critical for achieving the goal of much higher x-ray and ion production rates.

We have constructed a test stand for measuring the compressibility of the electron beam from our newly fabricated guns. The test stand uses a novel x-ray imaging technique that is completely different from the scanning techniques used in the microwave tube industry and elsewhere. As shown in Fig. 1., the beam from an electron gun under test is injected along the axis of a solenoid magnet. In this respect the test stand resembles an EBIT. The magnet consists of room temperature coils split to allow x-ray observation in the coil midplane. The profile of the compressed beam is revealed by the bremsstrahlung x-rays produced as beam electrons collide with background gas atoms. The x-ray emission may be increased by introducing argon gas into the vacuum chamber, from which 3-keV line radiation is produced. A 25-μm imaging slit located close to the beam is used to produce a magnified image of the beam profile on a position sensitive proportional counter located outside the vacuum chamber. The test stand is constructed mostly of common vacuum components with very few custom parts.

The compressibility of the electron beam is determined by the magnetic field on the cathode, by the quality of the electrode design and fabrication, and by the conditions of launching the beam into the main magnetic field. Even though the 5-kG field in the test stand is ten times smaller than that of the Intense EBIT, it is sufficient to diagnose all of these effects. The test-stand electron beam collector is water cooled and capable of handling the full dc beam from at least the first of the Intense EBIT guns.

An unexpected benefit of our new imaging technique is its ability to diagnose the intensity and approximate energy of secondary electrons returning from the collector. This is important because secondary and back-scattered electrons from the collector may limit the maximum electron beam in an EBIT, and there has been no other way to observe them.

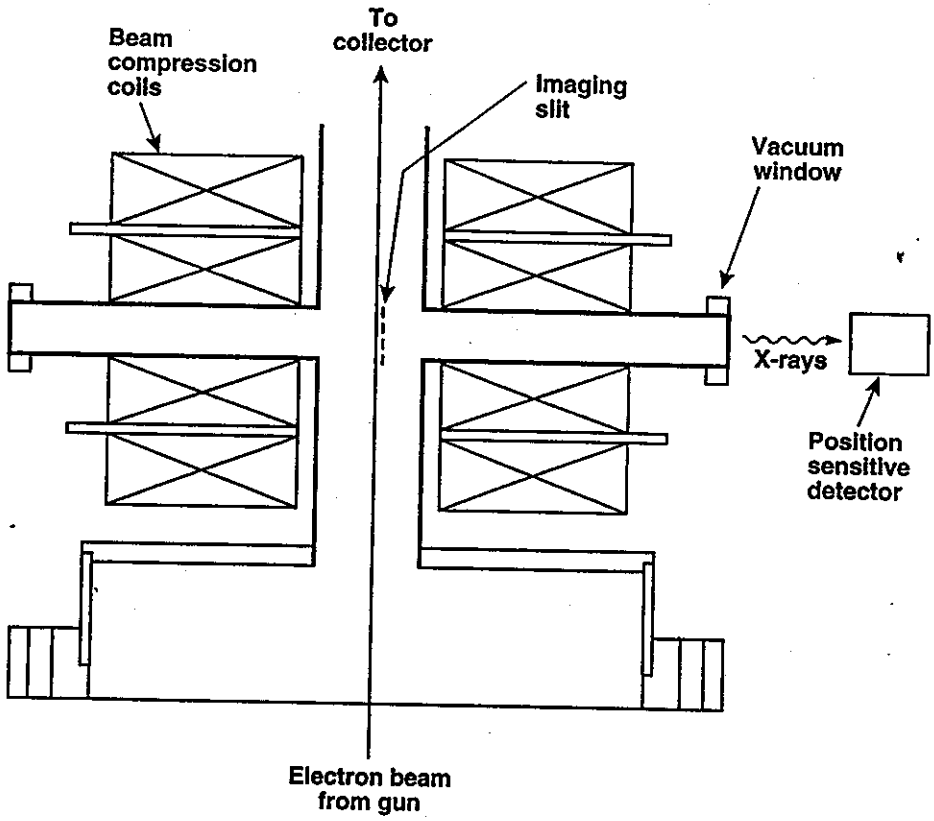

Fig. 1. Arrangement used for imaging the profile of a magnetically compressed electron beam. The slit is parallel to the electron beam, and the proportional counter is position sensitive in the direction perpendicular to the plane of the figure. Electron gun assemblies (not shown) are mounted on the 10-inch diameter flange at the bottom of the figure.

FT-ICR Analysis of the Magnetic Trapping Mode of an Electron Beam Ion Trap

P. Beiersdorfer[1], B. Beck[1], St. Becker[2,3], and L. Schweikhard[3]
[1]*Lawrence Livermore National Laboratory, Livermore, CA 94550*
[2]*iC-Haus, D-55294 Bodenheim, Germany*
[3]*Gutenberg Universität, D-55099 Mainz, Germany*

Until recently, the properties of EBIT have been analyzed both theoretically [1,2] and experimentally [1,3] only in the context of ion confinement in the presence of an electron beam. We refer to this mode of operation as the "electron trapping mode". The electrostatic fields of the electron beam are an integral part of the EBIT design to provide ion confinement in the radial direction. By contrast, the trapping properties in the absence of the electron beam, which we call the "magnetic trapping mode," seemed irrelevant to the performance of the EBIT facility as a spectroscopic or ion source. In the absence of the electron beam, however, ions should continue to be confined in the radial direction by the presence of a strong axial magnetic field (typically B = 3 T) that is used in the electron trapping mode to compress the electron beam. Moreover, the ions are confined axially by the potential applied to the end electrodes of the cylindrical trap, even under standard EBIT operating conditions. Typically, the axial potential applied to the end drift tubes relative to the middle range from V_{ax} = 10 V to 500 V. It is therefore possible to operate the facility as an ion trap after the electron beam is turned off, i.e., in the magnetic trapping mode. The main questions that arise are: How many of the highly-charged ions produced in the electron trapping mode remain in the trap after the beam is turned off? How long can they be stored? What are the ion-loss processes?

We performed a series of experiments to provide some of the answers to these questions [4]. In these measurements we rely on the Fourier transform – ion cyclotron resonance (FT-ICR) technique to analyze the ions remaining in the EBIT trap after the electron beam is turned off. The FT-ICR technique represents an excellent diagnostic tool for the characterization of the ions in the trap after the electron beam is turned off and has only recently been applied to the highly charged atomic ions found in an EBIT device [5]. It allows an estimation of the absolute number of ions in the trap [6] as well as to determine the relative abundance of each ion species. Moreover, by following the temporal evolution of the FT-ICR signal a lower limit on the ion storage time can be placed.

In our experiments [4], we found that the number of highly charged ions and the relative species abundance is the same just before and just after turning off the electron beam. In fact, a comparison with the absolute number of ions determined with x-ray spectroscopic techniques when the electron beam is on shows that switching EBIT from the electron to the magnetic trapping mode has no obvious effect on the number of ions or the relative ion abundance in the trap. About 10^5 ions per highly charged species, such as hydrogenic $^{84}Kr^{35+}$, were shown to exists in the trap. Moreover, by probing the stored ions at different times after the beam was turned off we could place a lower limit of 1.5 s on the ion storage time, as illustrated in Fig. 1.

Our measurements thus show that the electron trapping mode represents an ideal method for filling the trap *in situ* without the losses associated with transfering the ions from external sources. In addition, the length of the ion storage time is sufficient for a multitude of experiments which may be carried out in the future and which are impossible in the presence of

an electron beam. The magnetic trapping mode thus represents a new opportunity for studying the physics of highly charged ions in regimes that have been previously inaccessible.

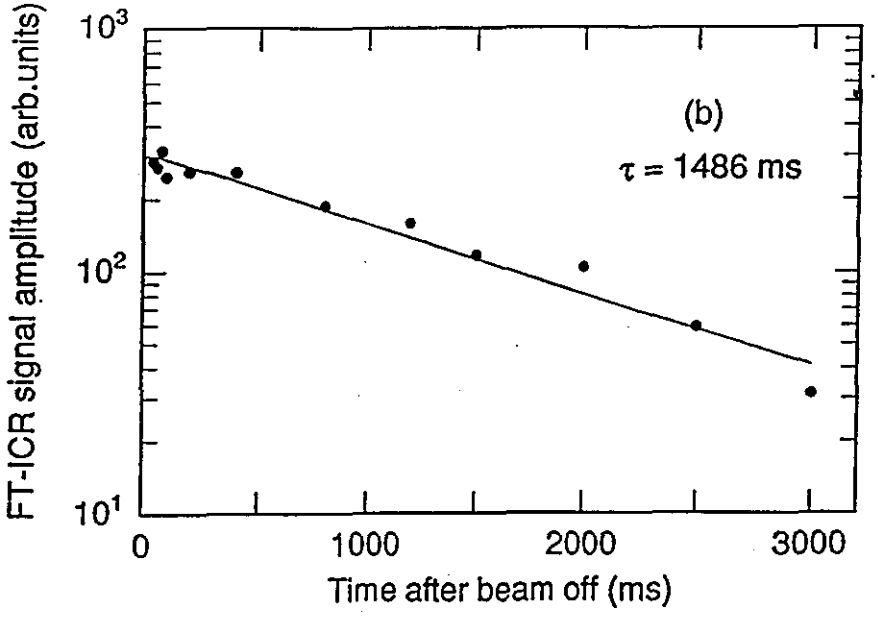

Fig. 1. FT-ICR signal amplitude of $^{84}Kr^{34+}$ ions observed as a function of the delay before ICR excitation commences after turning off the electron beam . The result of an exponential fit to the data is shown as a solid line.

References:

[1] M. A. Levine, R. E. Marrs, J. R. Henderson, D. A. Knapp, and M. B. Schneider, Phys. Scripta **T22**, 157 (1988).

[2] B. M. Penetrante, J. N. Bardsley, D. DeWitt, M. Clark, and D. Schneider, Phys. Rev. A **43**, 4861 (1991); B. M. Penetrante, J. N. Bardsley, M. A. Levine, D. A. Knapp, and R. E. Marrs, Phys. Rev. A **43**, 4873 (1991); B. M. Penetrante, D. Schneider, R. E. Marrs, and J. N. Bardsley, Rev. Sci. Instrum. **63**, 2806 (1992).

[3] M. B. Schneider, M. A. Levine, C. L. Bennett, J. R. Henderson, D. A. Knapp, and R. E. Marrs, in *International Symposium on Electron Beam Ion Sources and Teir Applications* AIP Conf. Proc. No. 188, ed. by A. Hershcovitch (AIP, New York, 1988), p. 158.

[4] P. Beiersdorfer, B. Beck, St. Becker, and L. Schweikhard, Intern. J. Mass Spectrom. Ion Proc. (in press).

[5] P. Beiersdorfer, B. Beck, R. E. Marrs, S. R. Elliott, and L. Schweikhard, Rapid Commun. Mass Spectrom. **8**, 141 (1994); P. Beiersdorfer, St. Becker, B. Beck, S. Elliott, L. Schweikhard, and K. Widmann, Nucl. Instrum. Meth. in Phys. Research **B98**, 558 (1995); L. Schweikhard, J. Ziegler, P. Beiersdorfer, B. Beck, St. Becker, S. Elliott, Rev. Sci. Instrum. **66**, 448 (1995).

[6] P. A. Limbach, P. B. Grosshans, and A. G. Marshall, Anal. Chem. **65**, 135 (1993).

This work was supported by NATO Collaborative Research Grant CRG-930125.

Implementation of a High-Resolution Transmission-Type Spectrometer on SuperEBIT for X-ray Transitions above 30 keV

K. Widmann[a,b], P. Beiersdorfer[a]

[a]Department of Physics and Space Technology, Lawrence Livermore National Laboratory, Livermore, CA 94551, USA

[b]Institut für Experimentalphysik, Technische Universität Graz, A–8010 Austria

High–resolution x–ray measurements on EBIT have so far been performed only with reflection–type crystal spectrometers. These have worked efficiently for x–ray energies up to 13 keV, e.g., the K–shell radiation of He–like krypton[1]. In order to extend crystal spectrometer measurements to higher–energy x rays from higher–Z elements, we have designed a transmission–type crystal spectrometer[2]. It enabled us to observe the $1s2p\,^3P_1 \rightarrow 1s^2\,^1S_0$ and $1s2s\,^3S_1 \rightarrow 1s^2\,^1S_0$ transitions individually, which have never before been spectroscopically resolved. Precision measurements of He–like and H–like xenon Kα transitions have been performed by Briand et al.[3] using a germanium detector with a resolution of 270 eV. The current setup improves the spectral resolution by more than an order of magnitude.

Our transmission–type spectrometer design is based on the DuMond geometry[4] employing a cylindrically bent crystal. The radius of curvature of the crystal is the diameter of the so–called Rowland circle (see Fig. 1). Placing the x–ray source, i.e., the trap region of SuperEBIT, on the Rowland circle strongly reduces the bandwidth of the diffracted x rays with the advantage that the throughput is tremendously increased at a given wavelength of interest. If the opening angle of the crystal is small enough, the diffracted x rays are quasimonochromatic. Therefore, no position sensitive detector is necessary, and solid state detectors, such as high–purity germanium detectors, can be used with almost 100% counting efficiency for 30 keV photons. To obtain a spectrum we rotate the crystal using a stepper motor mounted on a modified rotation stage. At each crystal position we count the number of photons reaching the detector and tag this number with the current position of the stepper motor. We normalized each step using the countrate of directly excited lines, emitted by the highly charged ions in the trap, which were measured with a second germanium detector.

A layout of the transmission–type crystal spectrometer for SuperEBIT is shown in Fig. 1. The spectrometer was set up to observe Kα radiation of He–like xenon, Xe^{52+}, which is situated near

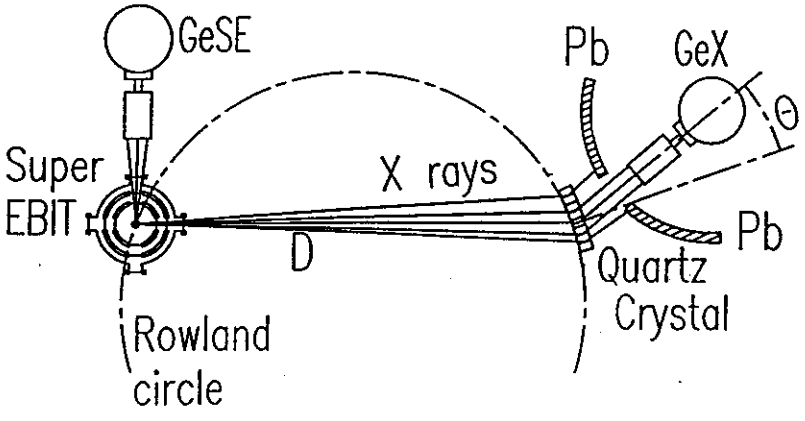

Figure 1: Layout of the transmission–type crystal spectrometer in the horizontal plane of SuperEBIT. The electron beam is perpendicular to the page. GeSE and GeX are high-purity germanium detectors; θ...Bragg angle; D...distance source to crystal; Pb...lead shielding;

31 keV. We use a Quartz crystal cut perpendicular to the $(13\bar{4}0)$ planes, $2d = 2.3604$ Å. Thus, the nominal Bragg angle is around $\theta = 9.9°$. The change in the Bragg angle is $0.000741° \pm 0.000001°$ per step which is equivalent to an energy change of about 2.2 eV for the diffracted photons at these x-ray energies. The radius of curvature of the crystal is $R_c = (2713.8 \pm 3.2)$ mm and was measured using an optical setup. The illuminated area of the crystal is $(60 \times 40)\text{mm}^2$. Positioning the crystal so that the electron beam is part of the Rowland circle is non trivial. At perfect alignment the energy spread of the diffracted x-ray photons reaching the detector is less than 0.5 eV across the detector area. If the distance between the crystal and SuperEBIT is off by $\pm$ 10 mm, the bandwidth of the diffracted x rays is increased to $\approx$ 3.5 eV. The influence of the finite width of the source, i.e., the width of the electron beam $\Delta x_{beam} = 60\mu m$, is about 4 eV for every diffracted x-ray photon. Therefore, the nominal resolution of our transmission-type spectrometer cannot be better than $\Delta E = 4.5$ eV, and the resolving power not better than $E/\Delta E = 6800$ for this setup. Further limitation of the resolving power is due to the quality of the focus of the bent crystal.

Figure 2 presents the result of the high-resolution measurement of some He-like Kα transitions using the transmission-type crystal spectrometer. The spectrum shows the $1s2s\,^3S_1 \rightarrow 1s^2\,^1S_0$, and $1s2p\,^3P_1 \rightarrow 1s^2\,^1S_0$, transitions in He-like Xe^{52+}. It took 131 hours to collect the amount of counts shown in Fig. 2. One channel represents the sum of the counts obtained during three consecutive steps. Thus, the dispersion is 6.6 eV per channel. Using a simple Gaussian fit we obtain a full width at half maximum of (20 ± 5) eV for these transitions. Therefore, the measured resolving power of our transmission-type crystal spectrometer is about 1500. This shows that the resolving power is limited by the quality of the focus of the crystal, as discussed above. Further improvment of the resolution depends on the ability of bending the crystal with a smaller focal width.

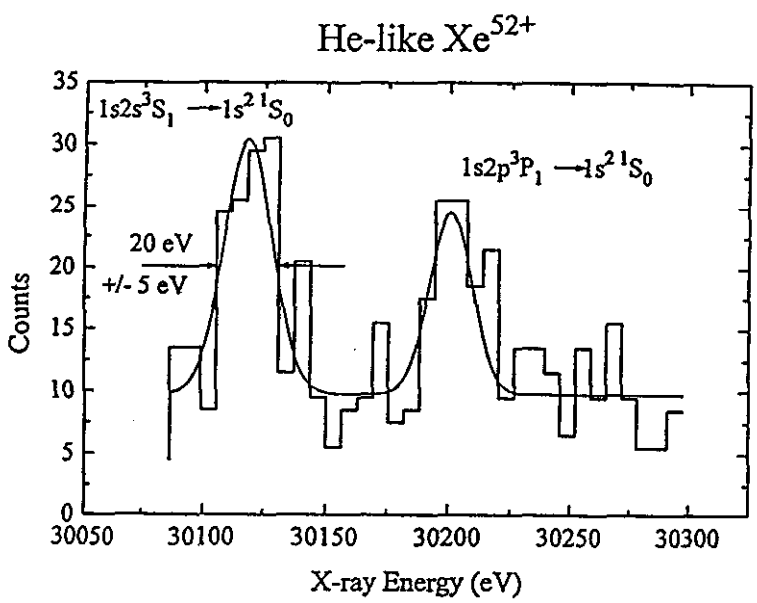

Figure 2: First resolved spectrum of the $1s2p\,^3P_1 \rightarrow 1s^2\,^1S_0$ and $1s2s\,^3S_1 \rightarrow 1s^2\,^1S_0$ transitions in helium-like Xe^{52+} observed with the transmission-type crystal spectrometer.

References

[1] K. Widmann, P. Beiersdorfer, V. Decaux, Phys. Rev. A **53**, 2200 (1996).

[2] K. Widmann, P. Beiersdorfer, G.V. Brown, J.R. Crespo López Urrutia, V. Decaux, D.W. Savin, submitted to Rev. Sci. Instrum. (May 1996).

[3] J.P. Briand, P. Indelicato, A. Simionovici, V. San Vicente, D. Liesen, and D. Dietrich, Europhys. Lett. 9, 225 (1989).

[4] J.W.M. DuMond, Rev. Sci. Instrum. 18, 626 (1947).

Installation of a Laser System for Ion Cooling in RETRAP

L.Gruber, J. Steiger, B. Beck, D. Schneider
Lawrence Livermore National Laboratory, Livermore, CA 94550

In the past year a laser lab has been set up adjacent to EBIT. It consists of a high power Argon-ion pump-laser and an actively stabilized dye ring laser. The maximum output power of the pump is 25 W, but only 7-8 W at 415.5 nm are used. This makes the pumping of a second dye laser feasible. The dye used is Kiton Red, with a tuning range from 600 to 650 nm. Due to active stabilization the linewidth of the laser does not exceed 500 kHz. In addition the frequency can be scanned over 30 GHz.

An intracavity frequency doubler ($LiIO_3$) is used to achieve the desired wavelength of 313 nm. The output power at this wavelength has been measured to 7 mW.

Undoubled light transmitted through the high-reflector (which replaces the output-coupler of the non-doubled setup) is used to measure the properties of the laserbeam. A spectrum analyzer, a wavelength-meter and an Iodine-cell (see Figure 1) measure frequency distribution and wavelength (accuracy 0.1 pm).

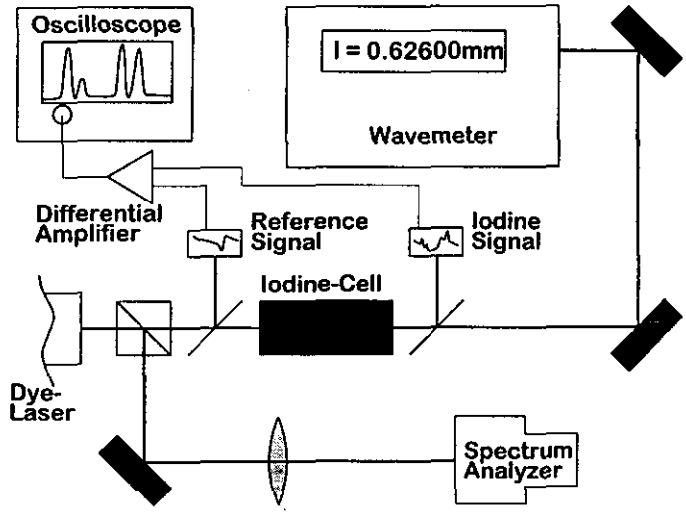

Figure 1: Schematics of the experimental setup to analyze the quality and the wavelength of the laserlight

Safety regulations required us to install the laser in a room adjacent to EBIT rather than close to the experiment. Therefore the building of a beamtransport-system was necessary. To maintain the good beam qualities the transport by means of mirrors was chosen. These mirrors were mounted on special vibrationally insulated stands

and each one of those is standing on small optical tables. The beam is transported to an optical table, which is part of the RETRAP-system where a telescope expands the beam from a 0.5" diameter to 1.5". A focusing lens focuses the beam in one of the hyperbolical traps in RETRAP.

The beam diameter after focusing was measured with the help of a chopper wheel and a photodiode. The chopper was moved in the region of the focal point to get a rough estimate of the shape of the beam waist in the trap. Figure 2 shows the beam diameter as a function of the position of the chopper.

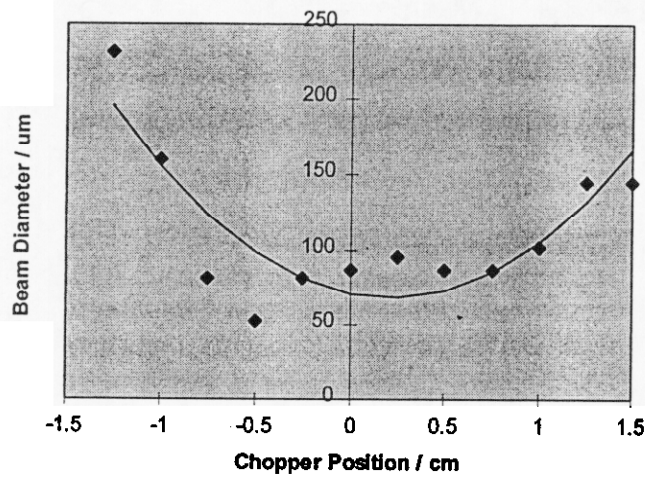

Figure 2: Beam diameter as a function of the chopper position. This measurement was used to obtain a rough estimate of the beam waist in the focal region.

It was found that the beam diameter is smaller than 100 μm over a region of about 2 cm. Therefore the alignment is not very sensitive in this direction.

The Laser can be operated remotely with a second electronic control unit installed next to RETRAP. In addition the control unit next to the laser can be accessed by a LabView-program which reads the data from the Iodine-cell and sets the laser to the desired frequency. The wavemeter has been equipped with a GPIB-interface to monitor the frequency stability on-line.

Appendix

A. Publications, Invited Talks, and Conference Contributions

   1. Publications

   2. Contributed Conference Papers

   3. Conference Organization

   4. Invited Talks and Seminars

B. Scientific Activities Centered Around EBIT

   1. Visitors and Participating Guests

   2. EBIT Seminar Series in N-Division of LLNL

C. Education

D. Scientific Cooperations

E. Personnel

A. Publications, Invited Talks, and Conference Contributions

A-1 Publications (Refereed Journals published in 1995)

Structure and Lamb Shift of $2s_{1/2}$-$2p_{3/2}$ Levels in Lithiumlike Th^{87+} through Neonlike Th^{80+}
P. Beiersdorfer, A. Osterheld, S. R. Elliott, M.Chen, D. Knapp, K. Reed
Phys. Rev. A 52 2693-2706 (1995).

High-Resolution Measurement, Line Identificiation, and Spectral Modeling of the Kß Spectrum of Heliumlike Ar^{16+}
P. Beiersdorfer, A. L. Osterheld, T. W. Phillips, M. Bitter, K. W. Hill, S. von Goeler
Phys. Rev. E 52 1980-1992 (1995).

Measurements of Line Overlap for Resonant Spoiling of X-ray Lasing Transitions in Nickellike Tungsten
S. R. Elliott, P. Beiersdorfer, B. J. MacGowan, Joseph Nilsen
Phys. Rev. A 52 2689-2692 (1995).

Measurements of the Radiative Lifetime of the 1s2s $^3S_1$ Level in Heliumlike Magnesium
G. S. Stefanelli, P. Beiersdorfer, V. Decaux, K. Widmann
Phys. Rev. A 52 3651-3654 (1995).

Spectral Measurements of Few-Electron Uranium Ions Produced and Trapped in a High-Energy Electron Beam Ion Trap
P. Beiersdorfer
Nuclear Instruments and Methods in Physics Research 99 114-116 (1995).

Fourier Transform Ion Cyclotron Resonance Mass Spectrometry - A New Tool for Measuring Highly Charged Ions in an Electron Beam Ion Trap
P. Beiersdorfer, St. Becker, B. Beck, S. Elliott, K. Widmann, L. Schweikhard
Nuclear Instruments and Methods in Physics Research 98 558-561 (1995).

Measurement of the Temperature of Cold Highly Charged Ions Produced in an Electron Beam Ion Trap
P. Beiersdorfer, V. Decaux, K. Widmann
Nuclear Instruments and Methods in Physics Research B 98 566-568 (1995)

The Super Electron Beam Ion Trap
R. E. Marrs, P. Beiersdorfer, S. R. Elliott, D. A. Knapp, Th. Stoehlker
Physica Scripta T59 183-188 (1995).

Wavelength Measurements of the He-like Krypton K-Shell Spectrum
K. Widmann, P. Beiersdorfer, V. Decaux
Nuclear Instruments and Methods in Physics Research B 98 45-47 (1995).

Excitation Mechanisms of $2s_{1/2}$-$2p_{3/2}$ and $2p_{1/2}$-$2p_{3/2}$ Transitions in U^{82+} Through U^{89+}
V. Decaux, P. Beiersdorfer, A. Osterheld
Nuclear Instruments and Methods in Physics Research B 98 129-131 (1995).

Measurement of Doubly Excited Levels in Lithiumlike and Berylliumlike Cobalt
A. J. Smith, P. Beiersdorfer, V. Decaux, K. Widmann, A. Osterheld, M. Chen
Physical Review A 51, 2808-2814 (1995).

Photo-Pumping Resonance for Modifying the Kinetics of a Neonlike La^{47+} Laser
P. Beiersdorfer, J. Nilsen, J. Scofield, M. Bitter, S. von Goeler, K. W. Hill
Physica Scripta 51 322-325 (1995).

Experiments with Highly Charged Ions up to Bare U^{92+} on the Electron Beam Ion Trap
P. Beiersdorfer
In *Proceedings of 14th Int. Conf. on Atomic Physics*, AIP Conf. Proceedings No. 323, ed. by D. J. Wineland, C. E. Wieman, and S. J. Smith (AIP, NewYork 1995), 116-129.

Measurement of the 3d-4f Transition in Ni-like Er for Use in a Photo-Pumped X-ray Laser Scheme
S.R. Elliott, P. Beiersdorfer, and J. Nilsen
Physical Review A 51, 1683-1686 (1995).

High-resolution Measurements of the He-β Spectra of Heliumlike Chromium for Possible Diagnostic of Laser-produced Plasmas
V. Decaux, P. Beiersdorfer, S. Elliott, A. Osterheld, E. Clothiaux
Rev. Sci. Instruments 66, 758-760 (1995).

High-Pressure Position-Sensitive Proportional Counter
David Vogel, P. Beiersdorfer, V. Decaux, K. Widmann
Rev. Sci. Instruments 66, 776-778 (1995).

Electron Impact Excitation Cross Section Measurements of Highly Charged Heliumlike and Lithiumlike Ions
K.L. Wong, P. Beiersdorfer, K.J. Reed, and D.A. Vogel.
Phys. Rev. A 51, 1214-1220 (1995).

High-resolution Measurement of the Kα Spectra of Low Ionization Species of Iron: New Spectral Signature of Non-Equilibrium Ionization conditions in Young Supernova Remnants
V. Decaux, P. Beiersdorfer, A. Osterheld, M. Chen, S.M. Kahn
Astrophysical Journal 443, 464-468 (1995).

Excitation and Detection of ICR Modes for Control and Analysis of a Multi-Component Plasma
L. Schweikhard, J. Ziegler, P. Beiersdorfer, B. Beck, St. Becker, and S.R. Elliott
Rev. Sci. Instruments 66, 448-450 (1995).

Studies of He-like Krypton for Use in Determining Electron and Ion Temperatures in Very High-temperature Plasmas
K. Widmann, P. Beiersdorfer, V. Decaux, S.R. Elliott, D. Knapp, A. Osterheld, M. Bitter, A. Smith
Rev. Sci. Instruments 66, 761-763 (1995).

Temperature of the Ions Produced and Trapped in an Electron Beam Ion Trap
P. Beiersdorfer, V. Decaux, S.R. Elliott, K. Widmann, K. Wong
Rev. Sci. Instruments 66, 303-305 (1995).

Observation of Interference Between Dielectronic Recombination and Radiative Recombination in Highly charged Uranium Ions
D. A. Knapp, P. Beiersdorfer, M. H. Chen, J. H. Scofield, and D. Schneider
Physical Review Letters 74, 54-57 (1995).

Measurements of Line Overlap for Resonant Spoiling of X-ray Lasing Transitions
P. Beiersdorfer, S.R. Elliott, B.J. MacGowan, and J. Nilsen
In *Proceedings of 4th Int. Colloquium on X-ray Lasers*, AIP Conf. Proc. No. 332, ed. by D. C. Eder and D. L. Matthews (AIP, NewYork 1995) 512-516.

EBIT X-ray Spectroscopy Studies for Applications to Photo-Pumped X-ray Lasers
S.R. Elliott, P. Beiersdorfer, and J. Nilsen
In *Proceedings of 4th Int. Colloquium on X-ray Lasers*, AIP Conf. Proc. No. 332, ed. by D. C. Eder and D. L. Matthews (AIP, NewYork 1995) 307-311.

Complex Substate Amplitudes Formed in Double Electron Capture
H. Khemlich, M.H. Prior, D. Schneider
Phy. Rev. Lett. 74, 25, 5015 (1995).

High Resolution, Broad Band X-ray Spectroscopy of Ion-Surface Interactions Using a Microcalorimeter
M. LeGros, E. Silver, D. Schneider, J. McDonald, S. Bardin,
NIM A357, 110 (1995).

Electron Emission From Foils Induced by Energetic Heavy Ion Collisions
R. A. Sparrow, R. Olson, D. Schneider
J. Phys. B 28, 3427-3439 (1995).

Time Ordering Effects in K-Shell Excitation of 170 MeV Ne^{7+} Colliding with Gas Atoms: Double Excitation
N. Stolterfoht, A. Mattis, D. Schneider, G. Schiwietz, B. Skogvall, B. Sulik, S. Rice
Phys. Rev. A 51, 1, 350 (1995).

Auger Decay of Na-like Si^{3+} ($2p^5$ 3lnl) States Formed by Slow $Si^{5+} \rightarrow$ He and Ar Ion-Atom Collisions
D. Schneider, R. Bruch, A. Shlyaptseva, T. Brage, D. Ridder
Phys. Rev. A 51, 6, 4652 (1995).

AFM Studies of a New Type of Radiation Defect on Mica Surfaces Caused by Highly Charged Ion Impact
C. Ruehlicke, M.A. Briere, D. Schneider
NIM B99, 528 (1995).

Recent Results from the LLNL Electron Beam Ion Trap
D. Schneider
Physica Scripta T59, 189 (1995).

Charge Exchange Between Xe^{44+} and H_2 in an Ion Trap
J. Steiger, G. Weinberg, B. Beck, D.A. Church, J. McDonald, D. Schneider
NIM B98, 569 (1995).

Two-Center Electron Emission in Collisions of Fast, Highly Charged Ions with He: Theory and Experiment,
N. Stolterfoht, H. Platten, G. Schiwietz, T. Schneider, D. Schneider, L. Gulas, P. Fainstein, A. Salin
Phys. Rev. A, 52, 3796 1995.

Electron Beam Ion Traps,
R. E. Marrs, in Experimental Methods in the Physical Sciences Vol. 27A, edited by F.B. Dunning and R.G. Hulet, Academic Press, San Diego, 1995, p391.

Highly Charged Science with the Electron Beam Ion Trap,
R. Marrs and D. Schneider,
Physics News in 1994 (AIP, New York, 1995), p. 16.

A Wire Probe as an Ion Source for an Electron Beam Trap,
S.R. Elliott and R. E. Marrs,
Nucl. Instrum. Methods B 100, 529 (1995).

Measurement of Two-Electron Contributions to the Ground-State Energy of Heliumlike Ions,
R.E. Marrs, S.R. Elliott, and Th. Stoehlker,
Phys. Rev. A52, 3577 (19950.

Recent Results from the Super EBIT,
R.E. Marrs
The Physics of Electronic and Atomic Collisions XIX International Conference, edited by L.J. Dube, J.B.A. Mitchell, J.W. McConkey, and C.E. Brion, AIP Conference Proceedings No. 360 (AIP, New York, 1995), p. 705.

A-2 Contributed Conference Papers

Detailed Measurements and Modeling of the n=3 → n=1 Spectrum of He-like Argon (Ar^{16+})
P. Beiersdorfer, K. Widmann, V. Decaux, A. Osterheld, M. Bitter, K. Hill, S. vonGoeler, A. Smith
37th Annual Meeting, APS Division of Plasma Physics, Louisville, KY, Nov. 6-10, 1995.

Measurement of the Radiative Lifetime of the 1s2s $^3S_1$ Level in Heliumlike Magnesium
G.S. Stefanelli, P. Beiersdorfer, V. Decaux, K. Widmann
XIX ICPEAC, Whistler, BC, Canada, July 26-Aug. 1, 1995

Electron Impact Excitation Cross Section Measurements of Highly Charged Heliumlike and Lithiumlike Ions
K.L. Wong, P. Beiersdorfer, K.J. Reed, D. A. Vogel
XIX ICPEAC, Whistler, BC, Canada, July 26-Aug. 1, 1995

Search for $^3S_1$-$^3P_2$ Decay in U^{90+}
P. Beiersdorfer, Th. Stöhlker, S. Elliott
XIX ICPEAC, Whistler, BC, Canada, July 26-Aug. 1, 1995

Measurement of Dielectronic Recombination Resonances in Heliumlike and Lithiumlike Cobalt
A. J. Smith, P. Beiersdorfer, V. Decaux, K. Widmann, A. Osterheld, M. Chen
XIX ICPEAC, Whistler, BC, Canada, July 26-Aug. 1, 1995

Production of Cold Highly Charged Ions for Spectroscopic Studies
P. Beiersdorfer, V. Decaux, K. Widmann, S. Elliott
XIX ICPEAC, Whistler, BC, Canada, July 26-Aug. 1, 1995

Optical Diagnostics of Highly Charged Ions in Super-EBIT
J. R. Crespo Lopez-Urrutia, P. Beiersdorfer, K. Widmann, V Decaux
XIX ICPEAC, Whistler, BC, Canada, July 26-Aug. 1, 1995

Wavelengths Measurements of the Kα Transitions of Heliumlike Krypton
K. Widmann, P. Beiersdorfer, V Decaux, S.R. Elliott, M. Bitter
XIX ICPEAC, Whistler, BC, Canada, July 26-Aug. 1, 1995

First Lifetime Measurement of the Metastable $2s^22p^5(^2P^o_{3/2})3s(J=2)$ Ne-Like Fe^{16+} Ion
J. R. Crespo Lopez-Urrutia, P. Beiersdorfer, V Decaux, K. Widmann
XIX ICPEAC, Whistler, BC, Canada, July 26-Aug. 1, 1995

Production of Cold Highly Charged Ions for Spectroscopic Studies
P. Beiersdorfer, V. Decaux, K. Widmann, S. Elliott
1995 Annual Meeting of the Division of Atomic, Molecular, and Optical Physics, Toronto, Canada, May 16-19, 1995

Visible Light from Highly Charged Ions in EBIT
J. R. Crespo Lopez-Urrutia, P. Beiersdorfer, K. Widmann, V Decaux
1995 Annual Meeting of the Division of Atomic, Molecular, and Optical Physics, Toronto, Canada, May 16-19, 1995

FT-ICR Mass Spectrometry of Very Highly Charged Atomic Ions
P. Beiersdorfer, S. Becker, L. Schweikhard, B. Beck
Am. Soc. of Mass Spectrometry, Atlanta, GA, May 22-26, 1995

Evidence for Coulomb Explosions Induced by the Impact of Slow Very Highly Charged Ions on Solids
M.A. Briere, T. Schenkel, A.E. Schach von Wittenau, and D.H. Schneider
Proceedings of the XIX ICPEAC, Whistler, Canada, July 26, 1995.

Time-of-Flight Secondary Ion Mass Spectroscopy Studies of Insulator Surfaces with Very Highly Charged Ions up to Th^{71+}
M.A. Briere, T. Schenkel, A.E. Schach von Wittenau, D. Schneider
Proceedings of the XIX ICPEAC, Whistler, Canada July 26, 1995

Measured Charge Exchange Between Highly Charged Ions and a Neutral Gas,
B.R. Beck, D. A. Church, J. McDonald, D. Schneider, J. Steiger, G. Weinberg
Proceedings of the XIX ICPEAC, Whistler, Canada July 26, 1995.

High Production Efficiency of Large Secondary Cluster Ions due to the Impact of Slow Very Highly Charged Ions
M.A. Briere, T. Schenkel, A.E. Schach vonWittenau, D. Schneider
Proceedings of the XIX ICPEAC, Whistler, Canada July 26, 1995.

A Single Detector Technique for Secondary Ion Mass Spectroscopy with Highly Charged Primary Ions
M. A. Briere, G. Schiwietz, T. Schenkel, A.E. Schach von Wittenau, and D.H. Schneider
Proceedings of the XIX ICPEAC, Whistler, Canada July 26, 1995.

On the Mechanisms of Electron Transfer in the Bulk in Ion Surface Interactions
J. P. Briand, S. Bardin, D.H. Schneider, H. Khemliche, J. Jin, M. Prior
Proceedings of the XIX ICPEAC, Whistler, Canada July 26, 1995.

On the Dynamics of the Filling of the L Shell of Hollow Atoms
J. P. Briand, S. Bardin, D.H. Schneider, H. Khemliche, J. Jin, M. Prior
Proceedings of the XIX ICPEAC, Whistler, Canada July 26, 1995.

First Observation of the Influence of the Chemical Nature of a Surface in the Interaction of Ar^{17+} Ions on Various Targets
J. P. Briand and D. Schneider
Proceedings of the XIX ICPEAC, Whistler, Canada July 26, 1995.

On the Auger Neutralization Processes of Highly Charged Ions on Surfaces
S. Bardin, D.H. Schneider, J.P. Briand, H. Khemliche, J. Jin, M. Prior
Proceedings of the XIX ICPEAC, Whistler, Canada July 26, 1995

K X-ray Spectra Emitted by C^{5+}, N^{6+} and O^{7+} Impinging on Clean Surfaces
S. Bardin, D.H. Schneider, J.P. Briand, H. Khemliche, J. Jin, M. Prior
Proceedings of the XIX ICPEAC, Whistler, Canada July 26, 1995.

X-rays from $Ar^{17,18+}$ Collisions with C_{60}: Relation to Above Surface Behavior1J.P. Briand, L. deBilly, J. Jin, H. Khemliche, M.H. Prior, Z. Xie, M. Necioux, and D.H. Schneider
Proceedings of the XIX ICPEAC, Whistler, Canada July 26, 1995.

Surface Species Identification Using SIMS with Highly-Charged Ions from an EBIT and Auger Spectroscopy
A.E. Schach von Wittenau, A. Schmid, M.A. Briere, T. Schenkel, D. Schneider
Proceedings of the XIX ICPEAC, Whistler, Canada July 26, 1995.

Strongly Enhanced Secondary Ion Yields in TOF-SIMS Studies with Very Highly Charged Primary Ions up to Th^{71+}
T. Schenkel, M.A. Briere, A.E. Schach vonWittenau and D. Schneider
Proceedings of the XIX ICPEAC, Whistler, Canada July 26, 1995; Proceedings of the 18th Surface/Interface Research Meeting, Santa Clara University, Santa Clara, CA, June 13, 1995.

Super TOF Secondary Ion Mass Spectroscopy Using Very Highly Charged Primary Ions up to Th^{70+}
M.A. Briere, T. Schenkel, D. Schneider
SIMS X Conference, Nov. 1995, Münster, Germany

Analysis and Modification of Materials Using Highly Charged Ions
M. A. Briere
ISIAC XIV, Seattle, WA, August 2-4, 1995

Crystalllization and Switching Behavior of Sputtered Magneto-optic Garnet Films on Glass
T. Schenkel, Th. Kessler, J. Taubert, H. Baumann, J. Reimann, R. Omet and K. Bethge
Preoceedings of the 40th Annual Conference Magnetism & Magnetic Materials, Philadelphia, PA, Nov.6-9, 1995.

A-3 Conference Organization

XIV International Symposium on Ion Atom Collisions (XIV ISIAC), Seattle, Washington, August 3-4, 1995.

Host: EBIT Program in N-Division of the Physics and Space Technology Directorate of the Lawrence Livermore National Laboratory

Chairman: Dieter Schneider
Co-Chairman: Robert DuBois

The conference topics covered the following areas of physics:

- Slow collisions
- Fast collisions
- New developments
- Interdisciplinary research activities

Funding for the conference was provided by Physics and Space Technology and the Office of Basic Energy Sciences at DOE.

A-4 Invited Talks and Seminars

Overview of Recent X-ray Measurements at the Livermore EBIT Facility
P. Beiersdorfer
Friedrich Schiller Universität Jena, Max-Planck-Institut für Röntgen Optik, Dec. 12, 1995

Highlights of Recent EBIT Experiments
P. Beiersdorfer
Johannes-Gutenberg-Universität Mainz, Institut für Physik, Dec. 6, 1995

Making Hot Ions Cold - Experiments with Highly Charged Ions near Nature's Limit
P. Beiersdorfer
University of Nevada, Reno, Department of Physics, Dec. 1, 1995

Atomic Physics with an (almost) Table-Top Device
P. Beiersdorfer
Morehouse College, Department of Physics, Oct. 31, 1995

Accuracy of Laboratory X-ray Data
P. Beiersdorfer
1st Annual AXAF Science Center Workshop on Rates, Codes, and Astrophysics
Harvard-Smithsonian Center for Astrophysics, Cambridge, MA, July 17-20, 1995

Overview of the Current Spectroscopy Effort on the Livermore Electron Beam Ion Trap
P. Beiersdorfer
1st Euroconference on Atomic Physics with Stored Highly Charged Ions
Heidelberg, Germany, Mar. 20-24, 1995

Spectroscopy on the Livermore Electron Beam Ion Trap
P. Beiersdorfer
Kansas State University, Department of Physics, Mar. 30, 1995

Producing and Studying the Ultimate Ions in a Table-Top Device
P. Beiersdorfer
Sonoma State University, Department of Physics and Astronomy, Mar. 13, 1995

Highly Charged Ion Research at the LLNL EBIT
D. Schneider
University of Mexico, Institut de Fisica, Cerenavaca, Mexico, Feb. 1996

The EBIT as a Versatile Experimental Physics Facility
D. Schneider
International Conference on Trapped Ions, Heidelberg, Germany, Feb. 1995

Experiments with very Highly Charged Ions
D. Schneider
University of Frankfurt Nuclear Physics Institut, Germany, Mar. 1995

Progress in Ion/Surface Interaction Studies at EBIT
D. Schneider
Hahn Meitner Institut, Berlin, Germany, Mar. 1995

Physics With Very Highly Charged Ions at the LLNL EBIT
D. Schneider
Vanderbilt University, Nashville, TN, Aug. 1995

Progress in Experimental Physics at EBIT
D. Schneider
University of Illinois, Chicago, IL, Mar. 1995

Highly Charged Ion Physics at EBIT
D. Schneider
Western Michigan University, Kalamazoo, MI, Mar. 1995

Physics at EBIT
D. Schneider
Lawrence Berkeley Laboratory, Berkeley, CA, Nov. 1995

Progress of the LLNL EBIT/RETRAP
B. Beck
International Conference of Physics of Strongly Coupled Plasmas, Binz, Germany, Sept. 13, 1996

Electron-Ion Collisions in the Livermore Super EBIT
R.E. Marrs
DAMOP Meeting, Toronto, Canada, May, 1995

Recent Results from the Super EBIT
R.E. Marrs
XIX International Conference on the Physics of Electronic and Atomic Collisions, Whistler, Canada, July 1995

Production of U^{92+} with an EBIT
R.E. Marrs
6th International Conference on Ion Sources, Whistler, Canada, Sept. 1995

B. Scientific Activities Centered Around EBIT

B-1 Visitors and Participating Guest

Date	Visitor	Institution	Host
JANUARY			
16-20	John Tanis	Western Michigan University, Kalamazoo, MI	Knapp
27-30	David Church	Texas A&M, College Station, TX	Schneider
FEBRUARY			
9	Daniel Dubin	UC San Diego, San Diego, CA	Beck
9	John Farley	University of Nevada, Las Vegas, NV	Schneider
9	Charles Gabrys	University of Chicago	Schneider
MARCH			
6-14	Lutz Schweikhard	University of Mainz, Germany	Beiersdorfer
APRIL			
1-7/1	Vincent Decaux	University of California, Berkeley, CA	Beiersdorfer
24-25	Reinhard Doerner	Lawrence Berkeley National Laboratory Berkeley, CA	Schneider /Briere
26	Joe Martinez	Dept. of Energy, Washington DC	Schneider
MAY			
16-20	David Church	Texas A&M, College Station, TX	Schneider
18	Edward Parilis	Cal Tech, Pasadena, CA	Briere
26	Andras Gottschild	University of Texas at Austin, TX	Schneider /Crespo
JUNE			
7-14	Jochen Biersack	Hahn-Meitner-Institute, Berlin, Germany	Briere
14-28	H. Schmidt-Böcking	University of Frankfurt, Germany	Schneider
21-8/25	John Autrey	Morehouse University, Atlanta, GA	Beiersdorfer
21-8/25	Augustine Smith	" " " "	Beiersdorfer
21-9/1	Jelani Mahiri	" " " "	Beiersdorfer
23-30	David Church	Texas A&M, College Station, TX	Schneider
26-6/3	Lutz Schweikhard	University of Mainz, Germany	Beiersdorfer
26-6/10	Thomas Stoehlker	GSI, Darmstadt, Germany	Beiersdorfer
JULY			
10	Norman Tolk	Vanderbilt University, Nashville, TN	Schneider
14	Joachim Ullrich	GSI, Darmstadt, Germany	Schneider
14	Paul Neill	University of Nevada, Reno, NV	Beiersdorfer

23-25	Dave Church	Texas A&M, College Station, TX	Schneider
28	John Farley	University of Nevada, Las Vegas, NV	Schneider
28	Matthew Cook	" "	Schneider
AUGUST			
7-8	Marc Pieksma	Oak Ridge National Laboratory, TN	Briere
7-8	Hein Folkerts	KVI Zernikelaan Institute, Gronigan The Netherlands	Briere
7-8	Johannes Limburg	" "	Briere
10-15	Helmut Winter	Humboldt-Universität zu Berlin, Germany	Schneider
12-19	Lutz Schweikard	University of Mainz, Germany	Beiersdorfer
17	Jorge Eichler	Hahn-Meitner-Institute, Germany	Schneider
18-26	Steve Elliott	University of Washington, Seattle, WA	Beiersdorfer
24-25	Norman Tolk	Vanderbilt University, Nashville, TN	Schneider
24-25	Alan Barnes	" "	Schneider
24-25	Jonathan Gilligan	" "	Schneider
24-25	Royal Albridge	" "	Schneider
24-25	John Farley	University of Nevada, Las Vegas, NV	Schneider
24-25	Ravi.Marawar	" "	Schneider
28	Ivan Berry	U.S. Dept. of Defense, Washington, DC	Briere
SEPTEMBER			
5-8	Chander Bhalla	Kansas State University, Manhattan, KS	Beiersdorfer
19	Evgueni Donets	Laboratory of High Energies, Moscow, USSR	Schneider
OCTOBER			
3	Kurt Becker	City College of the City University of New York, NY	Schneider
1-1/1	Torsten Werner	Technische Universitat Dresden, Germany	Marrs
1-1/1	Albrecht Ullrich	" "	Marrs
17-26	David Church	Texas A&M, College Station, TX	Schneider
23-11/20	Andreas Hoffknecht	Univeristy of Osnabrueck, Germany	Briere
30-11/3	Andreas Arnau	University of Del Pais Vasco, Spain	Briere
NOVEMBER			
13-14	Shunsuke Ohtani	University of Electron-Communications, Japan	Schneider
13-14	Fred Currell	" "	Schneider
16-21	Thomas Kühl	GSI, Darmstadt, Germany	Schneider
16-30	Peter Seelig	University of Mainz, Germany	Steiger
17	Robert DuBois	University of Missouri, Rolla, MO	Schneider
21	Tsukiyo Tanaka	University of Nevada, Reno	Schneider

B-2 EBIT-Seminar Series in N-Division at LLNL

January	John Farley	"Laser Spectroscopy on Highly Charged Ions"
February	Dan Dubin	"Lattice Structure and Normal Modes of a Cryogenic Non-neutral Plasma"
March	David Church	"Highly Charged Ion Cooling in Ion Traps"
April	Reinhard Doerner	"Recoil Ion Spectroscopy"
May	Edward Parilis	"Ion-Surface Interactions With Highly Charged Ions"
June	Jochem Biersack	"Application of the Trim-Code"
June	Bernard Rupp	"Instrumentation Aspects of High Resolution Cryocrystallography of Biological Macromolecules"
August	Alan Barnes	"Ion Solid Interactions"
September	Evgueni Donets	"The EBIS-New Developments"
October	Andreas Hoffknecht	"Energy Loss of Highly Charged Ions at an AI (110) Surface"
November	Andres Arnau	"Nonlinear Screening of Hollow Atoms in Metals"

C. Education

C Graduate Education

The education of graduate students represents a major part of the EBIT program. During 1995 a total of six graduate students had been active in the program. The students came from different institutions, both national and international. One student finished his thesis for the Ph.D. in physics (George Weinberg supervised by D. Church and D. Schneider).

The EBIT program also routinely involves undergraduate students. Twice a year students from the Undergraduate Summer Institute Research Program have a chance to actively participate in ongoing research for a two-week period. During 1995, six undergraduates took advantage of this opportunity. The EBIT program has a continuing commitment to minority participation in its activities. A detailed description of our collaborative efforts with students and faculty from Historically Black Colleges and Universities is given in the following

List of Students at EBIT:

Lukas Gruber	Technische Universität Graz, Austria. Research on trapped highly charged ions towards a Ph.D. thesis.
Joe McDonald	Western Michigan University, Kalamazoo, MI. Research in ion/surface interactions towards Ph.D. thesis.
Christiane Ruehlicke	University of Bielefeld, Germany. Research on biomolecule fragmentation with highly charged ions towards a Ph.D. thesis.
Thomas Schenkel	University of Frankfurt, Germany. Research in ion/surface interactions toward Ph.D. thesis.
George Weinberg	Texas A&M University, College Station, TX. Research on trapped highly charged ions
Klaus Widmann	University of Technology, Graz, Austria. Research in atomic structure towards Ph.D. thesis.

Collaboration with Historically Black Colleges and Universities

Principal Collaborators: Peter Beiersdorfer (EBIT), Augustine J. Smith (Morehouse)

Collaborators: Vincent Decaux (EBIT), Klaus Widmann (EBIT), José Crespo López-Urrutia (EBIT)

Students: Jelani Mahiri (Morehouse), John Autrey (Morehouse), Michelle Slater (Spelman)

Abstract

A collaborative research effort between Historically Black Colleges and Universities (HBCU) and the EBIT program was started in October 1993 and was very intense and successful in 1995. The collaboration involved faculty and students from Morehouse College and Spelman College, Atlanta, and centered on the investigation of x-ray spectra and their diagnostic applications in magnetic and laser fusion. In 1995 several run periods were devoted to collaborative experiments on the EBIT facility. Most of these were during the summer months, but several others were scheduled during winter and spring breaks. Data analysis and reduction was carried out at LLNL and at HBCU facilities. For this purpose, Livermore provided Morehouse College with a computer workstation and software as well as salary support for employment of undergraduate students funded by the LLNL Research Collaborations Program for Historically Black Colleges and Universities. The collaborative efforts has resulted in several major scientific accomplishments in 1995.

Scientific Objectives

The ion and electron temperature and density are crucial parameters that quantify the conditions necessary for achieving thermonuclear fusion, both in magnetically and inertially confined plasmas. Techniques have been developed that rely on the interpretation of the x-ray line emission of highly charged heavy impurity ions to diagnose these plasma parameters. One method, applied extensively in tokamak diagnostics, is to observe the He-α ($n = 2 \rightarrow 1$) emission from transition-metal impurities embedded in the plasma. In the very dense plasmas produced in inertial-confinement (ICF) research, the He-α emission is optically thick, and the He-β ($n = 3 \rightarrow 1$) spectrum of argon or titanium is used for diagnostic purposes. In order to reliably infer the ion and electron temperature and density from such spectral measurements accurate atomic data are a prerequisite.

The objective of our research is to provide the atomic data needed for the interpretation of the spectral data from fusion plasmas and their use as temperature and density diagnostics as well as for benchmarking atomic physics calculations. Exploiting the precisely controlled experimental conditions provided by the Livermore Electron Beam Ion Trap facility our objective is to perform detailed studies of He-α and He-β spectra of the ions employed in plasma diagnostics. Our measurements include line positions, degree of polarization, electron-impact excitation cross sections, and dielectronic recombination rate coefficients. By extending these measurements to selected very high-Z elements atomic calculations are tested throughout the entire isoelectronic sequence.

Progress during 1995

The x-ray emission by dielectronic satellites pertaining to the $n = 2 \rightarrow 1$ He-α spectrum of heliumlike ions from the transition metals is an important diagnostic of electron temperature of magnetically confined fusion plasmas that allows the self-consistent modeling of the observed spectroscopic data. Using the Livermore Electron Beam Ion Trap facility we selectively excited the dielectronic resonances in heliumlike Co^{25+} and lithiumlike Co^{24+} and recorded the resulting x-ray emission with a high-resolution crystal spectrometer. A detailed analysis provided accurate atomic data on the line position and resonance strengths of the dielectronic satellites. Comparison with different theoretical results indicated several disagreements for several of the satellite intensities, as documented by Smith *et al.*, [1,2,3] that will significantly improve the accuracy with which the electron temperature can be inferred from the satellite intensity. Extending our investigations to higher-Z elements, we also carried out a measurement of the $n = 2 \rightarrow 1$ He-α spectrum of heliumlike Kr^{34+} [3,4]. Such an extension for heavier elements is especially important in the light of current efforts to design a high-temperature tokamak, such as the ITER tokamak, that attains ignition.

Our investigations have subsequently shifted to measurements of the dielectronic satellites pertaining to the $n = 3 \rightarrow 1$ He-β spectrum of heliumlike Ar^{16+} [5], which is an important diagnostic in laser fusion. Our analysis indicates that the intensity of the x-ray satellites that have a spectator electron with principal quantum number $n \geq 3$ are much larger than commonly assumed from the n^{-3} scaling expected from the n-dependence of the Auger rates [6]. In laser-produced plasmas, these satellites blend with the collisionally excited heliumlike line used to diagnose the electron density and result in a distortion and shift of the heliumlike line. Since our measurements show that the amount of dielectronic satellites blending with the heliumlike lines is larger than generally assumed, a reanalysis of the density diagnostic based on the He-β spectrum may be necessary.

The intensity of x-ray lines may not be isotropic if the lines are excited in collisons with directional electrons such those in a beam or directional electrons produced in short-pulse laser interactions. Instead, the emitted lines are linearly polarized. We have studied this phenomenon by recording the x-ray lines emitted from heliumlike Mg^{10+} under different conditions, and the effects of polarization of the lines was immediately obvious. A detailed analysis of the data, however, showed that the polarization of each line was somewhat less than expected. This is thought to be the result of thermal broadening of the beam that result in a partial depolariztion. We

are presently working out the theoretical framework to determine the amount of thermal broadening necesary to expain the observation. If successful, such measurements will provide a new spectral diagnostic for determining thermal effects on electron beams.

In many cases, our spectroscopic measurements provide wavelength information that is more accurate than data available from any other experiments or from calculations. As a result, our measurements represent benchmarks for testing atomic structure calculations, including the effects of relativity and quantum electrodynamics. In order to provide such benchmarks along the heliumlike isoelectronic sequence, we have extended our measurements to include heliumlike U^{90+}, i.e., the heliumlike ions of the heaviest naturally occurring element. These measurements were carried out at the high-energy EBIT facility using electron beams with 140-keV energy and very accurate wavelength data were obtained [7].

References

1. A. J. Smith, P. Beiersdorfer, V. Decaux, K. Widmann, A. Osterheld, M. Chen, *"Measurement of Doubly Excited Levels in Lithiumlike and Berylliumlike Cobalt"*, Phys. Rev. A **51**, 2808 (1995).

2. A. J. Smith, A. J., P. Beiersdorfer, V. Decaux, K. Widmann, A. Osterheld, M. Chen, *"Measurement of Dielectronic Recombination Resonances in Heliumlike and Lithiumlike Cobalt"*, Proceedings of the 19th International Conference on the Physics of Electron Atom Collisions, Whistler, BC, Canada, July 26-Aug. 1 (1995).

3. P. Beiersdorfer, G. Brown, J. Crespo López-Urrutia, V. Decaux, D. Savin, A. J. Smith, G. Stefanelli, K. Widmann, K. L. Wong, *"Overview of the Current Spectroscopy Effort on the Livermore Electron Beam Ion Traps"*, Hyperfine Interactions **99**, 203 (1995).

4. P. Beiersdorfer, K. Widmann, V. Decaux, A. Osterheld, M. Bitter, K. Hill, S. von Goeler, and A. Smith, *"Detailed Measurements and Modeling of the n=3 n=1 Spectrum of He-like Argon (Ar^{16+})"*, Bull. Am. Phys. Soc. **40**, 1795 (1995).

5. K. Widmann, P. Beiersdorfer, V. Decaux, S.R. Elliott, D. Knapp, A. Osterheld, M. Bitter, A. Smith, *"Studies of He-like Krypton for Use in Determining Electron and Ion Temperatures in Very High-temperture Plasmas"*, Rev. Sci. Instruments **66**, 761 (1995).

6. A. J. Smith, P. Beiersdorfer, V. Decaux, K. Widmann, K. J. Reed, M. Chen, *"Measurement of the Contributions of High-n Satellite Transitions to the Kβ Lines of He-like Ar^{16+}"*, Phys. Rev. A **54**, 462 (1996).

7. P. Beiersdorfer, S. R. Elliott, A. Osterheld, Th. Stöhlker, J. Autrey, G. Brown, A. J. Smith, and K. Widmann, *"Search for $1s2s\ ^3S_1$-$^3P_2$ Decay in U^{90+}"*, Phys. Rev. A **53**, 4000 (1996).

D. Scientific Cooperations

U.S. Cooperations:

Auburn University, Auburn, AL
California Institute of Technology, Pasadena, CA
Columbia University, New York, NY
Kansas State University, Manhattan, KS
Lawrence Berkeley National Laboratory, Berkeley, CA
Morehouse College, Atlanta, GA
Naval Research Laboratory, Washington, DC
Princeton Plasma Physics Laboratory, NJ
Texas A&M University, College Station, TX
University of California-Berkeley, Berkeley, CA
University of Nevada-Las Vegas, Las Vegas, NV
University of Nevada-Reno, Reno, NV
University of Washington, Seattle, WA
Vanderbilt University, Brentwood, TN
Western Michigan University, Kalamazoo, MI

International Cooperations:

GSI, Darmstadt, Germany
Hahn-Meitner-Institut, Berlin, Germany
Institut für Allgemeine Physik, Wien, Austria
Institut für Kernphysik, Frankfurt, Germany
Johannes Kepler Universität, Linz, Austria
Johannes Gutenberg Universität, Mainz, Germany
Friedrich Schiller Universität Jena, Germany
Manne Siegbahn Institute, Stockholm, Sweden
Technische Universität Graz, Austria
University of Paris, France

E. Personnel

Associate Director Physics & Space Technology: Richard J. Fortner
N. Division Leader: Mike Kreisler
EBIT Program: Dieter Schneider (SCHNEIDER2@.LLNL.GOV)

Scientific Staff Members:
- Peter Beiersdorfer
- Bret Beck (term)
- Michael Briere (term)
- Roscoe Marrs
- Dieter Schneider

Post-doctorals:
- Matt Cook (UNLV)
- Jose R. Crespo Lopez-Urrutia
- Vincent Decaux
- Daniel Savin (UCB)
- Joachim Steiger
- Alexis Schach von Wittenau

Students:
- Lukas Gruber
- Joseph McDonald
- Christiane Ruehlicke
- Thomas Schenkel
- George Weinberg
- Klaus Widmann

Technical Support Staff:
- Phil D'Antonio
- Ed Magee
- Dan Nelson
- Ken Visbeck

Guest Scientists:
- Peter Bauer
- Greg Brown
- David Church
- Lutz Schweikhard
- Augustine Smith
- Gregg Stefanelli
- Thomas Stoehlker

Secretary:
- Diane Rae
- Telephone No. (510) 422-8018
- Fax No. (510) 422-5940
- e-Mail: rae1@LLNL.GOV

Technical Information Department • **Lawrence Livermore National Laboratory**
University of California • Livermore, California 94551